



Light-Ion Induced Direct Reactions with Stored Radioactive Beams – The EXL Project at the Present ESR and at FAIR



Peter Egelhof
GSI Darmstadt, Germany

Symposium on
Physics of RARE-RI Ring

RIKEN, Tokio, Japan
November 10 - 12, 2011

- I. Motivation and Research Objectives of EXL*
- II. The EXL Detector Setup – Concept and Design Goals
- III. R&D on the EXL Recoil Detector
- IV. Feasibility Studies and First Experiments at the ESR
- V. Conclusions

* EXL: EXotic Nuclei Studied in Light-Ion Induced Reactions at the NESR Storage Ring

I. Motivation and Research Objectives of EXL

classical method of nuclear spectroscopy:

- ⇒ light ion induced direct reactions: (p,p), (p,p'), (d,p), ...
- ⇒ to investigate exotic nuclei: inverse kinematics

past and present experiments:

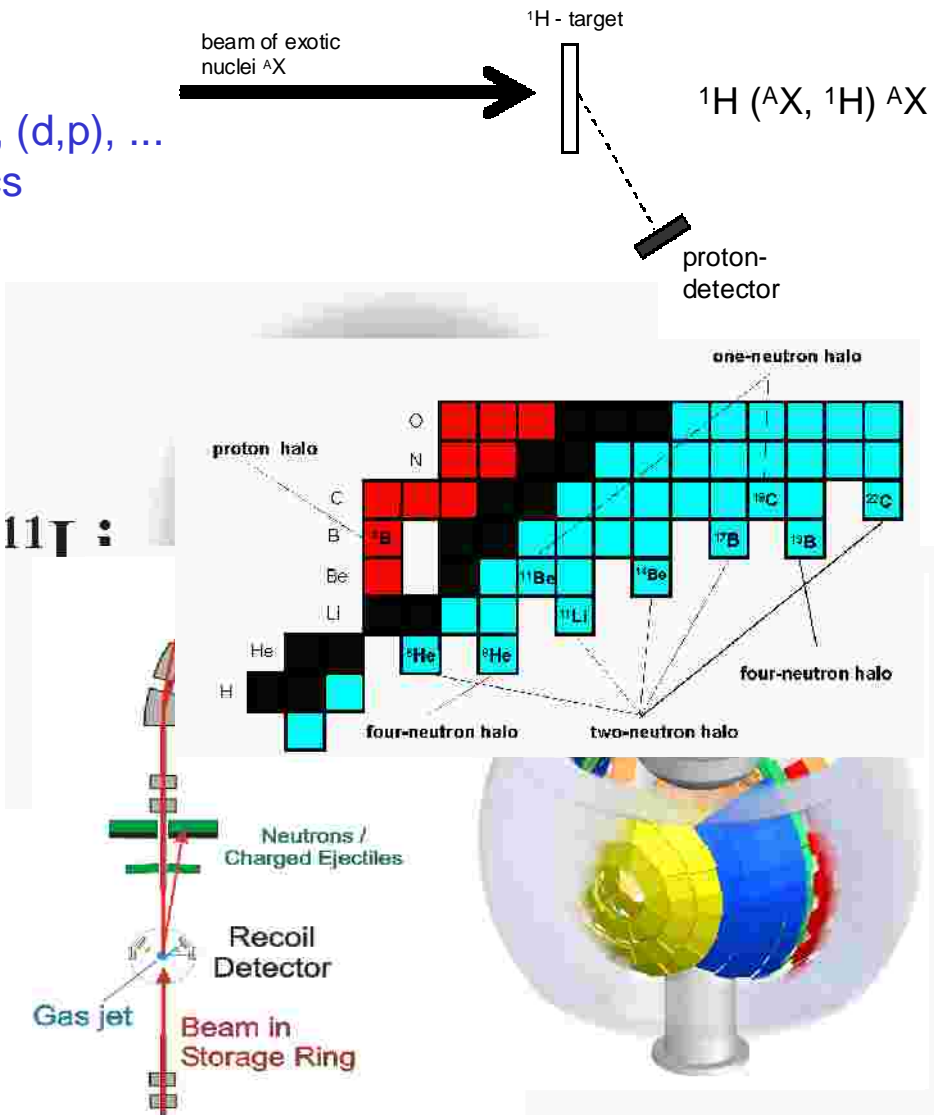
- ⇒ light neutron-rich nuclei: skin, halo structures
- ⇒ only at external targets

future perspectives at FAIR:

- ⇒ profit from intensity upgrade (up to 10^4 !!)
- ⇒ explore new regions of the chart of nuclides and new phenomena
- ⇒ use new and powerful methods:

EXL: direct reactions at internal NESR target

- ⇒ high luminosity even for very low momentum transfer measurements



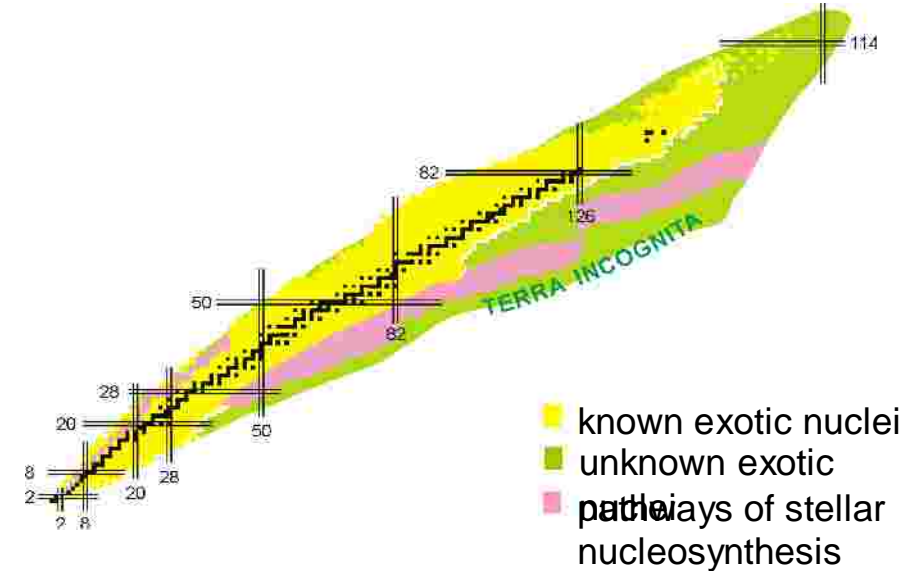
Perspectives at the GSI Future Facility FAIR

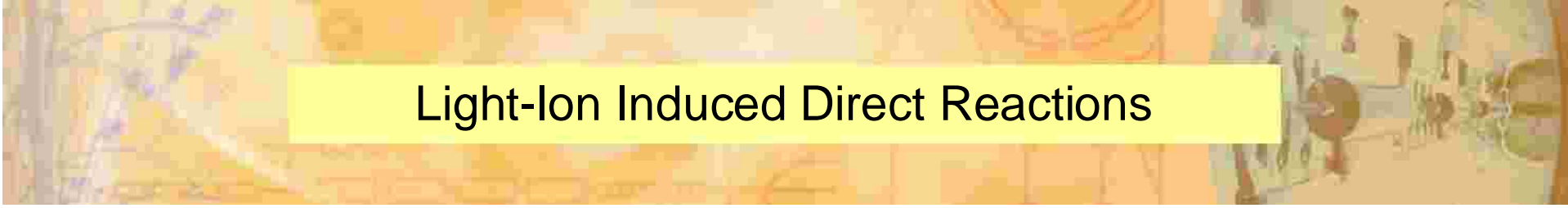
regions of interest:

⇒ towards the driplines for medium heavy and heavy nuclei

physics interest:

- | matter distributions (halo, skin...)
- | single-particle structure evolution (new magic numbers, new shell gaps, spectroscopic factors)
- | NN correlations, pairing and clusterization phenomena
- | new collective modes (different deformations for p and n, giant resonance strength)
- | parameters of the nuclear equation of state
- | in-medium interactions in asymmetric and low-density matter
- | astrophysical r and rp processes, understanding of supernovae





Light-Ion Induced Direct Reactions

- | elastic scattering (p,p), (α,α), ...
nuclear matter distribution $\rho(r)$, skins, halo structures
- | inelastic scattering (p,p'), (α,α'), ...
deformation parameters, $B(E2)$ values, transition densities, giant resonances
- | charge exchange reactions (p,n), ($^3\text{He},t$), ($d, ^2\text{He}$), ...
Gamow-Teller strength
- | transfer reactions (p,d), (p,t), ($p, ^3\text{He}$), (d,p), ...
single particle structure, spectroscopic factors
spectroscopy beyond the driplines
neutron pair correlations
neutron (proton) capture cross sections
- | knock-out reactions ($p,2p$), (p,pn), ($p,p, ^4\text{He}$)...
ground state configurations, nucleon momentum distributions, cluster correlations

The EXL Project @FAIR

FAIR: Facility for Antiproton and Ion Research

GSI today
GSI today

Future facility
Future facility

SIS 100/300

UNILAC

SIS 18

ESR

HESR

RESR CR

Rare-Isotope
Production Target

Super
FRS
Antiproton
Production Target

100 m

FLAIR

NESR

FAIR: Facility Characteristics

GSI today
GSI today

UNILAC SIS 18

ESR

HESR

RESR CR

100 fm

Rare-Isotope
Production Target

Super
FRS Antiproton
Production Target

FLAIR

NESR

Primary Beams

- $10^{12}/\text{s}$; 1.5-2 GeV/u; $^{238}\text{U}^{28+}$
- Factor 100-1000 over present in intensity
- $2(4)\times 10^{13}/\text{s}$ 30 GeV protons
- $10^{10}/\text{s}$ $^{238}\text{U}^{73+}$ up to 35 GeV/u
- up to 90 GeV protons

Secondary Beams

- Broad range of radioactive beams up to 1.5 - 2 GeV/u; up to factor 10 000 in intensity over present
- Antiprotons 3 - 30 GeV

Storage and Cooler Rings

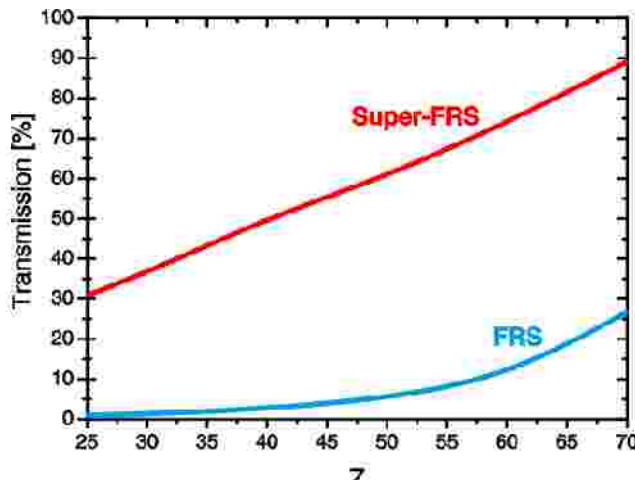
- Radioactive beams
- e – A collider
- 10^{11} stored and cooled 0.8 - 14.5 GeV antiprotons

Key Technical Features

- Cooled beams
- Rapidly cycling superconducting magnets

Nuclear Physics with Radioactive Beams at FAIR: NUSTAR: NUclear STructure, Astrophysics and Reactions

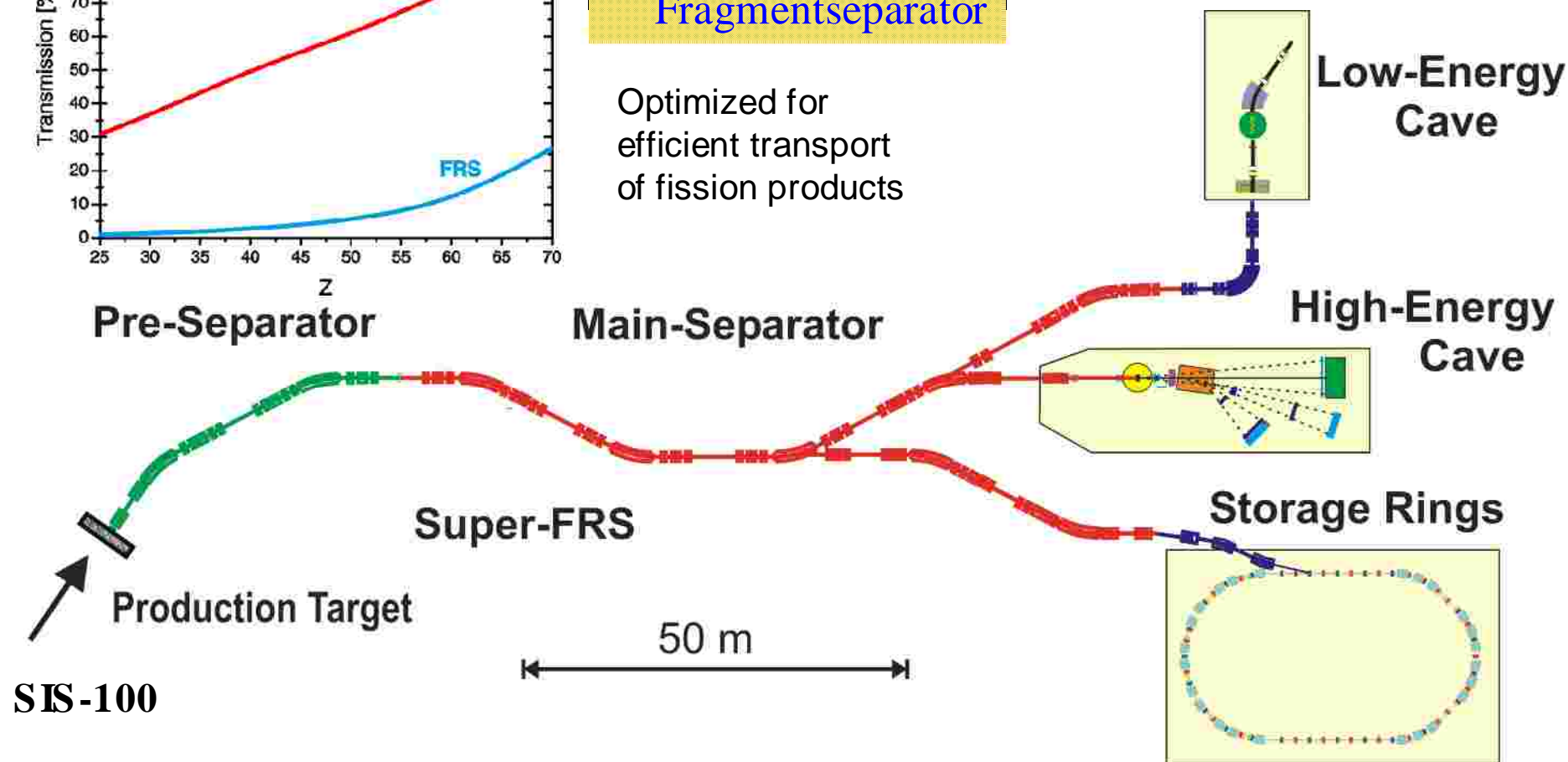
I High intensity primary beams from SIS 100 (e.g. $10^{12} \text{ }^{238}\text{U}$ / sec at 1 GeV/u)



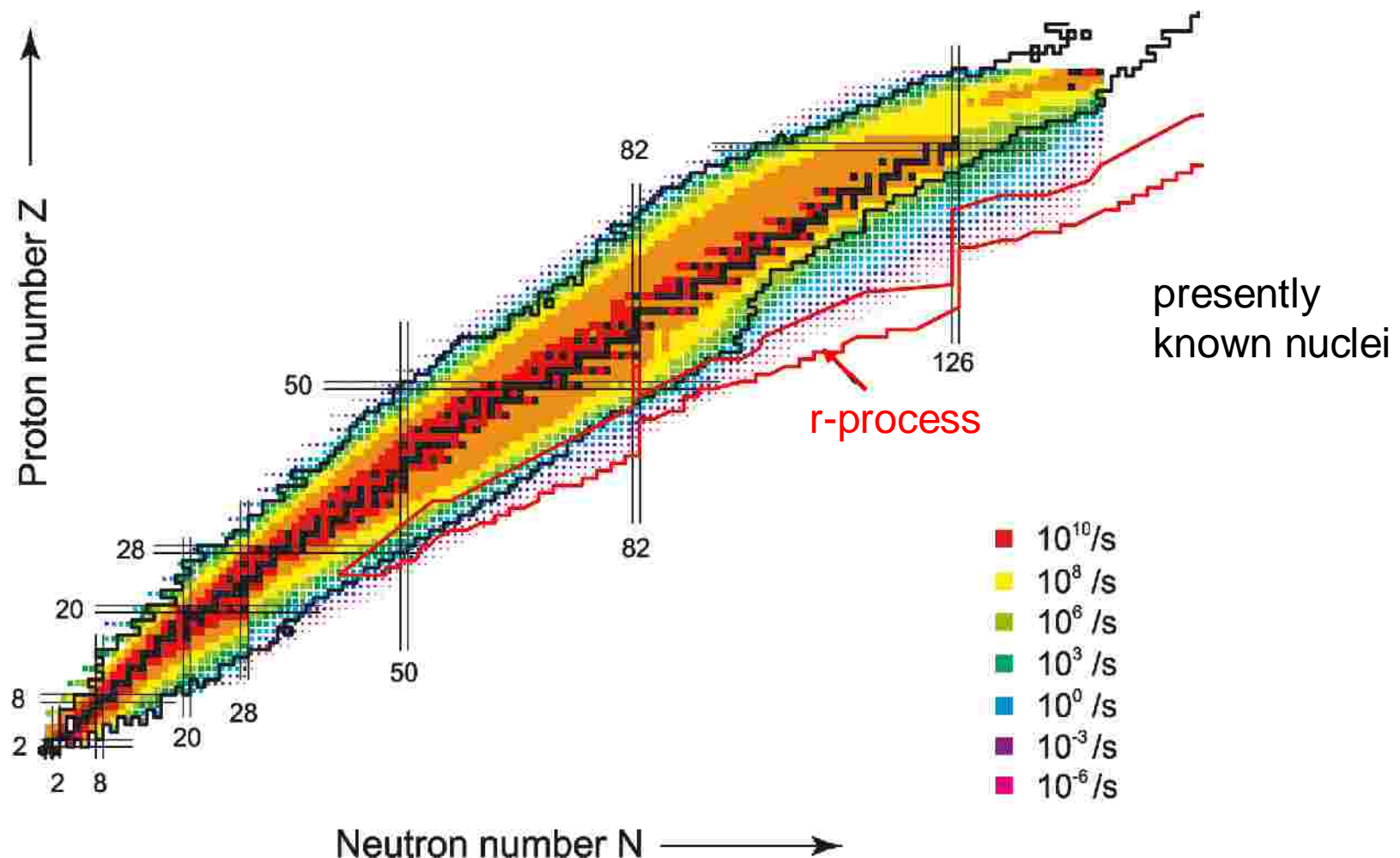
II Superconducting large acceptance Fragmentseparator

Optimized for efficient transport of fission products

III Three experimental areas



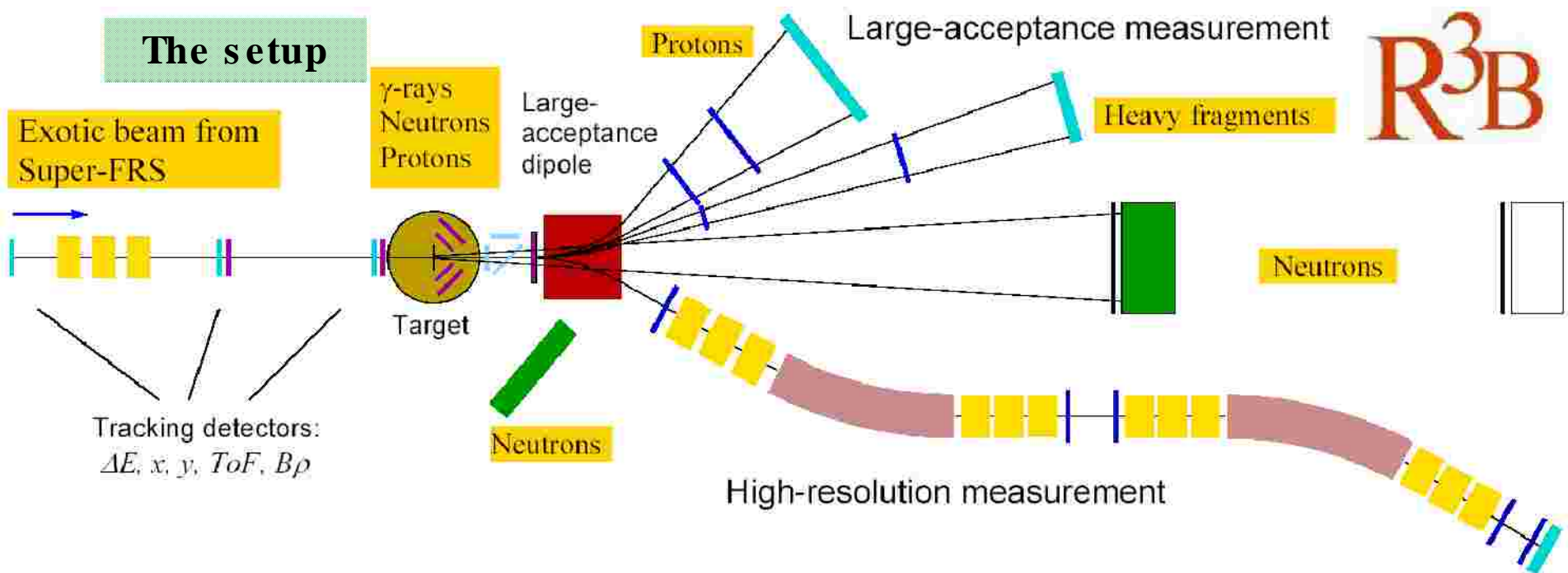
Expected Production Rates



Reactions with Relativistic Radioactive Beams at FAIR

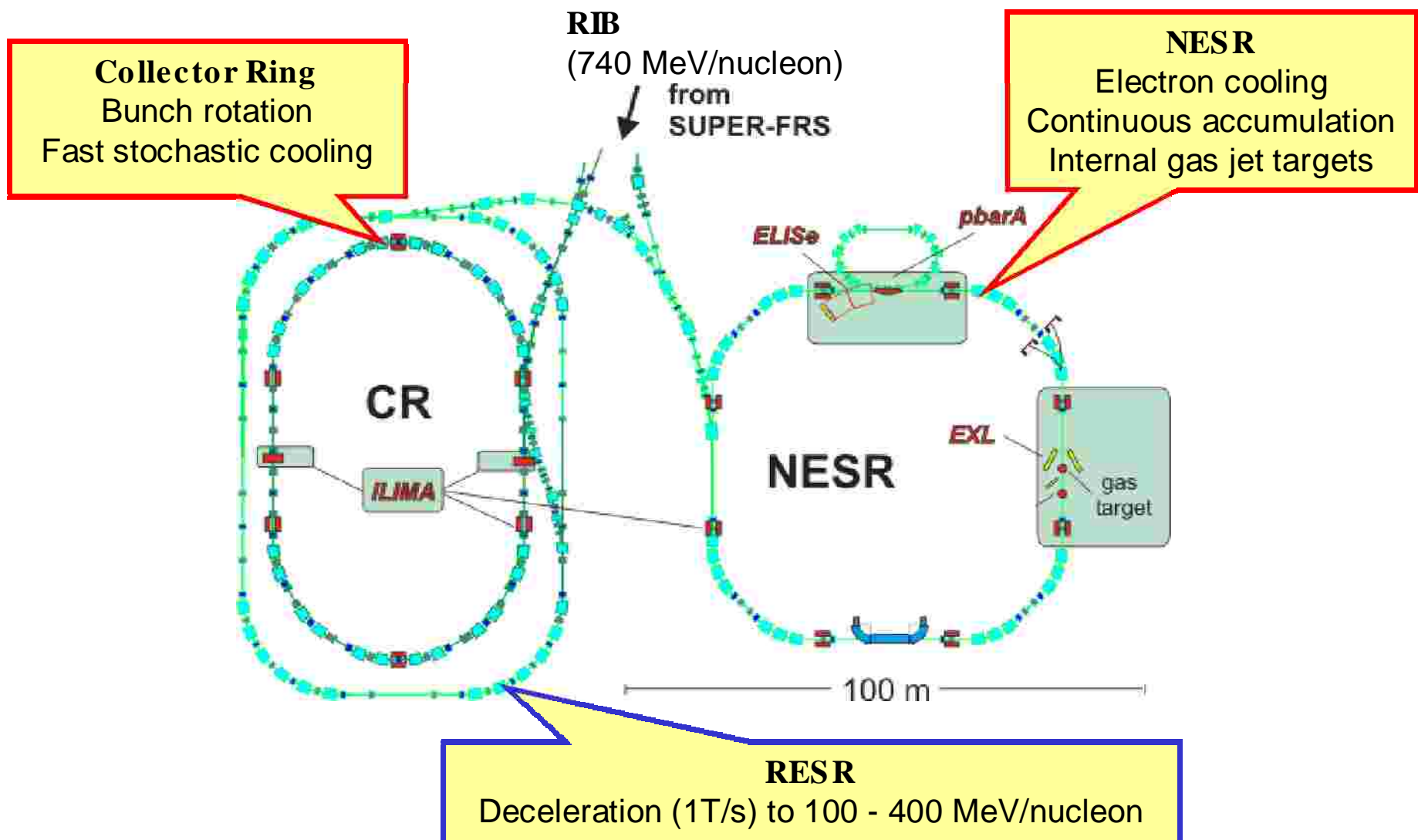
- R³B: Reactions with Relativistic Radioactive Beams
⇒ High Energy Branch
- EXL: Exotic Nuclei Studied in Light-Ion Induced Reactions at the NESR Storage Ring
⇒ Ring Branch
- ELISe: Electron Ion Scattering in a Storage Ring e-A Collider
⇒ Ring Branch
- AIC: Antiproton Ion Collider
⇒ Ring Branch

R3B: Reactions with Relativistic Radioactive Beams

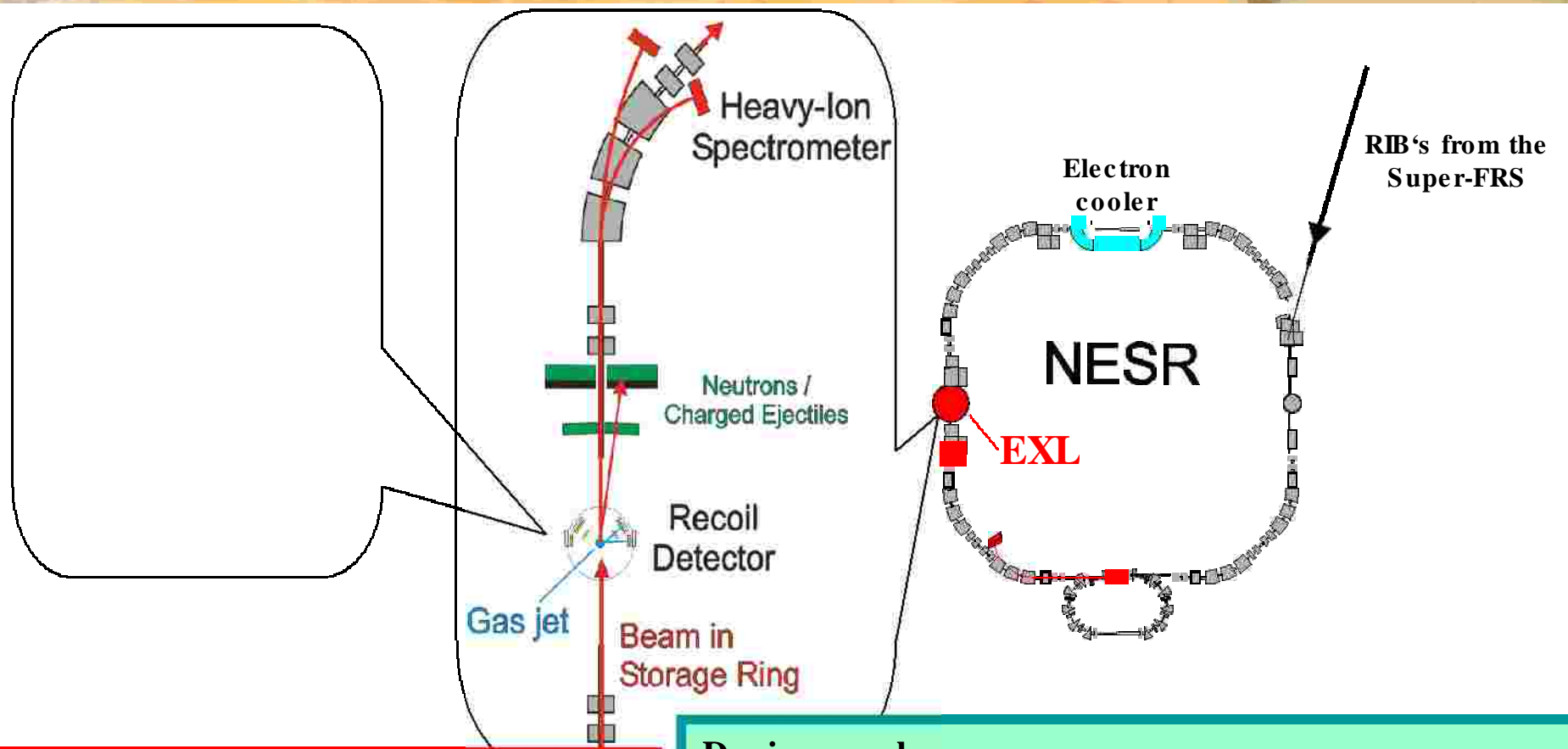


The R³B experiment: a universal setup for kinematical complete measurements

Experiments with Stored Exotic Nuclei



EXL: EXotic Nuclei Studied in Light-Ion Induced Reactions at the NESR Storage Ring



Detection systems for:

- | Target recoils and gammas ($p, a, n, ?$)
- | Forward ejectiles (p, n)
- | Beam-like heavy ions

Design goals:

- | Universality: applicable to a wide class of reactions
- | High energy resolution and high angular resolution
- | Large solid angle acceptance
- | Specially dedicated for low q measurements with high luminosity ($> 10^{29} \text{ cm}^{-2} \text{ s}^{-1}$)

Light-Ion Induced Direct Reactions at Low Momentum Transfer

- | elastic scattering (p,p), (α,α), ...
nuclear matter distribution $\rho(r)$, skins, halo structures
- | inelastic scattering (p,p'), (α,α'), ...
deformation parameters, $B(E2)$ values, transition densities, giant resonances
- | transfer reactions (p,d), (p,t), ($p, {}^3\text{He}$), (d,p), ...
single particle structure, spectroscopic factors, spectroscopy beyond the driplines,
neutron pair correlations, neutron (proton) capture cross sections
- | charge exchange reactions (p,n), (${}^3\text{He},t$), ($d, {}^2\text{He}$), ...
Gamow-Teller strength
- | knock-out reactions ($p,2p$), (p,pn), ($p,p {}^4\text{He}$)...
ground state configurations, nucleon momentum distributions

for almost all cases:

region of low momentum transfer
contains most important information

Speciality of EXL:

measurements at very low momentum transfer
⇒ complementary to R³B !!!

Experiments to be Performed at Very Low Momentum Transfer – Some Selected Examples

I Investigation of Nuclear Matter Distributions:

- ⇒ halo, skin structure
- ⇒ probe in-medium interactions at extreme isospin (almost pure neutron matter)
- ⇒ in combination with electron scattering (ELISe project @ FAIR):
separate neutron/proton content of nuclear matter (deduce neutron skins)

method: elastic proton scattering ⇒ at low q : high sensitivity to nuclear periphery

I Investigation of the Giant Monopole Resonance:

- ⇒ gives access to nuclear compressibility ⇒ key parameters of the EOS
- ⇒ new collective modes (breathing mode of neutron skin)

method: inelastic α scattering at low q

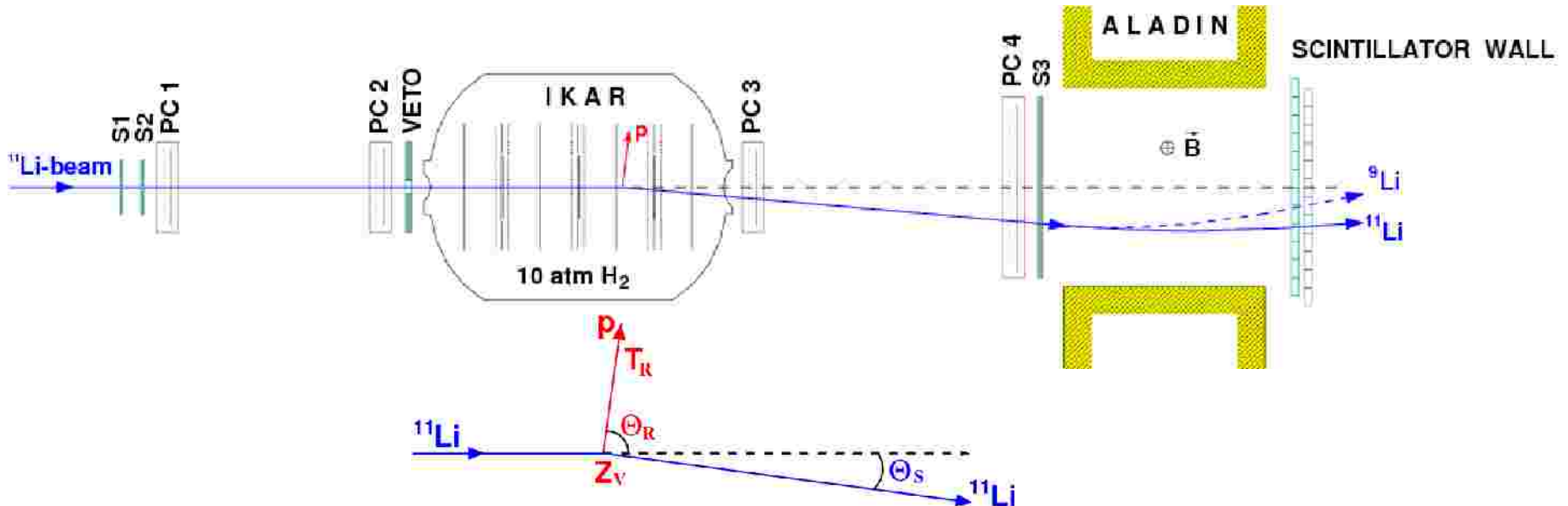
● Investigation of Gamow-Teller Transitions:

- ⇒ weak interaction rates for $N = Z$ waiting point nuclei in the rp-process
- ⇒ electron capture rates in the presupernova evolution (core collaps)

method: $(^3\text{He}, t)$, $(d, ^2\text{He})$ charge exchange reactions at low q

Investigation of Nuclear Matter Density Distributions of Halo Nuclei by Elastic Proton Scattering

Experimental Setup: Active Target IKAR and Aladin Magnet



target + recoil detector:

IKAR

} $\Rightarrow T_R, \theta_R, Z_V$

trajectory-reconstruction:

PC 1-4 (Multiwire proportional chambers)

} $\Rightarrow \theta_s$

beam identification:

S 1-3, Veto (plastic scintillators)

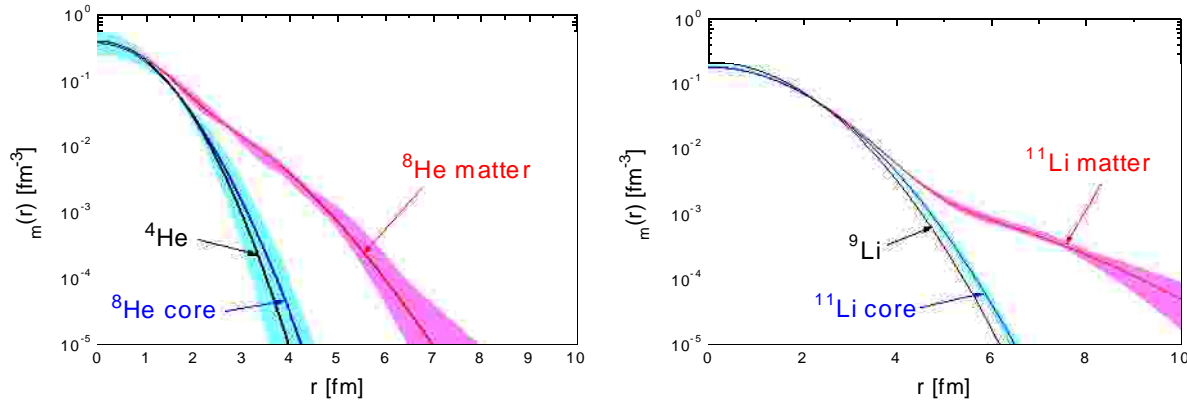
} $\Rightarrow \Delta E, \text{TOF, trigger}$

ALADIN-magnet
+ position sensitive scintillator wall

} \Rightarrow discrimination of projectile breakup

Investigation of Nuclear Matter Density Distributions of Halo Nuclei by Elastic Proton Scattering at Low Momentum Transfer

nuclear matter distributions:



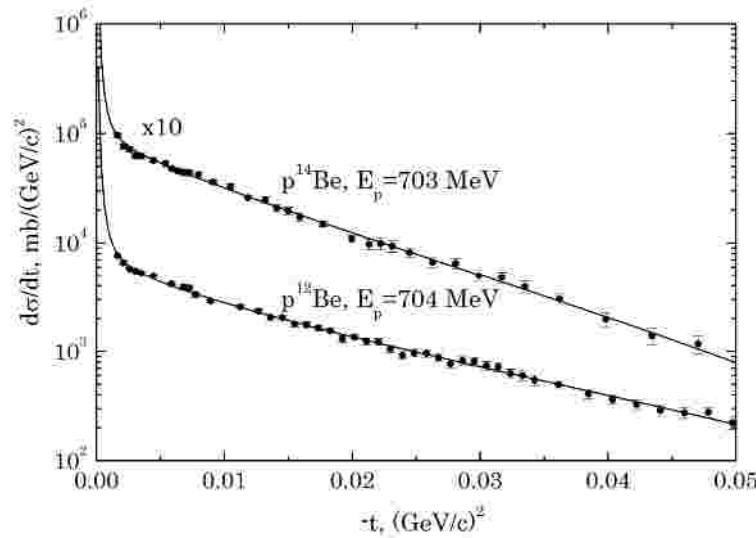
nuclear matter radii:

nucleus	R_{matter} , fm	R_{core} , fm	R_{halo} , fm
${}^4\text{He}$	1.49 (3)	--	--
${}^8\text{He}$	2.45 (7)	1.55 (15)	3.08 (10)
${}^9\text{Li}$	2.43 (7)	--	--
${}^{11}\text{Li}$	3.62 (19)	2.55 (12)	6.54 (38)

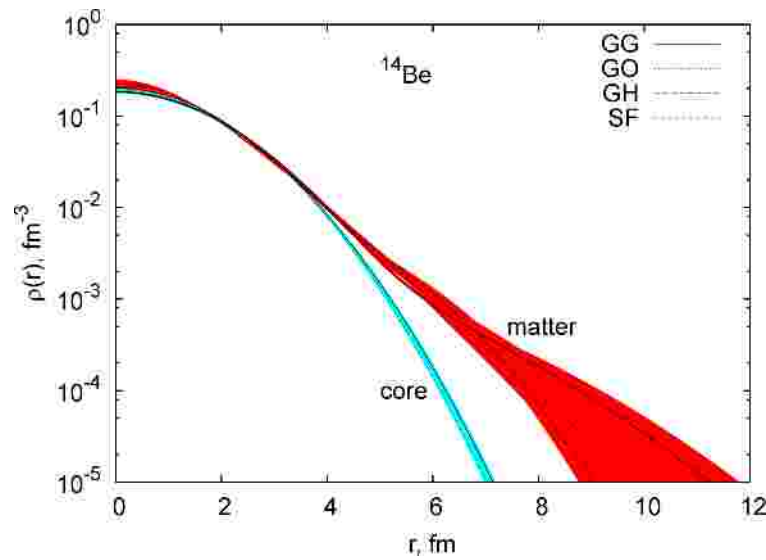
- | extended neutron distribution in ${}^8\text{He}$ and ${}^{11}\text{Li}$ obtained
- | size of core, halo and total matter distribution determined with high accuracy

Elastic Proton Scattering from ^{14}Be

differential cross section:



deduced nuclear matter distribution:



results for ^{14}Be :

$$\begin{aligned} R_{\text{matter}} &= 3.25 \pm 0.04 \pm 0.11 \text{ fm} \\ R_{\text{core}} &= 2.65 \pm 0.02 \pm 0.11 \text{ fm} \end{aligned}$$

- ^{14}Be exhibits a pronounced core-halo structure
- the picture of a ^{12}Be -core + 2 valence neutron structure is confirmed
- the present data favour a relatively large s-wave component
(see I. Thompson et. al, Phys. Rev. C53 (1996) 708)

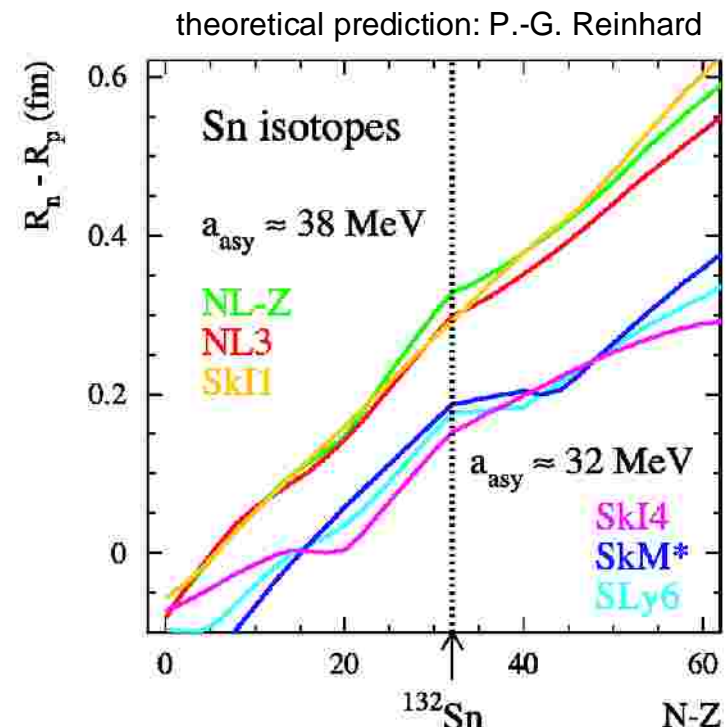
Proposed Experiments at FAIR

- | investigation of nuclear matter distributions along isotopic chains towards proton/neutron asymmetric matter
- | investigation of the same nuclei by (e,e) (ELISe) and (p,p) (EXL) scattering
 - ∅ separate neutron/proton content of nuclear matter
 - ∅ unambiguous and “model independent” determination of size and radial shape of neutron skins (halos)

example: Sn isotopes

at the nuclear surface:
almost pure neutron matter

- ∅ probe isospin dependence of effective in-medium interactions
- ∅ sensitivity to the asymmetry energy (volume and surface term!)



Experiments to be Performed at Very Low Momentum Transfer – Some Selected Examples

I Investigation of Nuclear Matter Distributions:

- ⇒ halo, skin structure
- ⇒ probe in-medium interactions at extreme isospin (almost pure neutron matter)
- ⇒ in combination with electron scattering (ELISe project @ FAIR):
separate neutron/proton content of nuclear matter (deduce neutron skins)

method: elastic proton scattering ⇒ at low q : high sensitivity to nuclear periphery

I Investigation of the Giant Monopole Resonance:

- ⇒ gives access to nuclear compressibility ⇒ key parameters of the EOS
- ⇒ new collective modes (breathing mode of neutron skin)

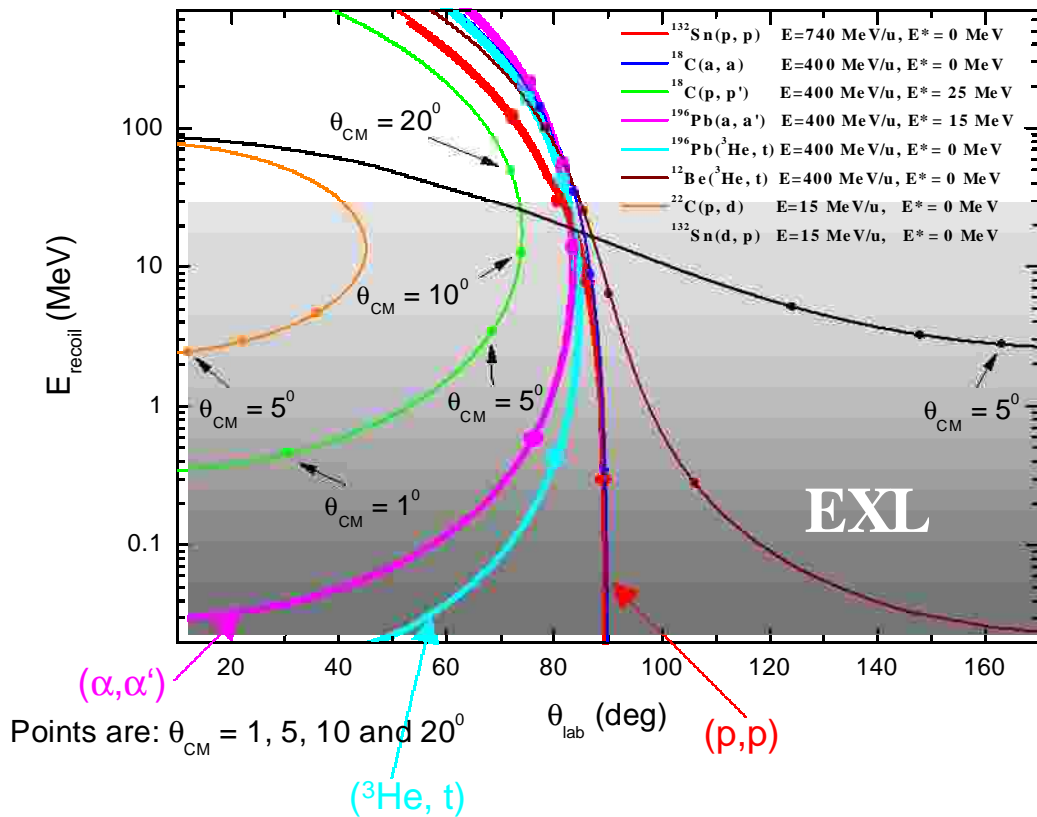
method: inelastic α scattering at low q

● Investigation of Gamow-Teller Transitions:

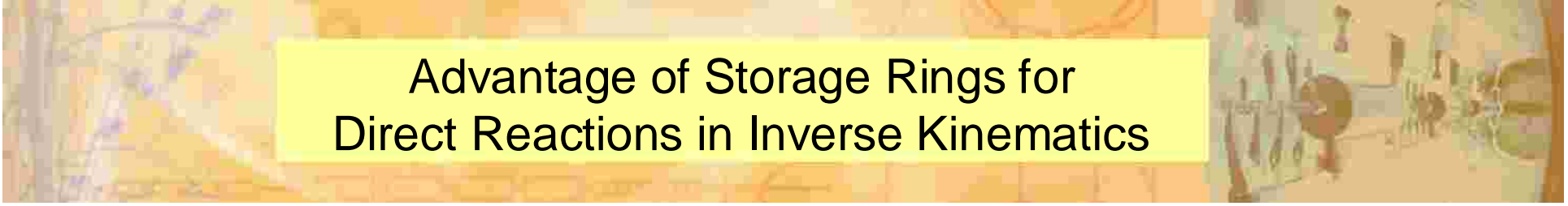
- ⇒ weak interaction rates for $N = Z$ waiting point nuclei in the rp-process
- ⇒ electron capture rates in the presupernova evolution (core collaps)

method: $(^3\text{He}, t)$, $(d, ^2\text{He})$ charge exchange reactions at low q

Kinematical Conditions for Light-Ion Induced Direct Reactions in Inverse Kinematics



- required beam energies:
 $E \approx 200 \dots 740 \text{ MeV/u}$
(except for transfer reactions)
- required targets: ${}^{1,2}\text{H}$, ${}^{3,4}\text{He}$
- most important information in
region of low momentum transfer
⇒ low recoil energies of
recoil particles
⇒ need thin targets for sufficient
angular and energy resolution

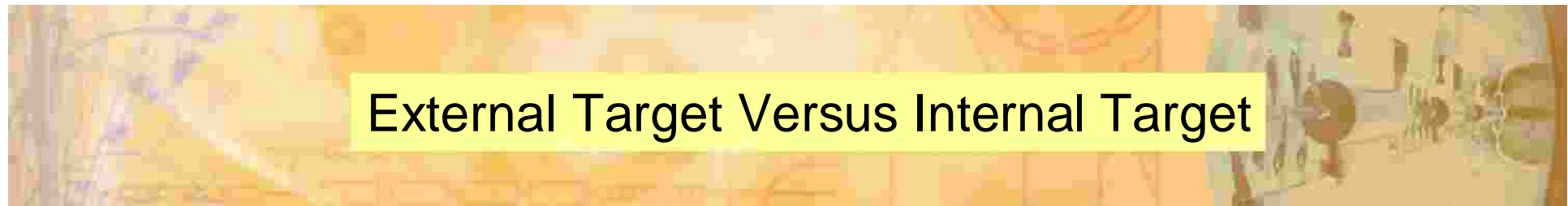


Advantage of Storage Rings for Direct Reactions in Inverse Kinematics

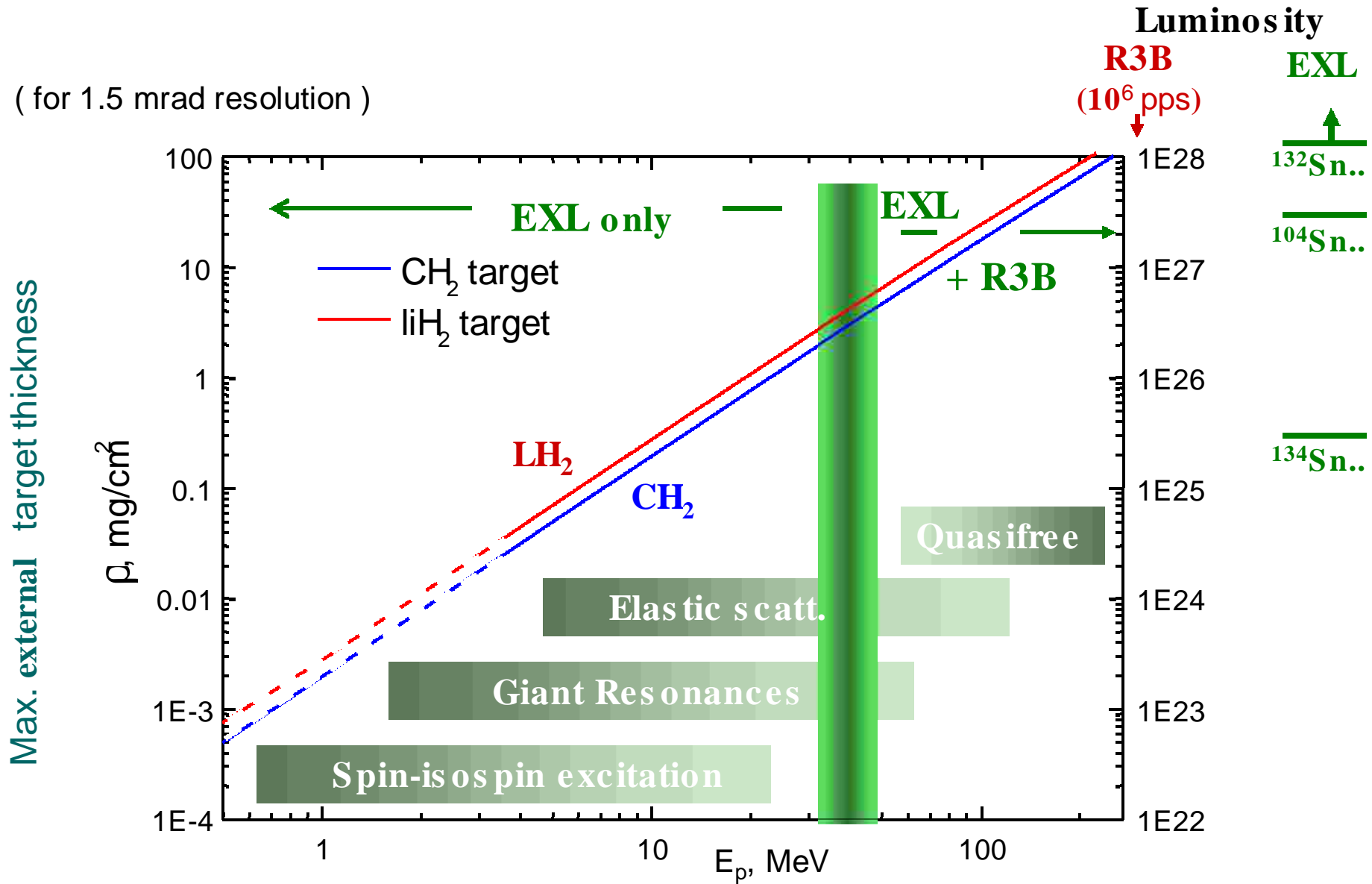
- | low threshold and high resolution due to: beam cooling, thin target (10^{14} - 10^{15} cm $^{-2}$)
- | gain of luminosity due to: continuous beam accumulation and recirculation
- | low background due to: pure, windowless $^{1,2}\text{H}_2$, $^{3,4}\text{He}$, etc. targets
- | experiments with isomeric beams

Experiments at very low momentum transfer can only be done at EXL
(except with active targets, but with substantial lower luminosity)

Only the world-wide unique combination of Super-FRS and NESR
provides high resolution experiments with high luminosity



External Target Versus Internal Target



Application of Internal and External Targets – a Comparison

assumptions:

- external target: $\leq 1 \text{ mg/cm}^2 (\text{CH}_2)_n$ P. Egelhof et al., Phys. Scripta T104 (2003) 151
- internal target: $10^{14}/\text{cm}^2$ hydrogen continuous accumulation and stacking
- charge exchange cross sections:
from T. Stöhlker et al.
(Phys. Rev. A 58 (1998) 2043)

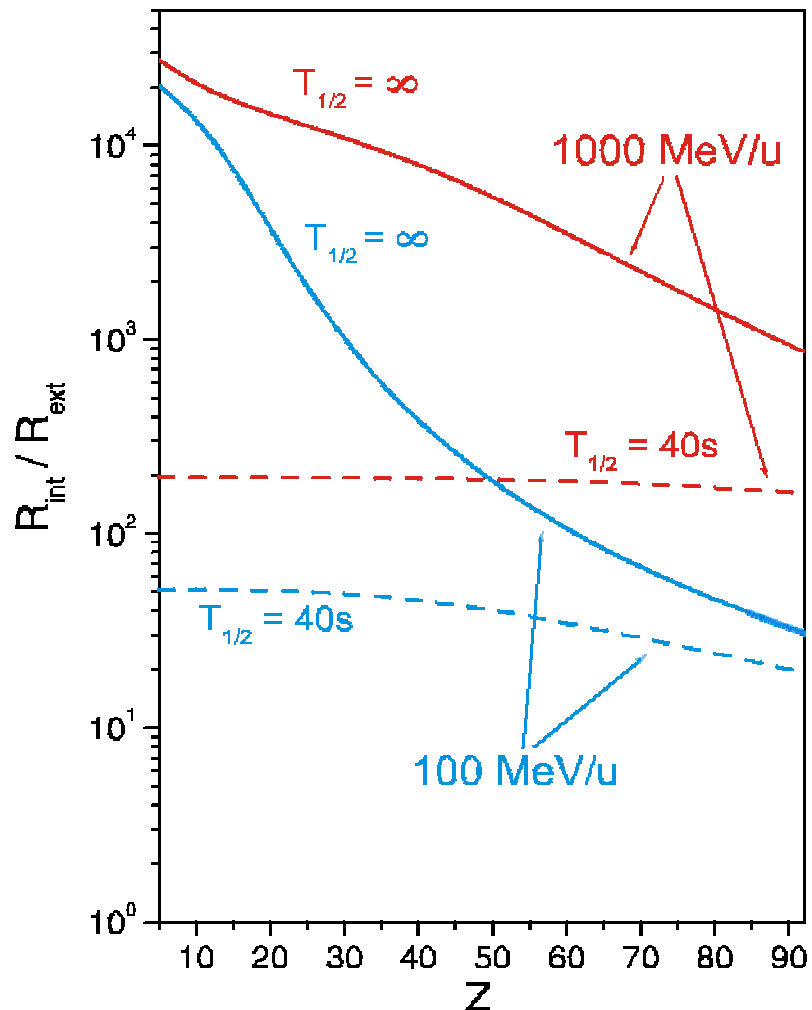
luminosity gain at internal target

depends on:

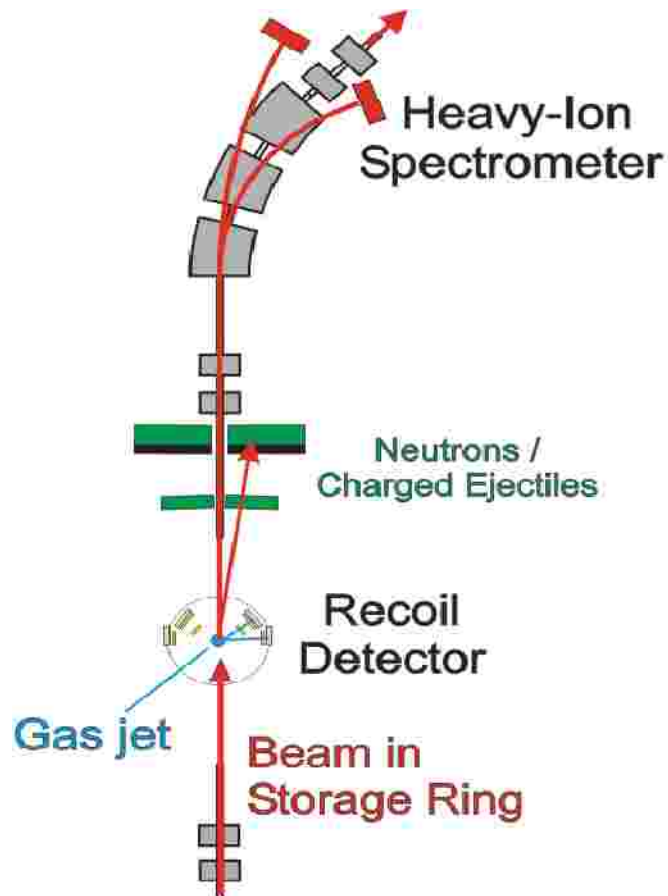
- Ø energy
- Ø atomic number
- Ø nuclear lifetime

limitations:

- Ø low E and high Z: charge exchange
- Ø high E: nuclear lifetime



II. The EXL Detector Setup - Concept and Design Goals



Detection systems for:

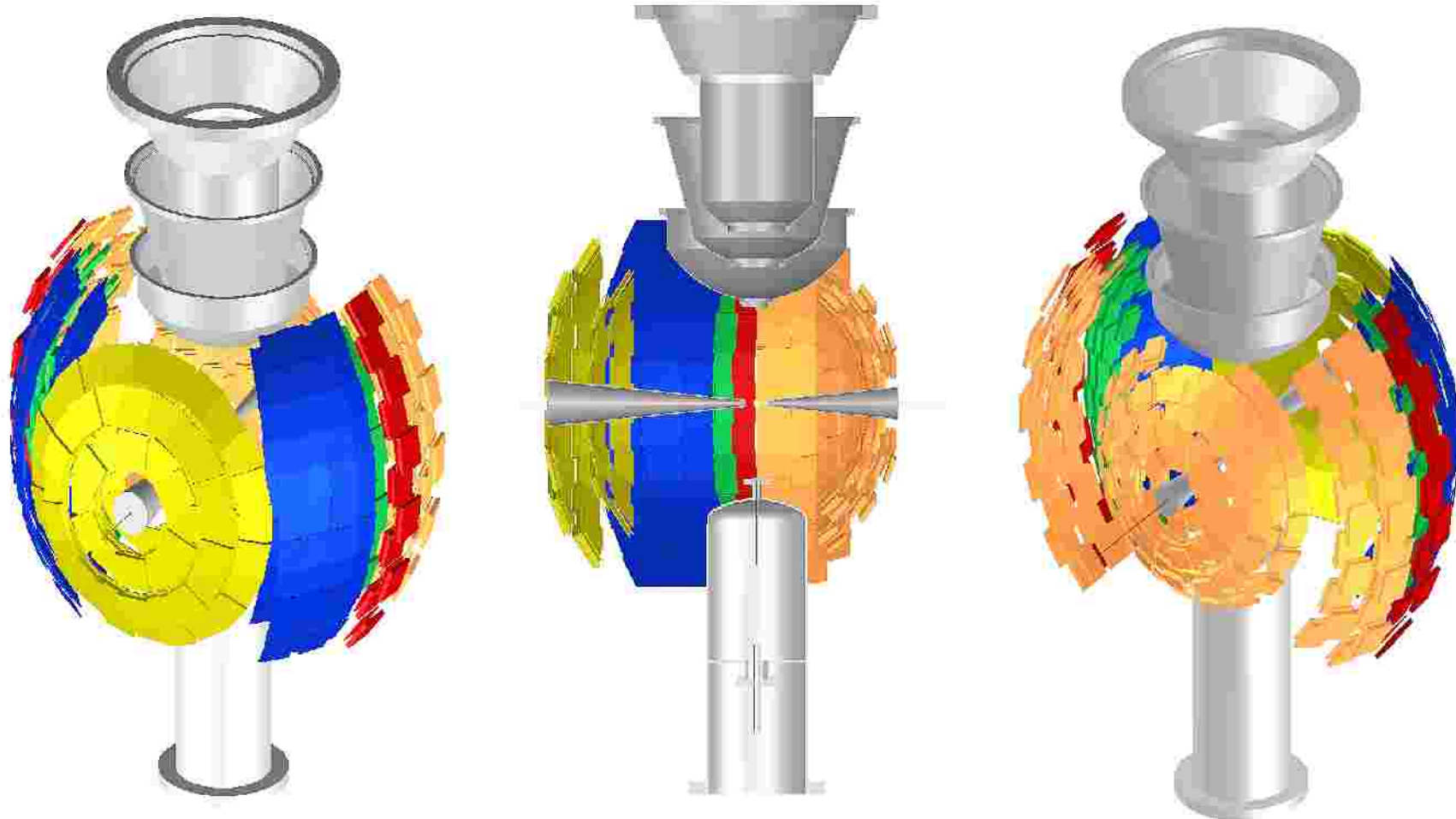
- | Target recoils and gammas ($p, \alpha, n, \gamma \dots$)
- | Forward ejectiles (p, n, γ)
- | Beam-like heavy ions

Design goals

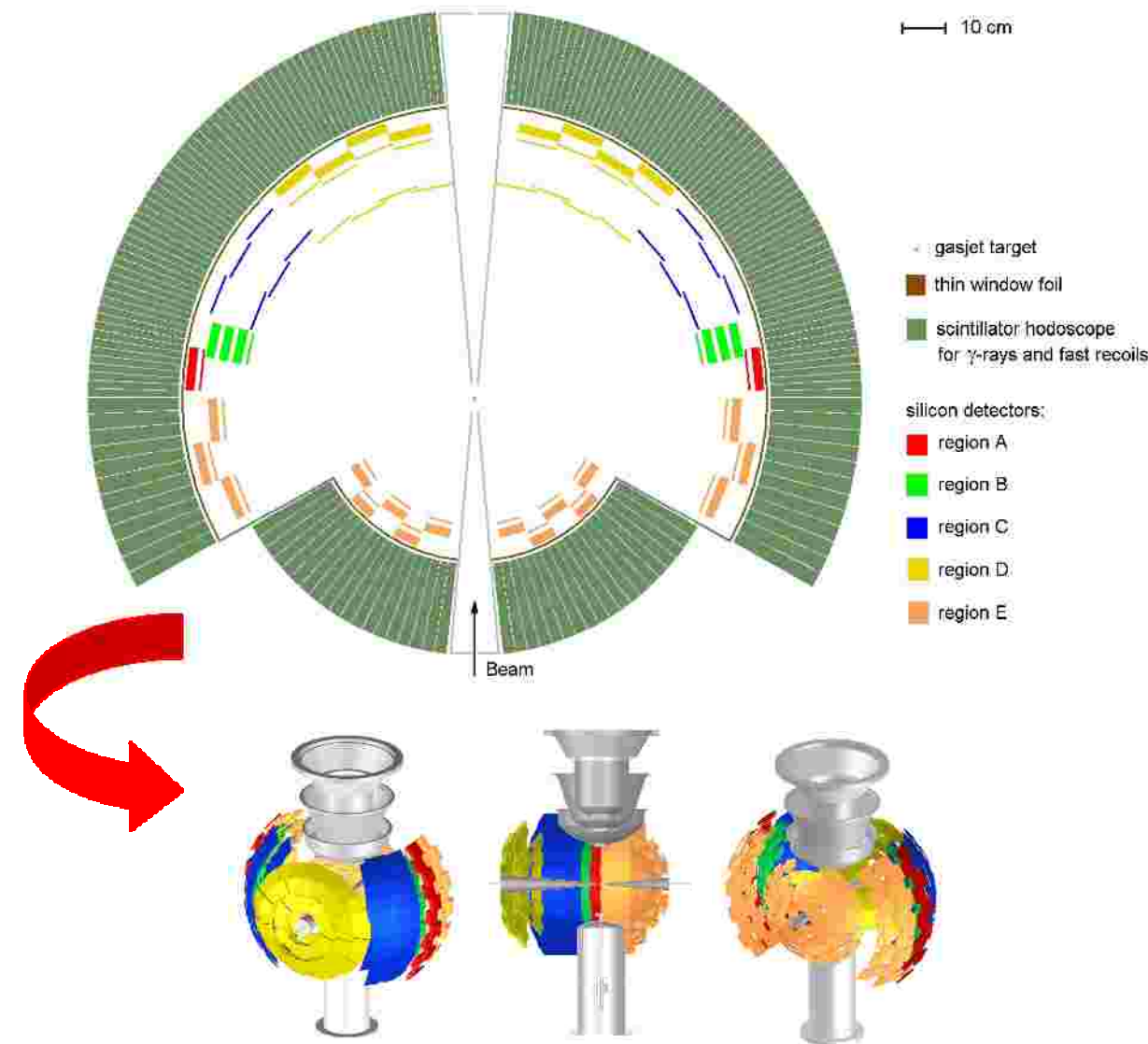
- | Universality: applicable to a wide class of reactions
- | High energy and angular resolution
- | Fully exclusive kinematical measurements
- | High luminosity ($> 10^{28} \text{ cm}^{-2} \text{ s}^{-1}$)
- | Large solid angle acceptance
- | UHV compatibility (in part)



The EXL Recoil Detector



The EXL Recoil and Gamma Array



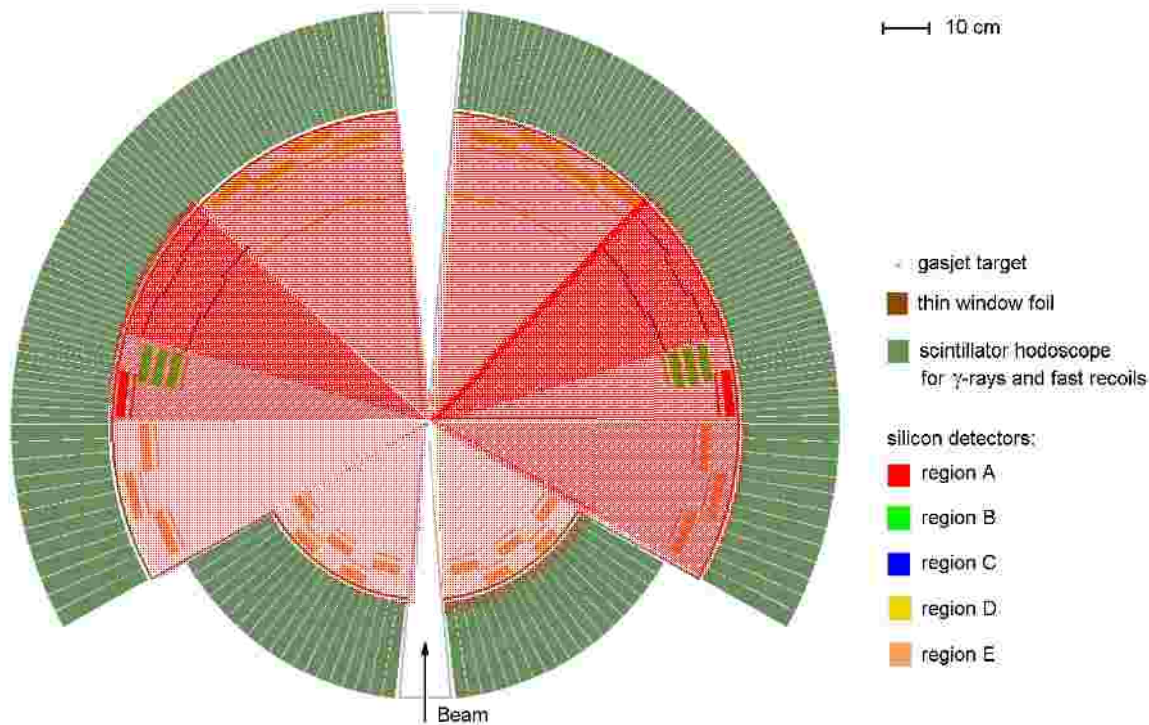
Si DSSD δ DE, x, y
300 μm thick, spatial resolution better than 500 μm in x and y,
? E = 30 keV (FWHM)

Thin Si DSSD δ tracking
<100 μm thick, spatial resolution better than 100 μm in x and y,
? E = 30 keV (FWHM)

Si(Li) δ E
9 mm thick, large area
100 x 100 mm^2 ,
? E = 50 keV (FWHM)

CsI crystals δ E, g
High efficiency, high resolution,
20 cm thick

The EXL Recoil and Gamma Array

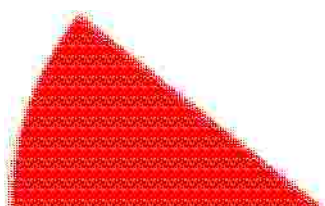


Si DSSD $\delta_{DE, x, y}$
300 μm thick, spatial resolution
better than 500 μm in x and y,
? E = 30 keV (FWHM)

Thin Si DSSD $\delta_{tracking}$
<100 μm thick, spatial resolution
better than 100 μm in x and y,
? E = 30 keV (FWHM)

Si(Li) δ_E
9 mm thick, large area
100 x 100 mm^2 ,
? E = 50 keV (FWHM)

CsI crystals $\delta_{E, g}$
High efficiency, high resolution,
20 cm thick



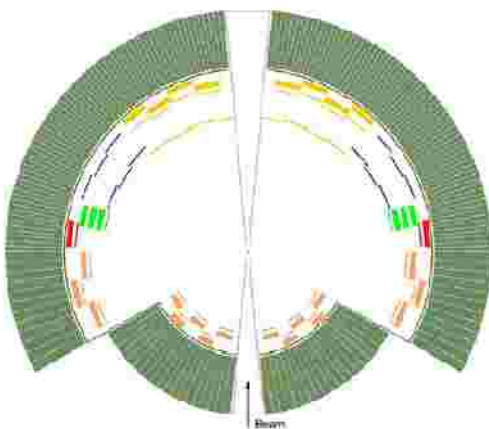
charge exchange reactions

Specifications of the Silicon Detectors for EXL

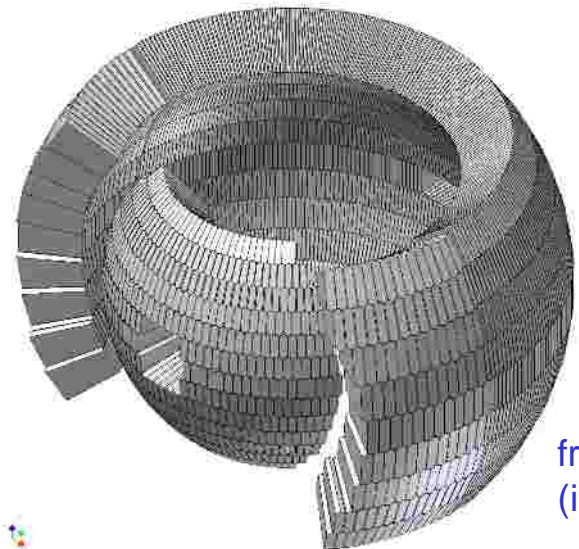
Angular region	T_{lab} [deg]	Detector type	Active area [mm ²]	Thickness [mm]	Distance from target [cm]	Pitch [mm]	Number of detectors	Number of channels
A	89 - 80	DSSD	87 x 87	0.3	59	0.1	20	34800
		Si(Li)	87 x 87	9	60	-	20	180
B	80 - 75	DSSD	50 x 87	0.3	50	0.1	20	27400
		Si(Li)	50 x 87	9	52	-	20	180
		Si(Li)	50 x 87	9	54	-	20	180
		Si(Li)	50 x 87	9	56	-	20	180
C	75 - 45	DSSD	87 x 87	0.1	50	0.1	60	104400
		DSSD	87 x 87	0.3	60	0.1	60	34800
D	45 - 10	DSSD	87 x 87	0.1	49	0.1	60	104400
		DSSD	87 x 87	0.3	59	0.1	80	139200
		Si(Li)	87 x 87	9	60	-	80	720
E	170 - 120	DSSD	50 x 50	0.3	25	0.5	60	6000
		Si(Li)	50 x 50	5	26	-	60	240
E'	120 - 91	DSSD	87 x 87	0.3	59	0.1	60	104400
		Si(Li)	87 x 87	5	60	-	60	540
Total		DSSD Si(Li)					420 280	555400 2220

Specifications of the Silicon Detectors for EXL

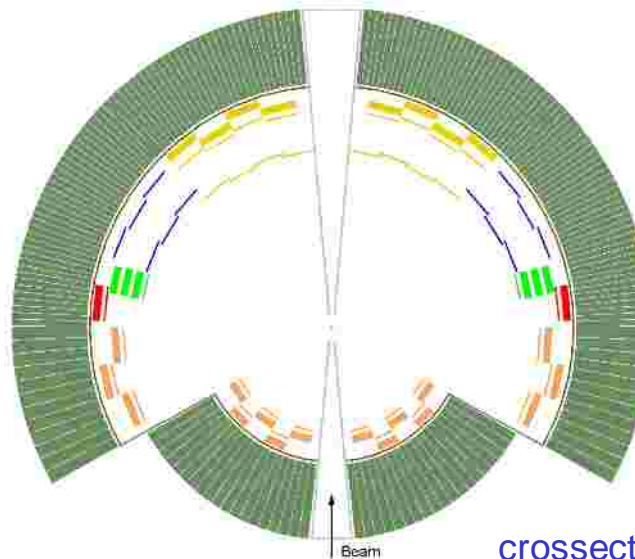
- low threshold = 40 keV
(\Rightarrow constraints on thickness of entrance windows)
- high energy resolution = 20 keV
- pitch size = 0.5 mm
- active area $65 \times 65 \text{ mm}^2$
- large dynamic range: 100 keV to 50 MeV
- readout of energy, time, PSA??
- self triggering
- moderate count rates
- UHV (HV) compatibility (partly)



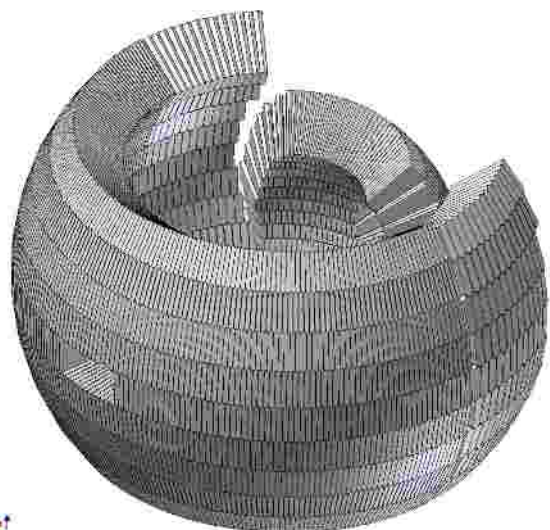
Design Study of the Gamma-Calorimeter



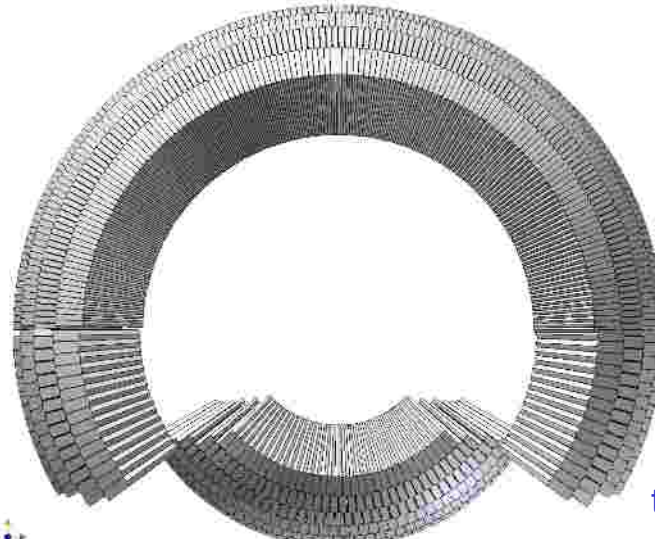
front view
(isometric)



crossection of basic concept



rear view
(isometric)

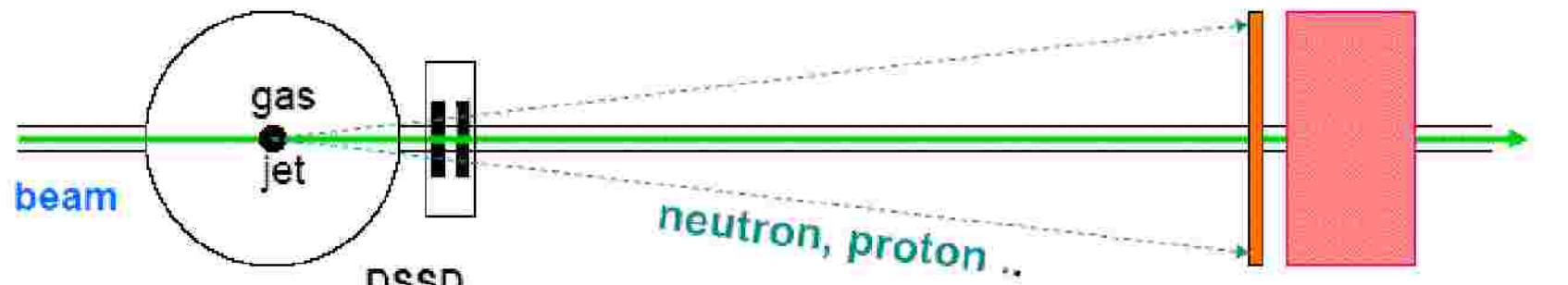


top view of 3D model

The EXL Forward Ejectile Detector

Kinematically complete measurements:

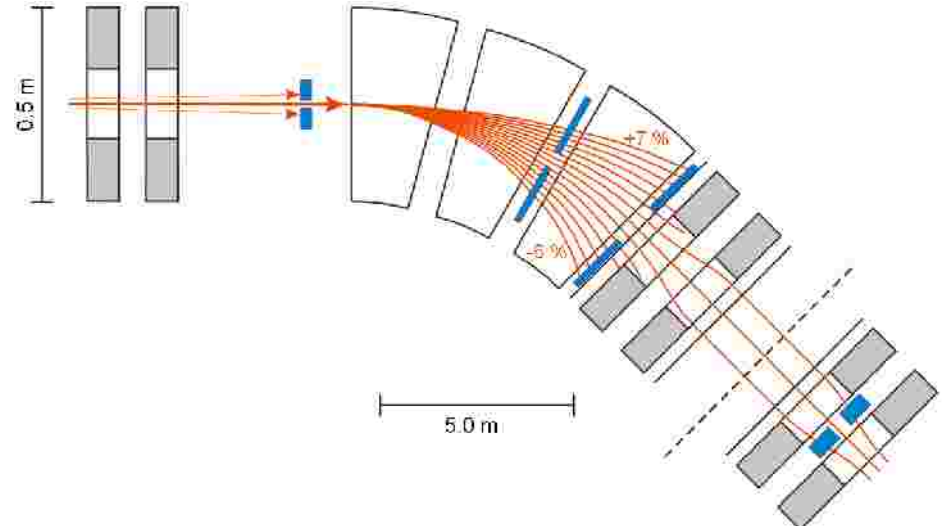
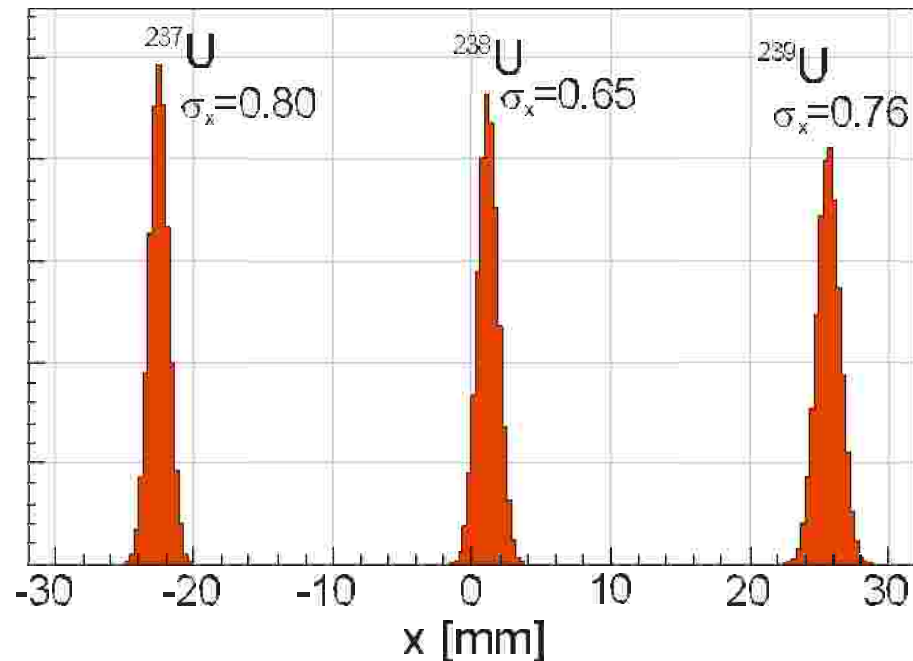
- detection of forward light particles emitted from the projectile (momenta measured)
- excitation energy of projectile residue, momentum (angular) correlations



(Phase I)

(Phase II)

- High-resolution TOF and position measurements
- Full solid angle (forward focus)
- Calorimeter: scintillator + iron converter (similar to LAND)



- ✓ Ion-optical mode for NESR as fragment spectrometer
- ✓ 3 heavy-ion detector stations:
 - in front of first dipole magnet for 'reaction tagging' (main mode)
 - inserted into dipole section for 'tracking' of fragments
 - inserted into quadrupole section for 'imaging' properties of magnetic Spectrometer (limited acceptance)

Predicted Luminosities

Target: 10^{14} H atoms cm⁻²; beam losses included

740 A.MeV **100 A.MeV**

Nucleus	production rate at S-FRS target [1/s]	Life time including losses in NESR [s]	Luminosity [cm ⁻² s ⁻¹]	Luminosity [cm ⁻² s ⁻¹]	Luminosity [cm ⁻² s ⁻¹] (preliminary)
¹¹ Be	2×10^9	36	$> 10^{28}$	$> 10^{28}$	8×10^{26}
⁴⁶ Ar	6×10^8	20	$> 10^{28}$	$> 10^{28}$	9×10^{23}
⁵² Ca	4×10^5	12	2×10^{26}	4×10^{25}	4×10^{10}
⁵⁵ Ni	8×10^7	0.5	6×10^{26}	5×10^{25}	5×10^{26}
⁵⁶ Ni	1×10^9	3800	$> 10^{28}$	$> 10^{28}$	2×10^{23}
⁷² Ni	9×10^6	4.1	2×10^{27}	3×10^{26}	3×10^{25}
¹⁰⁴ Sn	1×10^6	51	3×10^{27}	6×10^{26}	1×10^{27}
¹³² Sn	1×10^8	93	$> 10^{28}$	$> 10^{28}$	4×10^{20}
¹³⁴ Sn	8×10^5	2.7	3×10^{25}	5×10^{24}	5×10^{25}
¹⁸⁷ Pb	1×10^7	34	$> 10^{28}$	3×10^{27}	

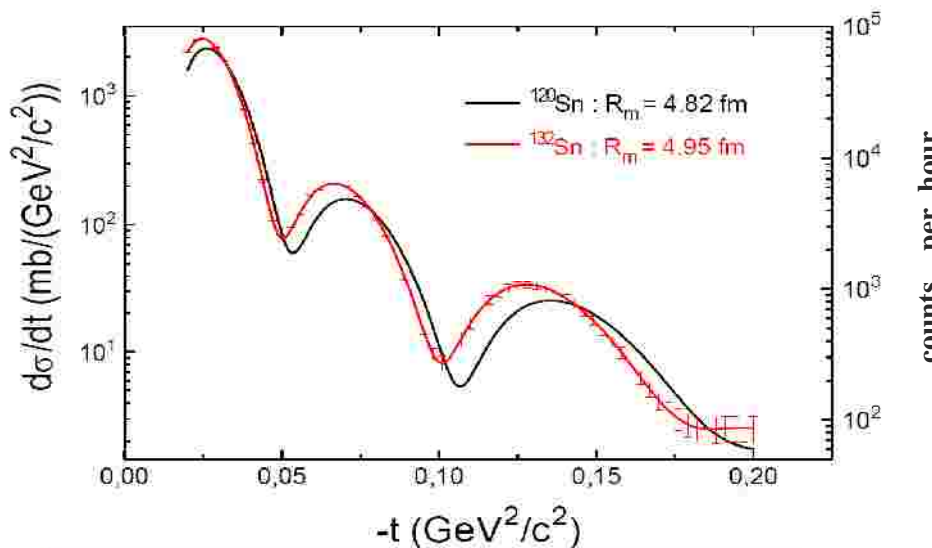
Options to be explored: Deceleration, Multi-charge state operation (*increase luminosity*) ?



Expected Performance

Elastic proton scattering ^{132}Sn (Matter Distribution)

Skin and halos in heavy neutron-rich nuclei

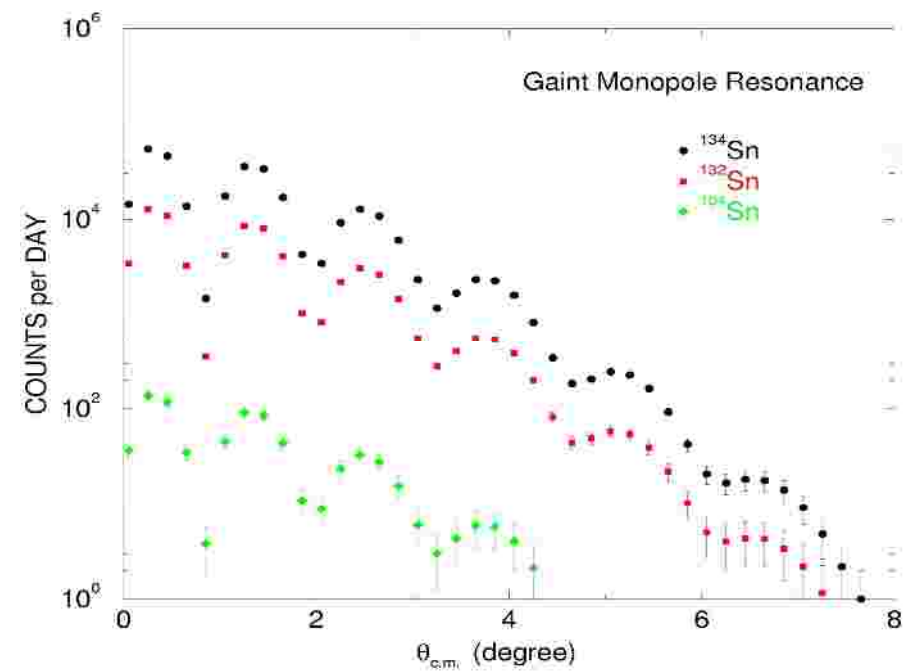


High sensitivity of the method
(simulation of experimental conditions
as expected at the NESR with a
luminosity of $10^{28} \text{ cm}^{-2} \text{ s}^{-1}$)

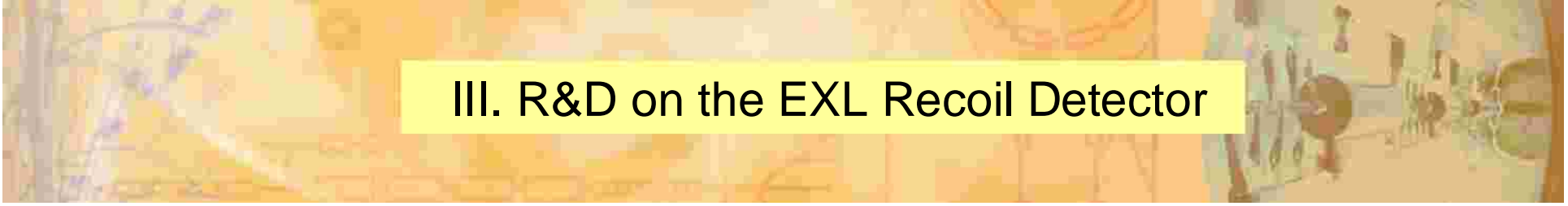
at present ESR: needs 500 days !!!

Inelastic alpha scattering on Sn isotopes (Giant Monopole Resonance)

Collective modes in asymmetric
nuclei, nuclear matter compressibility



at present ESR: needs 10000 days !!!



III. R&D on the EXL Recoil Detector

Aim: determine spectroscopic properties: ΔE , $\Delta(dE)$, efficiency, PSD
resolution of total energy reconstruction
UHV capability

Detectors: 1st series of DSSDs from PTI St. Petersburg
(8 sensors delivered April 2008/ September 2009)
2nd series of DSSD's with larger size (65 x 65 mm²)
(5 sensors delivered January 2010)

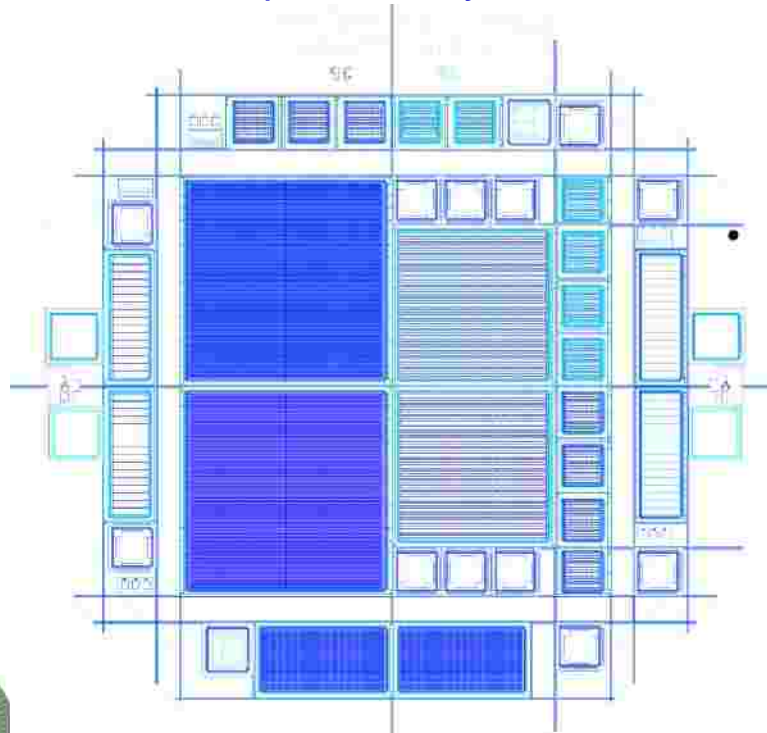
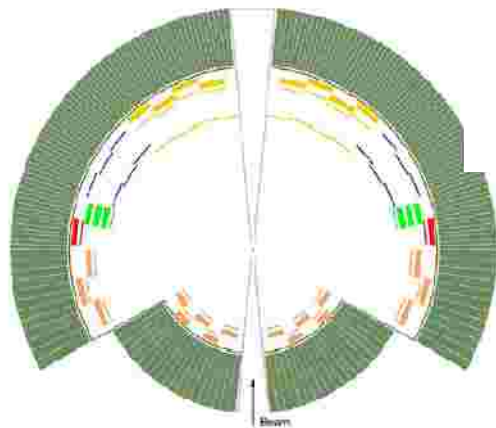
Tests:

2008/2009: GSI:	a sources
2008: Edinburgh:	a sources
April 2009: KVI Groningen:	protons of 50 MeV
July 2009: TU München:	a particles $E < 30$ MeV
September 2009: GSI:	protons of 100 and 150 MeV
April 2010: KVI Groningen:	protons of 135 MeV
January 2011: TU Tübingen:	protons of 1.5 MeV down to 70 keV

Status and Perspectives of R&D

Si - Detectors: DSSD`s

sensors provided by PTI St. Petersburg (V. Eremin et al.)



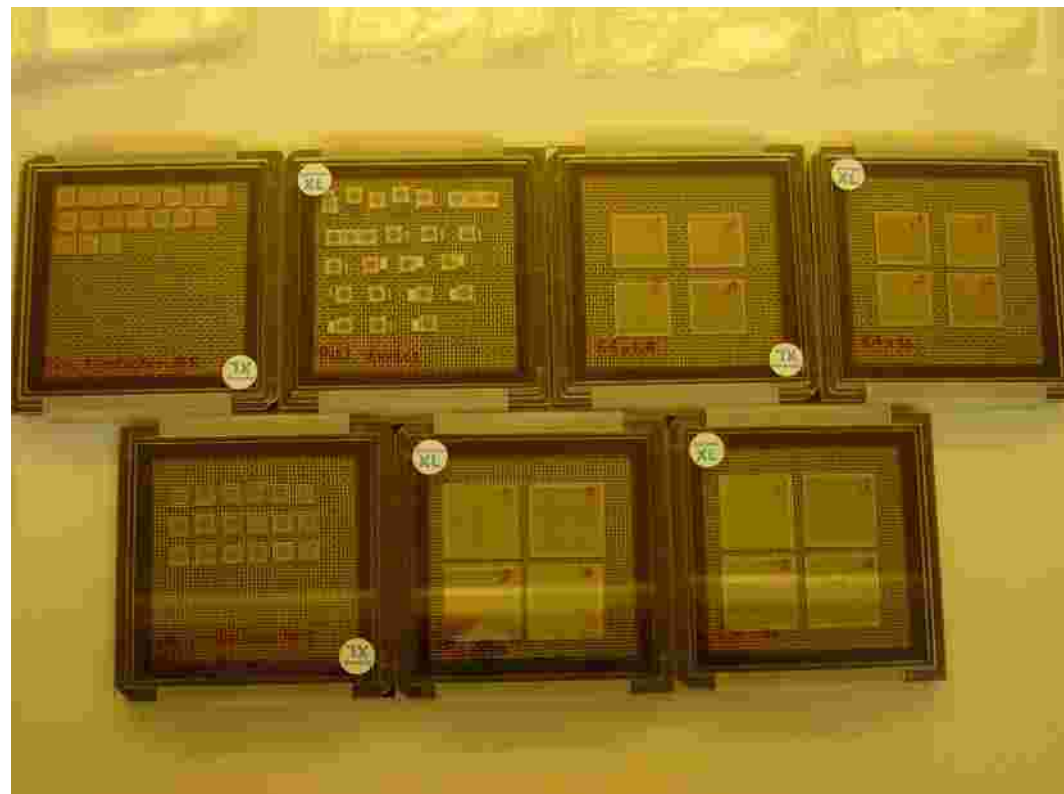
⇒ various test structures for R&D:

- a) $21 \times 21 \text{ mm}^2$, strip pitch $300 \mu\text{m}$ on both sides
- b) $27 \times 27 \text{ mm}^2$, strip pitch $100 \mu\text{m}$ on both sides
- c) $27 \times 27 \text{ mm}^2$, strip pitch $100 \mu\text{m}$, and 2.5 mm on the other side
- d) $21 \times 21 \text{ mm}^2$, strip pitch $300 \mu\text{m}$, and 1.25 mm on the other side
- e) many smaller-size test structures



Production – PTI St. Petersburg (Russia) Si wafer (300nm thick, 4")

Available DSSDs

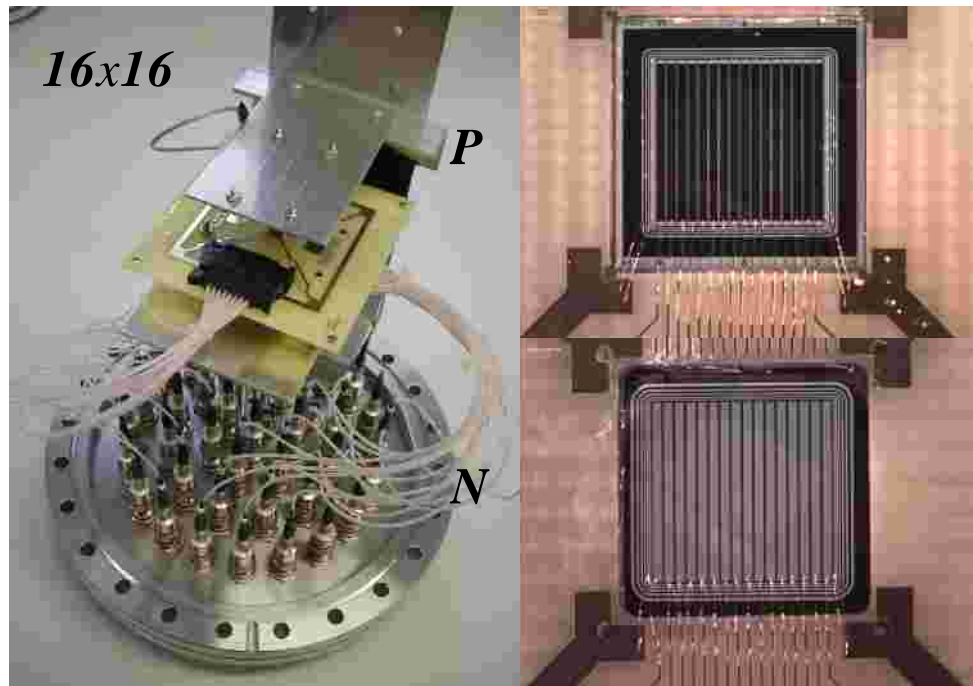


pitch	P⁺	N⁺	No
300µm	16	x 16 (FP):	20
300µm	16	x 16 (P ⁺):	20
300µm	64	x 16:	4
300µm	64	x 64:	4
100µm	256	x 16:	4
100µm	256	x 256:	4
		PIN:	30



Detector Construction at GSI

- Construction of prototype DSSDs at GSI: **16x16 (4)**, **64x64 (4) + 64x16 (4)**
- Both types use FR-4 PCB with epoxy-glued DSSD chips
- Wedge bonded

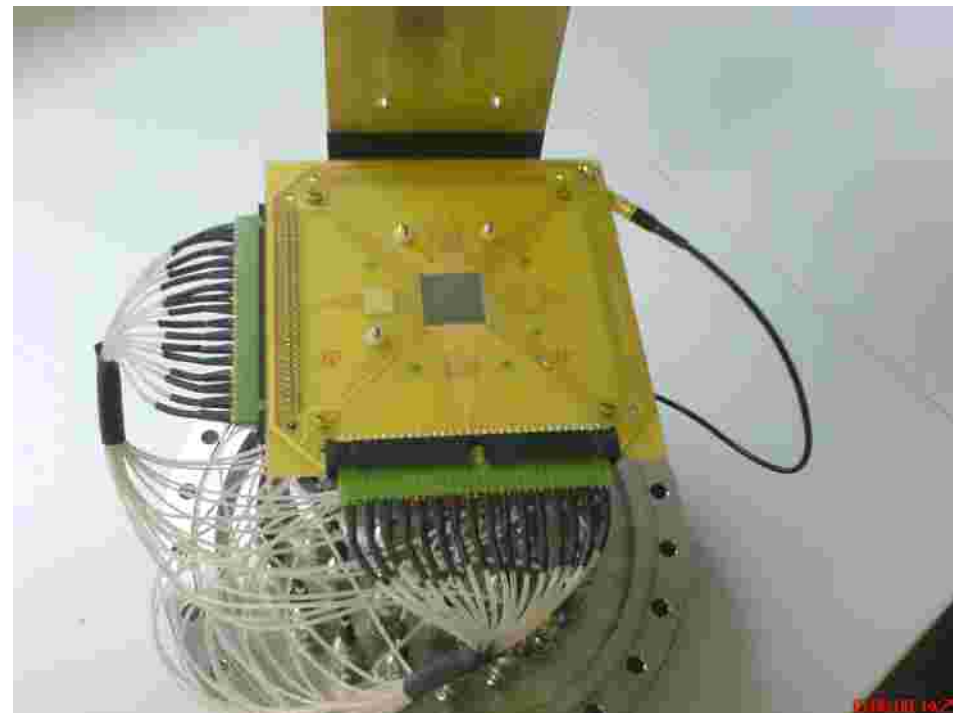
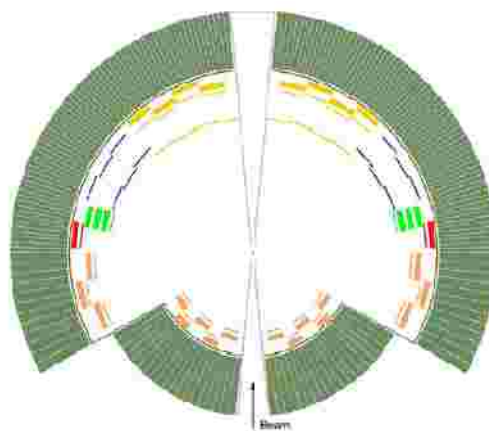


Status and Perspectives of R&D

Si - Detectors: DSSD`s

sensors provided by PTI St. Petersburg (V. Eremin et al.)

setup of working detectors (PCB-board, bonding, readout) at GSI
⇒ 9 detectors: 16X16, 64X16, 64X64 strips, d=300 µm



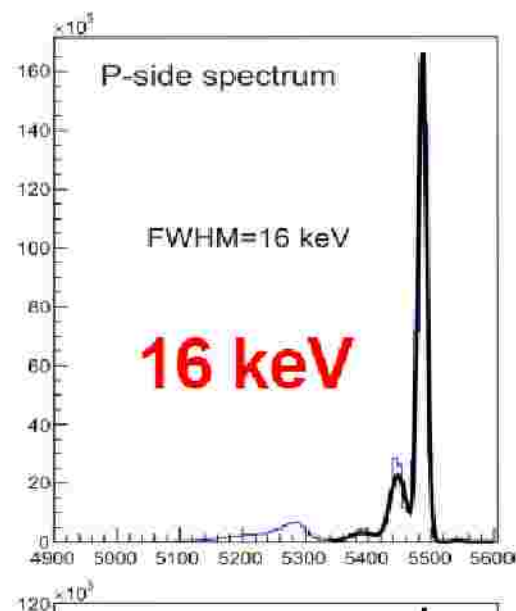
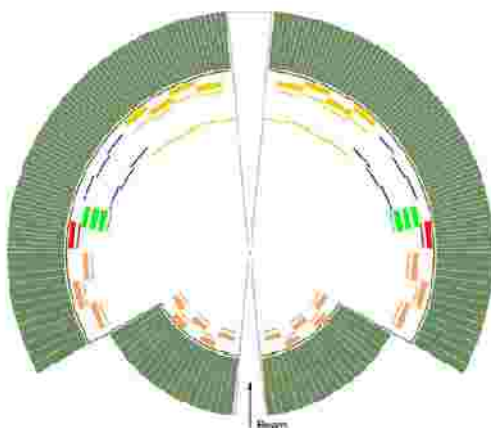
Status and Perspectives of R&D

Si - Detectors: DSSD`s

sensors provided by PTI St. Petersburg (V. Eremin et al.)

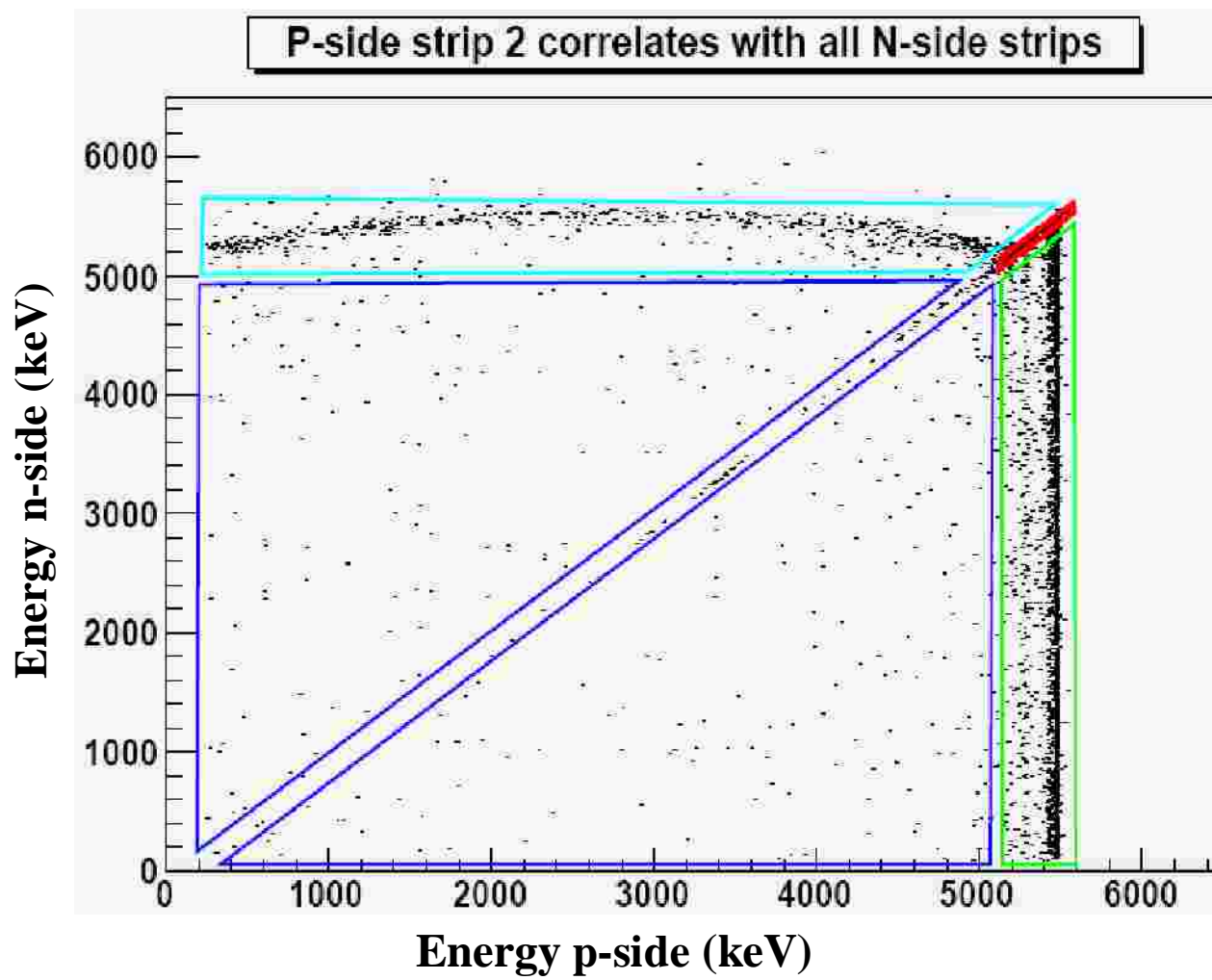
setup of working detectors (PCB-board, bonding, readout) at GSI
⇒ 9 detectors: 16X16, 64X16, 64X64 strips, d=300 µm

detector tests with a-source performed at GSI and Edinburgh
⇒ up to 128 channels read out, up to 99% working strips, ?E=16keV



front-rear correlation analysis
⇒ energy resolution and efficiency for p-side and n-side injection
⇒ results to be used as input for design of next generation detectors

Front-Rear Side Correlation Analysis



Event type

P - N

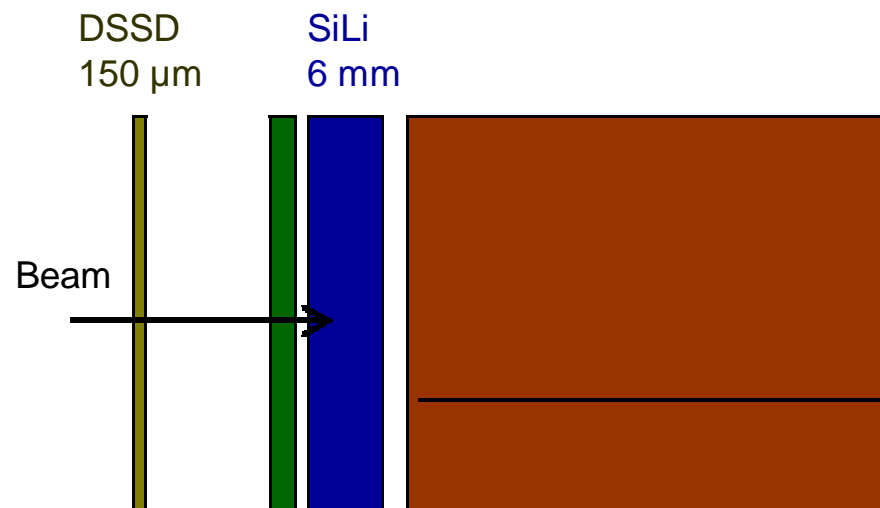
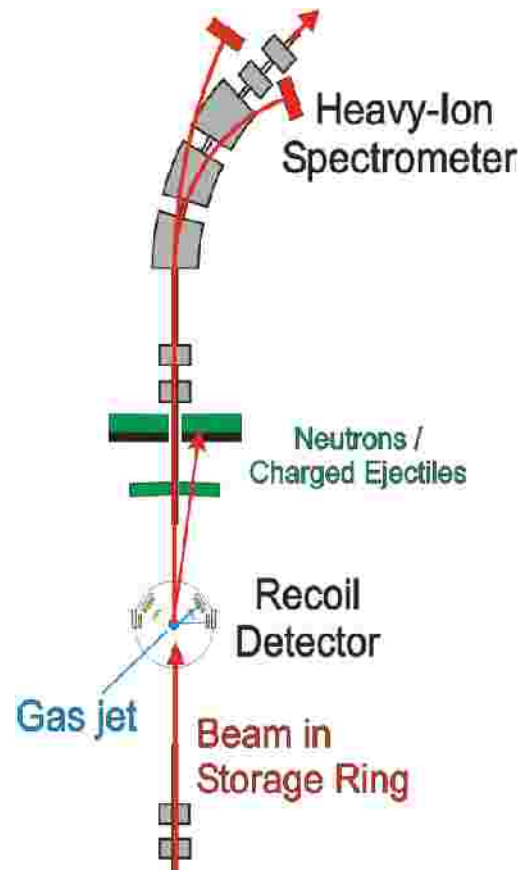
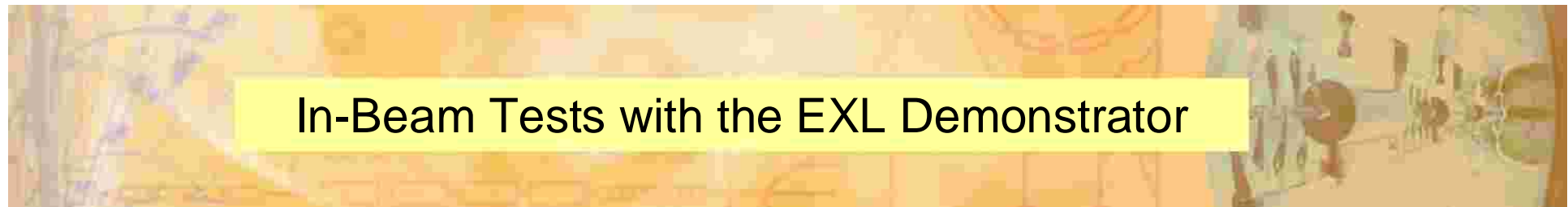
Strip – Strip **76.8 %**

Strip – Interstrip **18.2%**

Interstrip – Strip **4.1%**

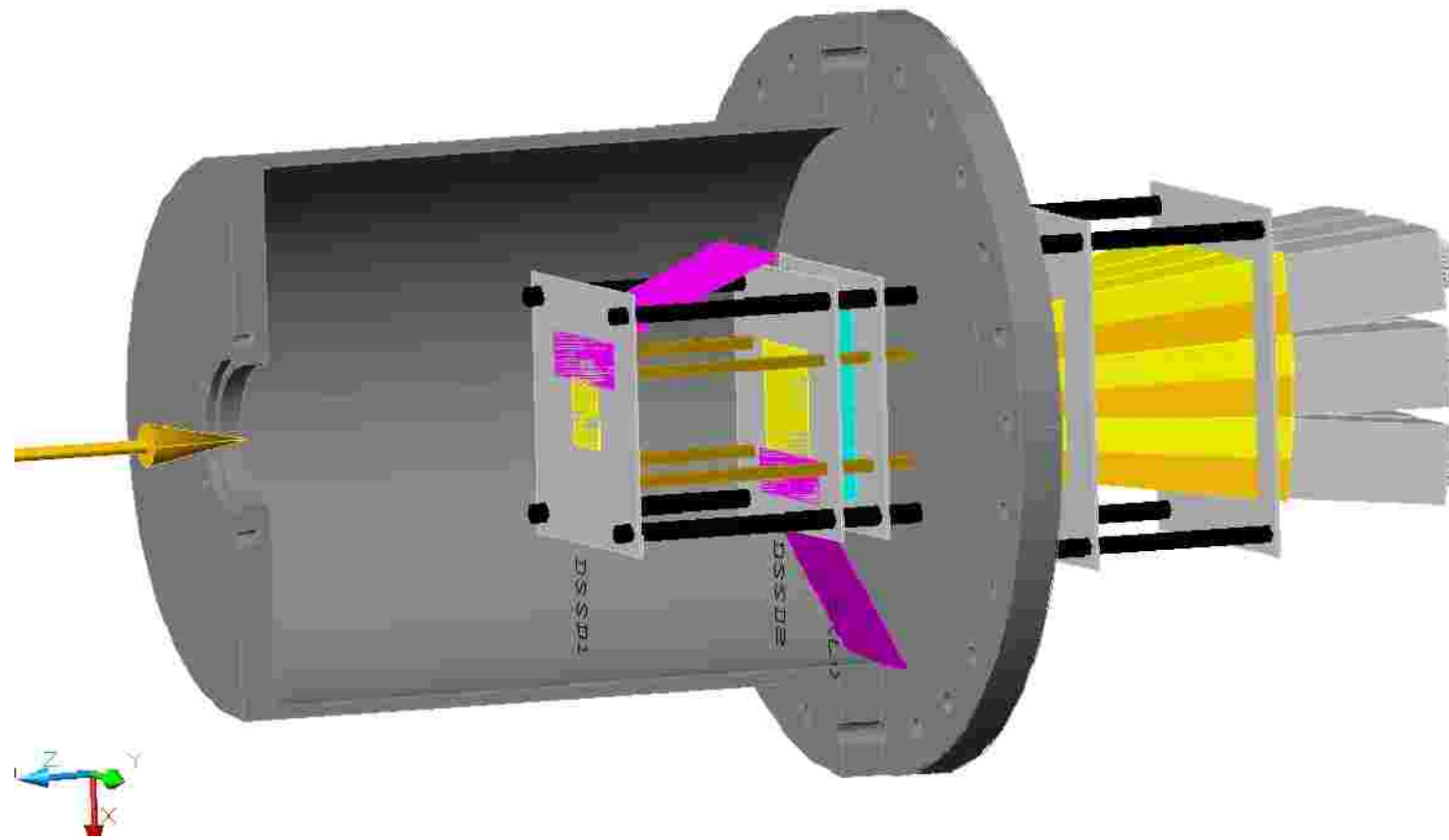
Interstrip – Interstrip **0.9%**

Probabilities
correspond to
pitch structure !

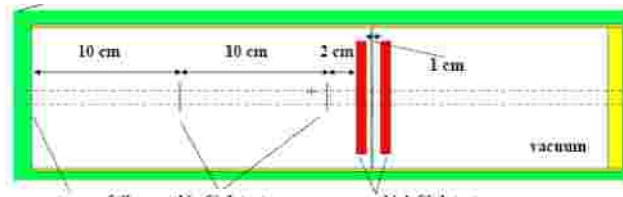


First DSSD – $3 \times 3 \text{ cm}^2$, 64 x 64 strips, pitch 300 μm
Second DSSD – $3 \times 3 \text{ cm}^2$, 64 x 64 strips, pitch 300 μm
SiLi – $9 \times 5 \text{ cm}^2$, 4 x 2 pads
CsI – 3 x 3 crystals with the individual readout

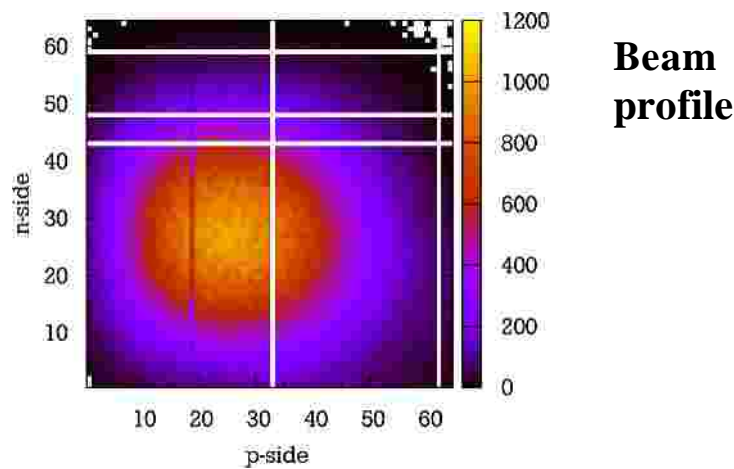
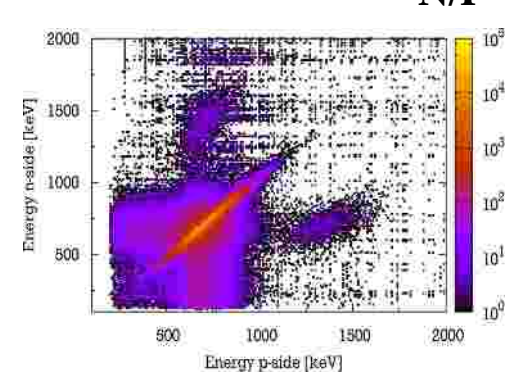
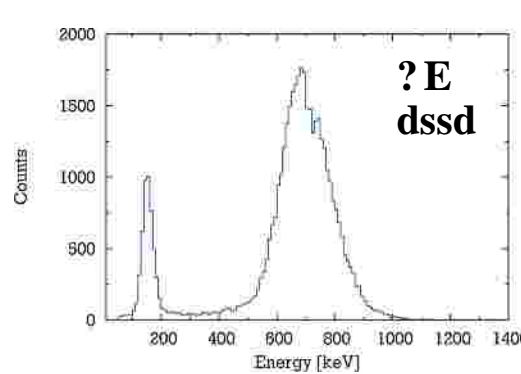
The EXL Demonstrator



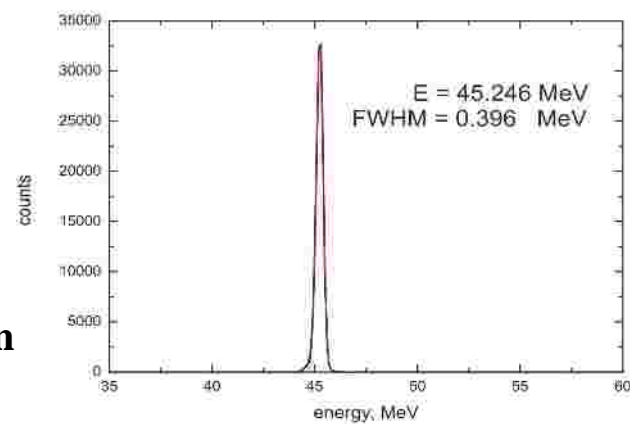
In-Beam Tests at KVI Groningen with 50 MeV Protons



set-up



Total energy reconstruction





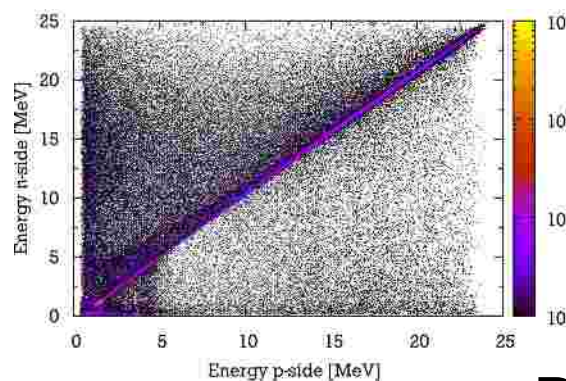
Pulse-Shape Discrimination with DSSD's

test with p, d, ${}^4\text{He}$ from
 ${}^{12}\text{C} + {}^{12}\text{C}$ @ 70 MeV
TU Munich

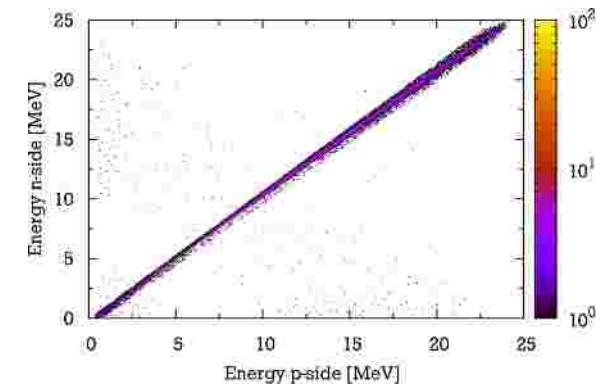


M. von Schmid et al.
NIM A629 (2011)197

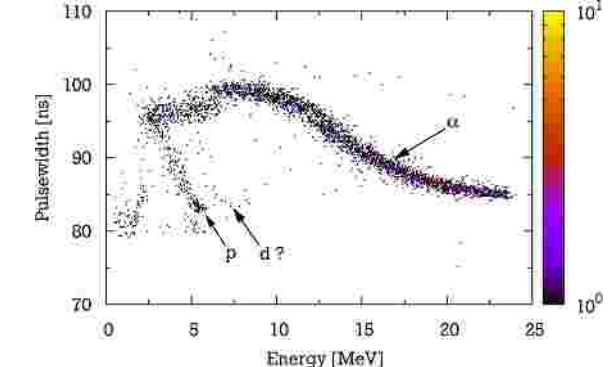
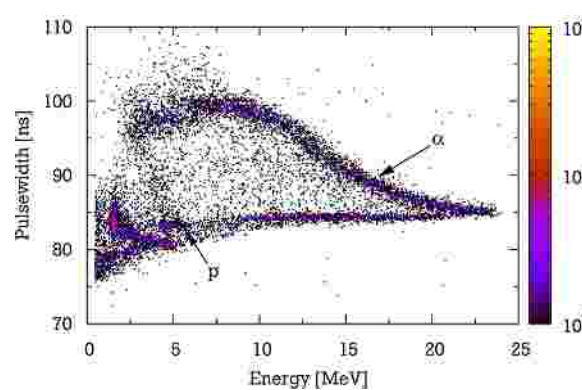
Strip & Interstrip



Strip (stopped a's)



P/N



PSD

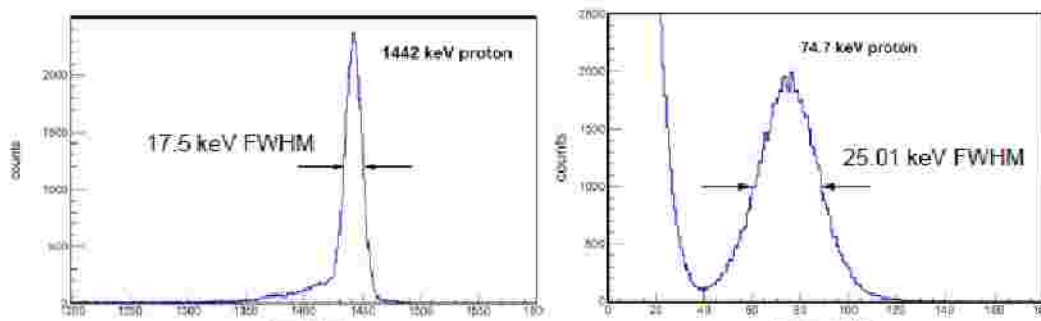
DSSD strip-strip events show PSD comparable with single PIN diodes

Response to very low energy recoil particles

experiment performed at the 1.5 MV
Van de Graf accelerator at the Univ. Tübingen

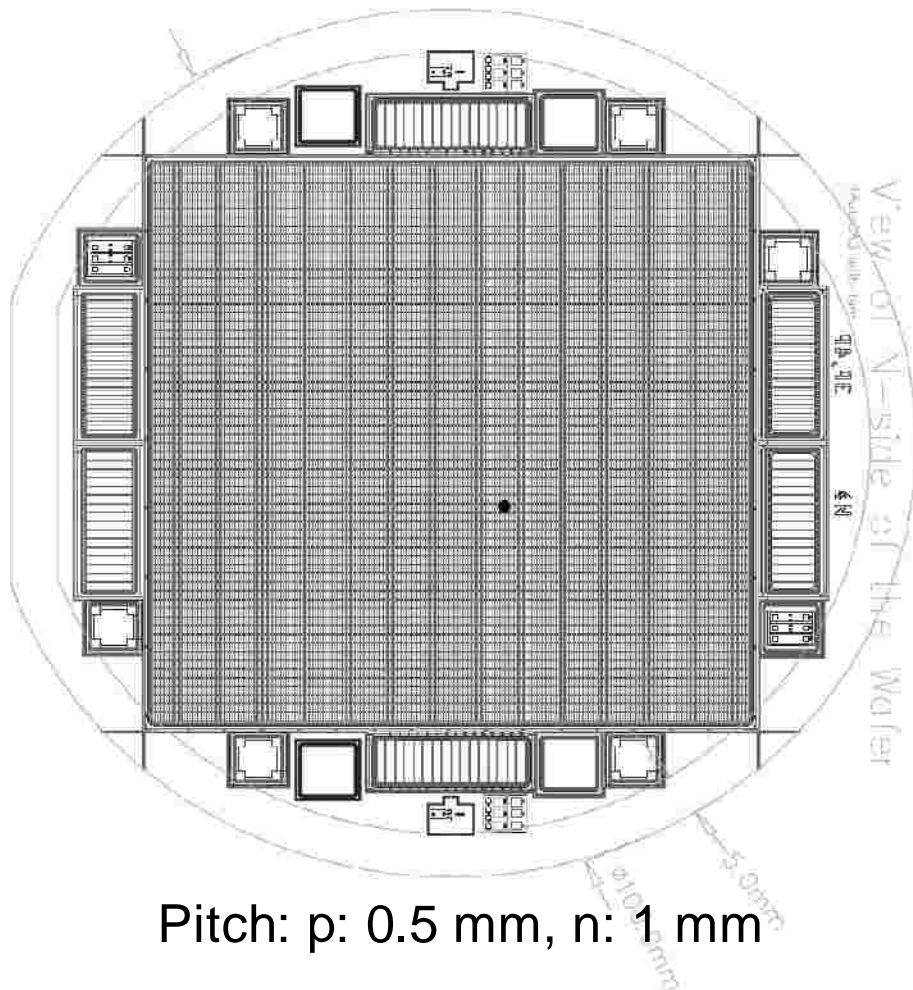


- 1503keV protons scattered from C target ($37\mu\text{g}/\text{cm}^2$)
- Spectrum shows strip #11 (p side)
- 818keV H_2 scattered from C target ($37\mu\text{g}/\text{cm}^2$),
~ $3.5\mu\text{m}$ Mylar degrader in front of DSSD
- Spectrum shows strip #11 (p side)



Pespectives: 2nd Series of DSSD's from PTI St. Petersburg: 64 X 64 mm²

65 x 65 mm²



Pitch: p: 0.5 mm, n: 1 mm

Specification:

Single-crystal silicon: 7 - 20 kOhm×cm

Diode structure: p+ (s trips) – i - n+ (s trips), orthogonal, n+ - s trip insulation, p+ implant

Diode area: 65 x 65 mm²

Diode topology: Strips on p+ side, 128
Strips on n+ side, 64

Diode thickness: 300 µm

Operational reverse voltage limit: > 100 V

Impact from GSI tests:

Improved p-side layout:

- P-side implantation depth reduced
- Smaller contact tips at p-side
- Inters trip gap reduced to 10 µm

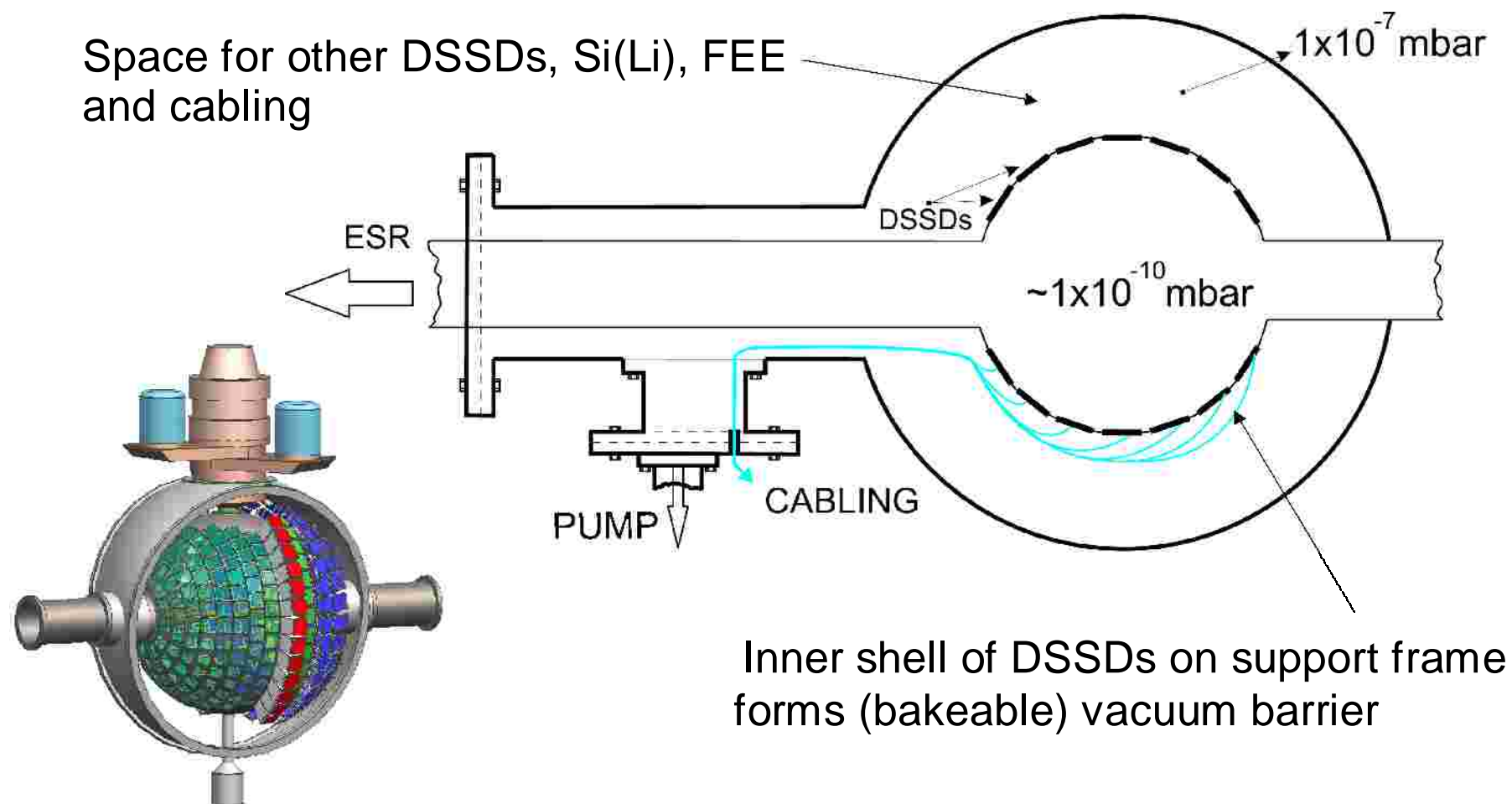
2nd Series of DSSD`s from PTI St. Petersburg: 64 X 64 mm²



UHV Capability of the EXL Silicon Ball: Concept: using DSSD's as high vacuum barrier

- Differential pumping proposed to separate NESR vacuum instrumentation (cabling, FEE, other detectors)

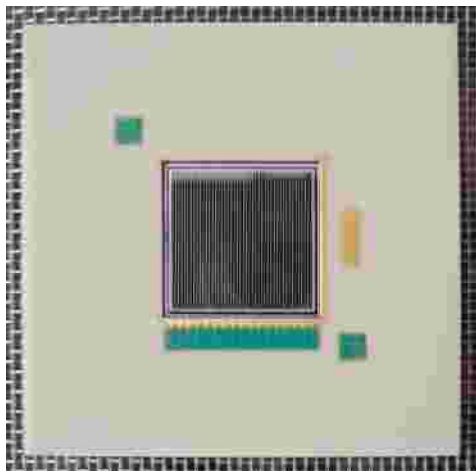
Space for other DSSDs, Si(Li), FEE
and cabling



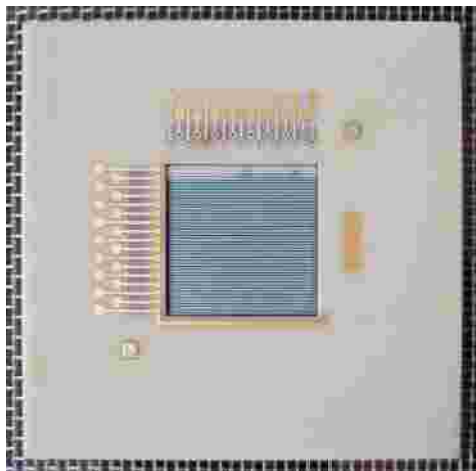
Inner shell of DSSDs on support frame
forms (bakeable) vacuum barrier

UHV-Barrier DSSD Prototype Design

P-side: in UHV



N-side



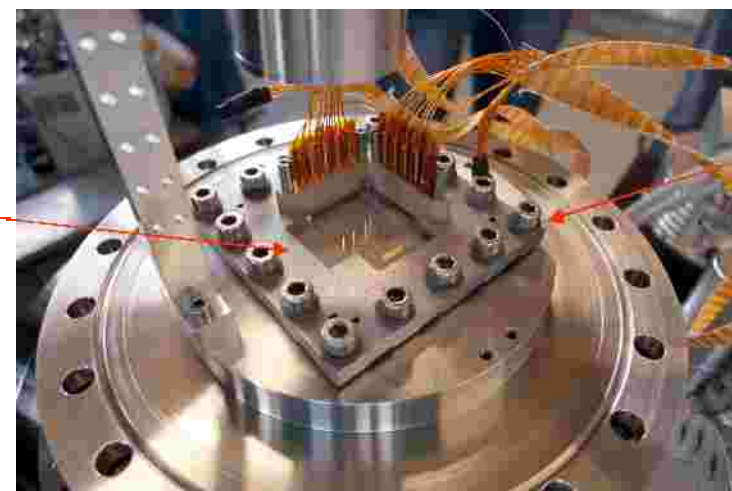
LUST
HYBRID-TECHNIK

21 x 21 mm²
DSSD with
64x64(16) strips
mounted into
AlN PCB of
60 x 60 mm²

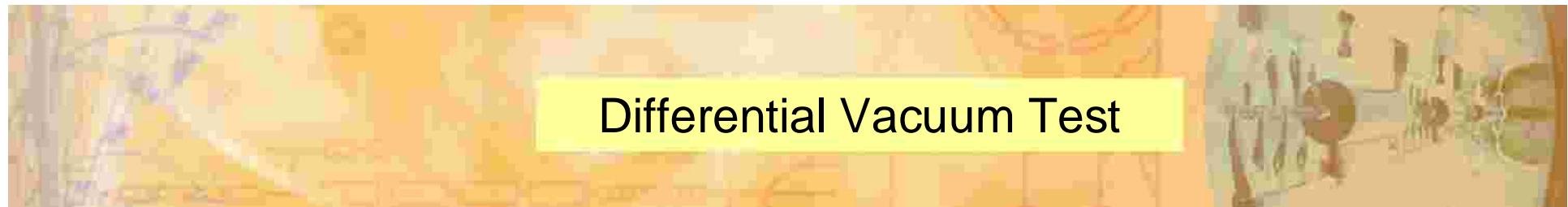
**P-side towards
UHV**

**N-side and
spring-pin
connectors at
auxiliary
vacuum**

IDI
INTERCONNECT TECHNOLOGIES INC.

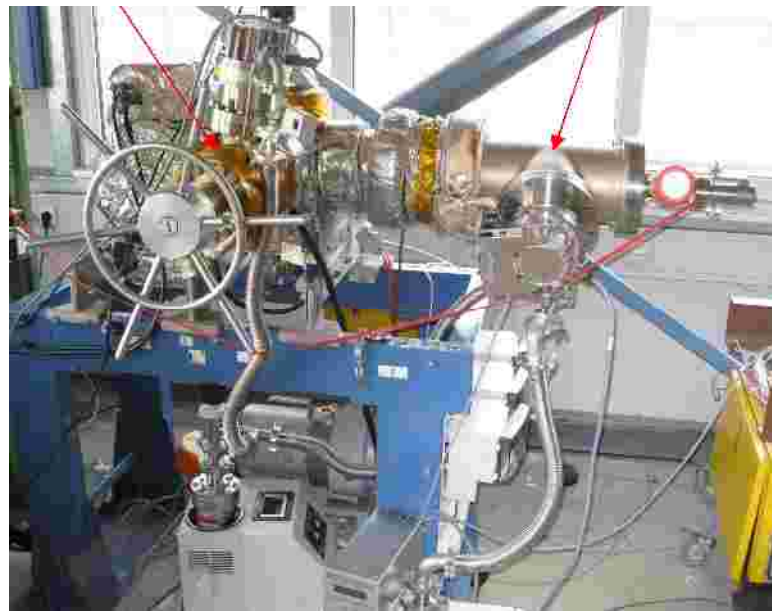


Cup springs



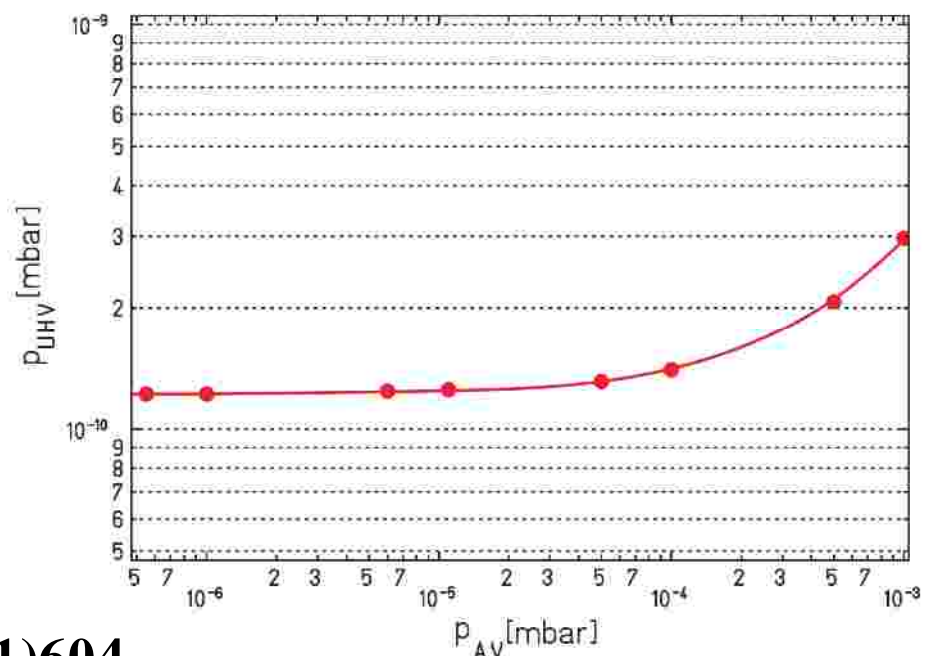
- Differential vacuum test using **real DSSD** as a vacuum barrier
 - **6 orders of magnitude difference between low and UH vacuum in wide pressure region**
- Vacuum of **$1.2 * 10^{-10}$ mbar** reached – pumping limit of the station

UHV part

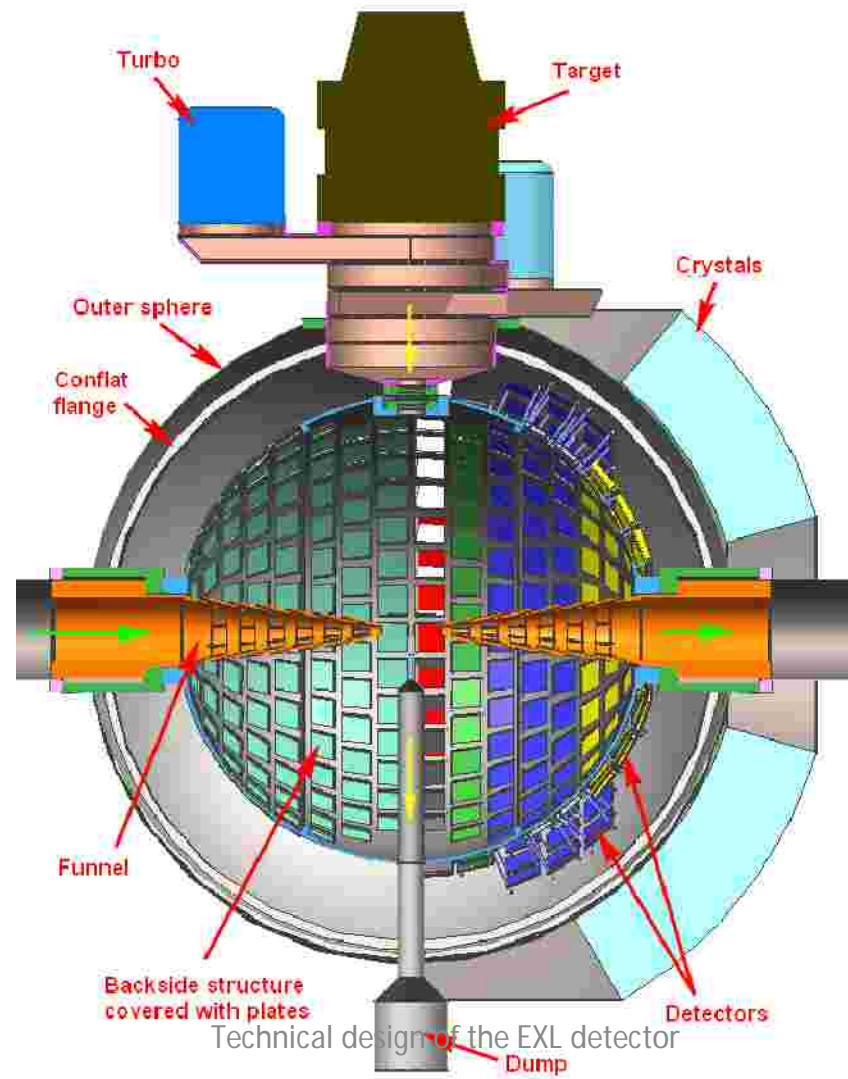


Low vacuum part

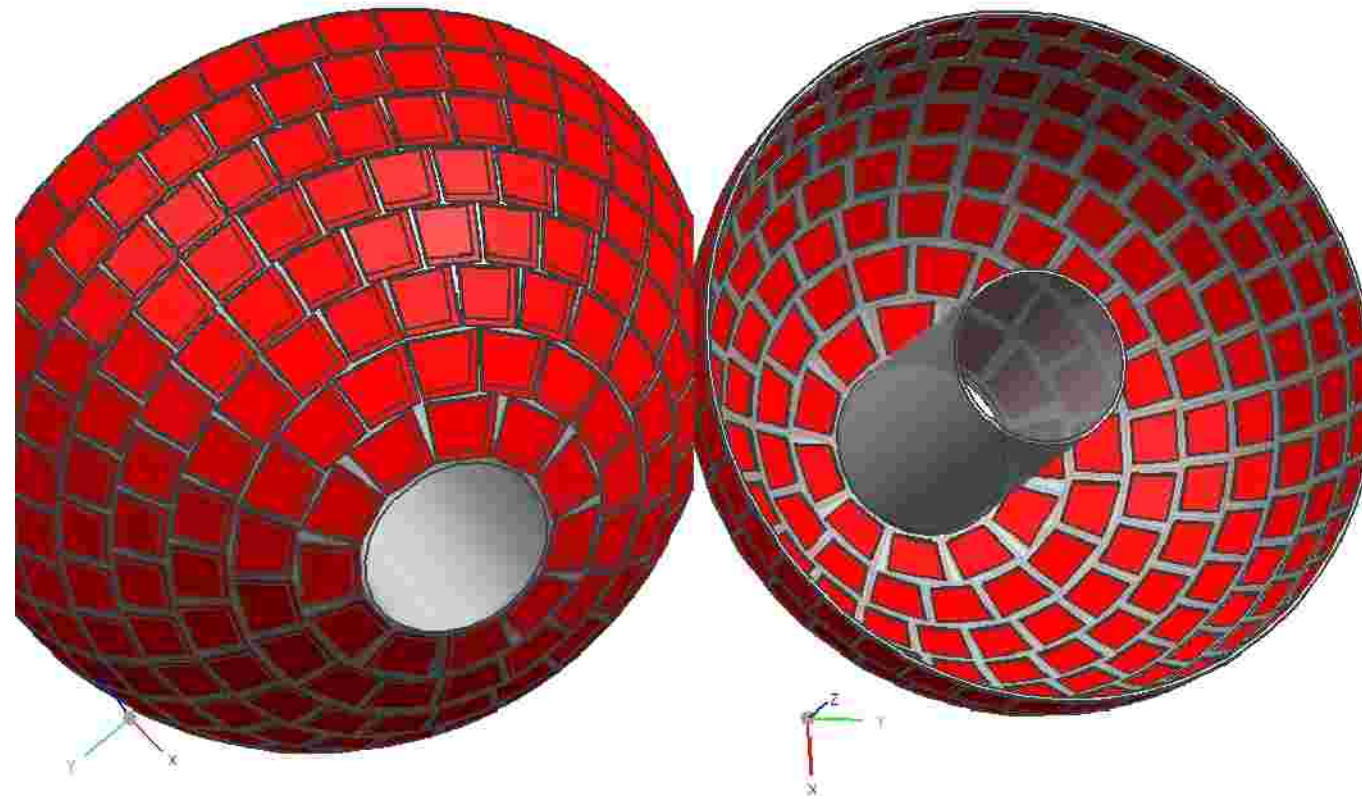
Vacuum separation

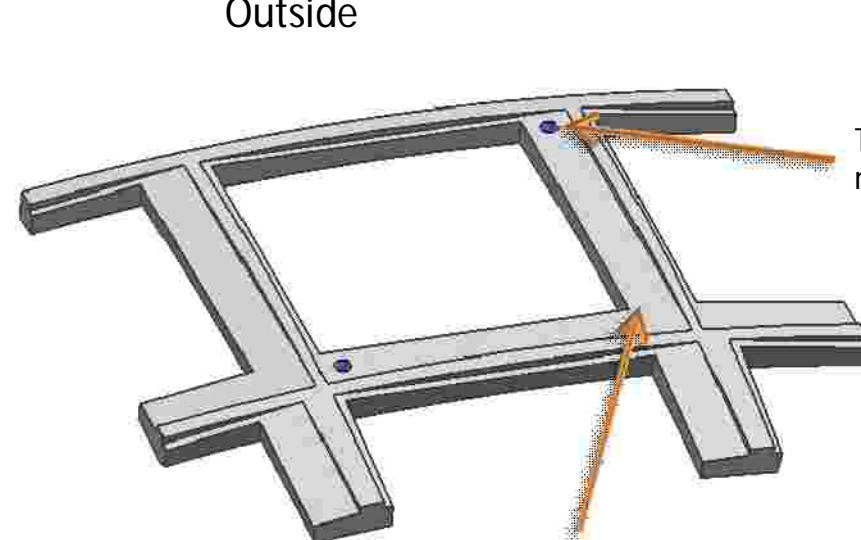


System Integration



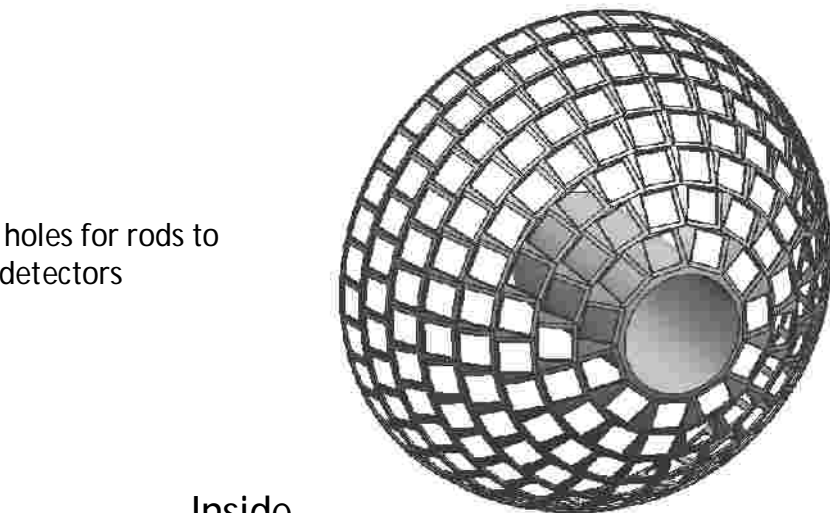
System Integration



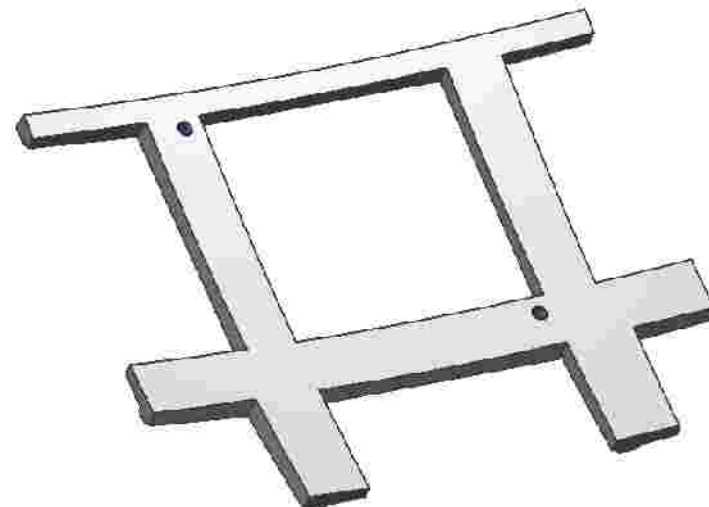


Thread holes for rods to
mount detectors

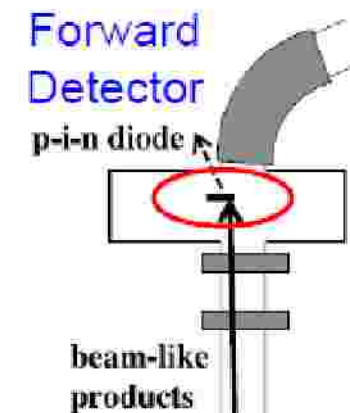
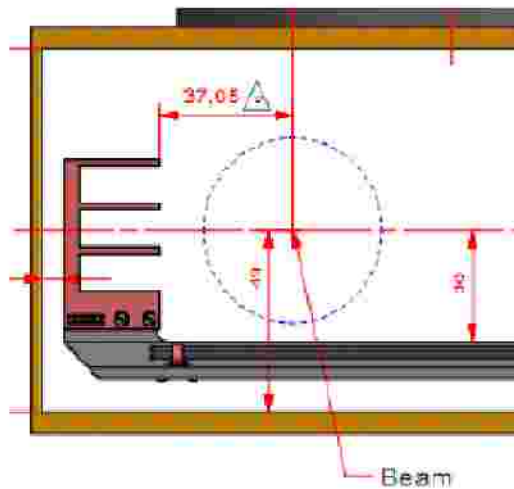
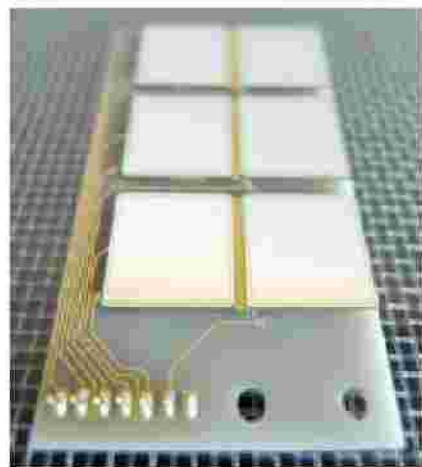
Flat cutouts to
support detector
and make it
vacuum tight



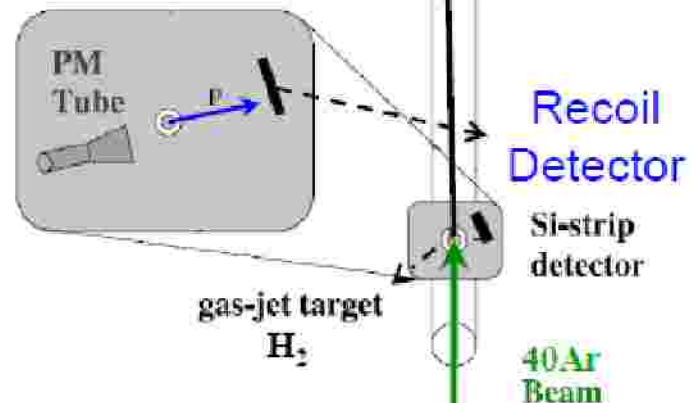
Inside



UHV capable Tagging Detector



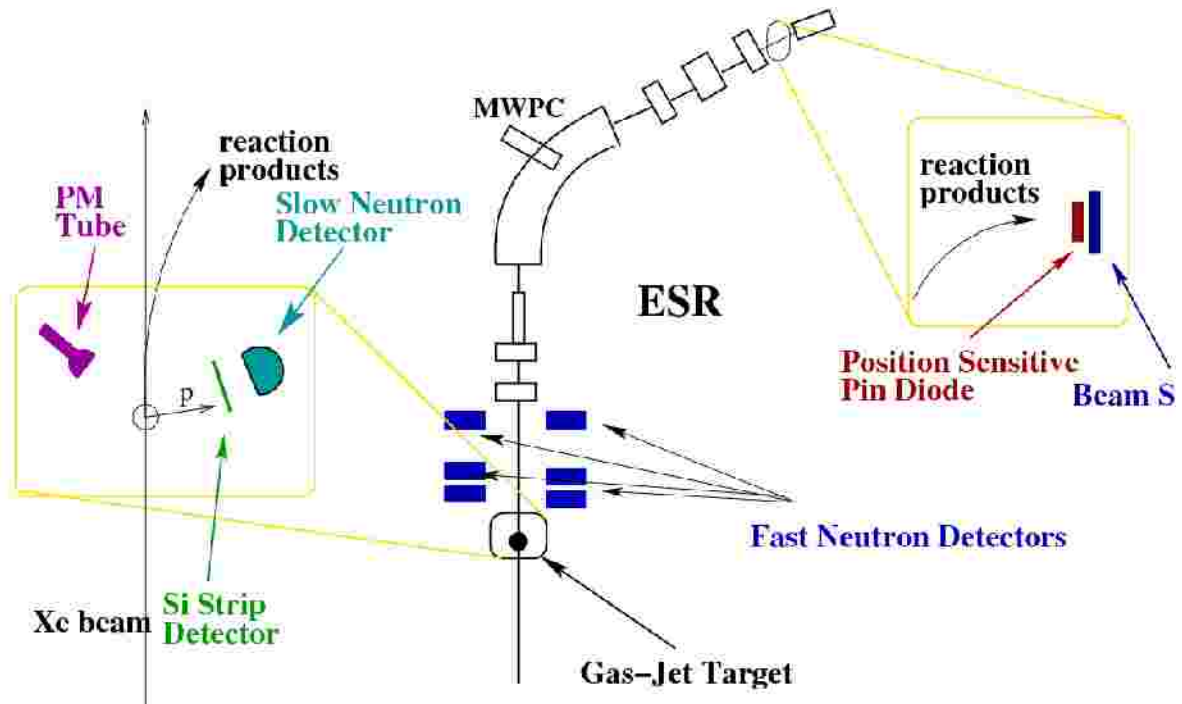
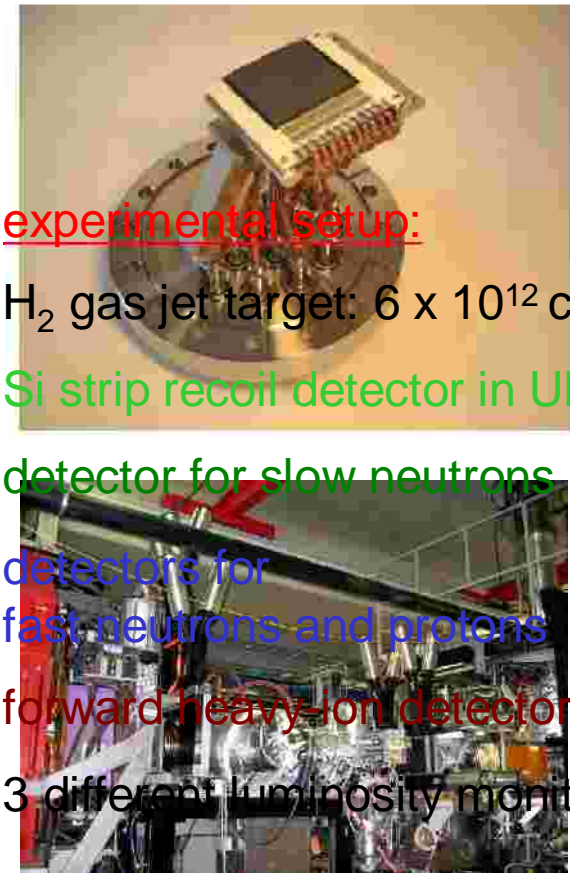
- Forward detector before the first dipole, detection of beam like reaction products in coincidence with recoils.
- 6 PIN diodes ($1 \times 1 \text{ cm}^2$) on AlN PCB, directly in the UHV
- Small dead edge, could be very close to the beam
- Baked at 250° C , passed vacuum Test.



IV. Feasibility Studies for EXL and First Experiments at the ESR

experimental conditions:

- ^{136}Xe beam, $E = 350 \text{ MeV/u}$
- 10^9 circulating ions in ring $\Rightarrow L \approx 6 \cdot 10^{27} \text{ cm}^{-2} \text{ sec}^{-1}$



Si-Strip Detector for Applications under UHV Conditions



- design:
 - active area: $40 \times 40 \text{ mm}^2$
 - thickness: 1 mm
 - 40 strips (pitch: 1mm) connected for readout in groups of 8
 - bakeable to $250^\circ \text{ Celsius}$
 - cables: home made

- performance:
 - energy resolution 35 keV FWHM
 - low outgassing rate



Selected Results

performance of luminosity monitors:

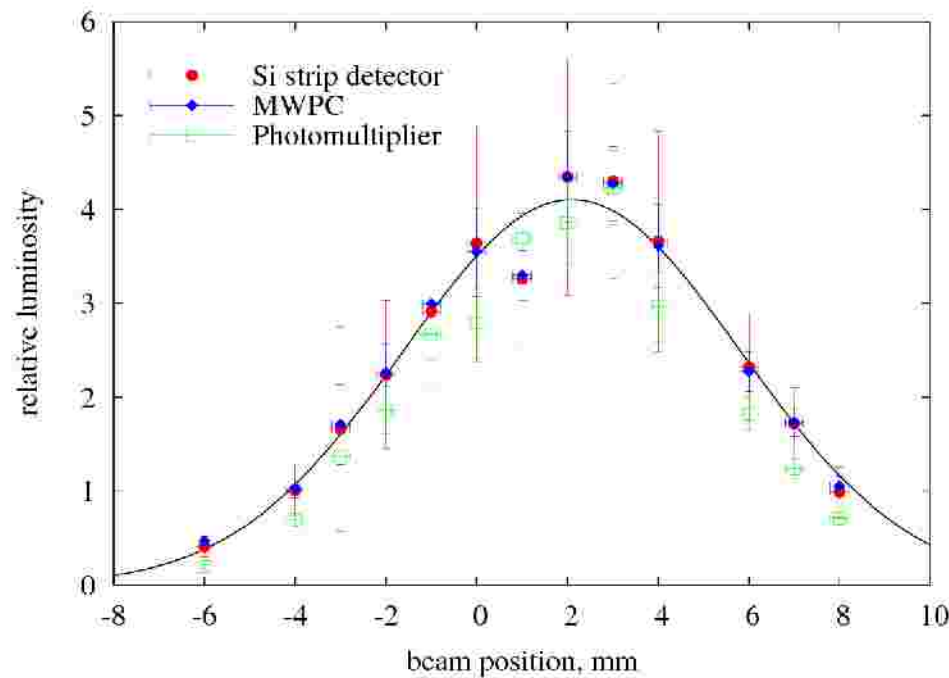
Si strip detector:

MWPC:

Photomultiplier:

elastic scattering

atomic charge exchange
light



size of gas jet target:

7.0 ± 0.2 mm

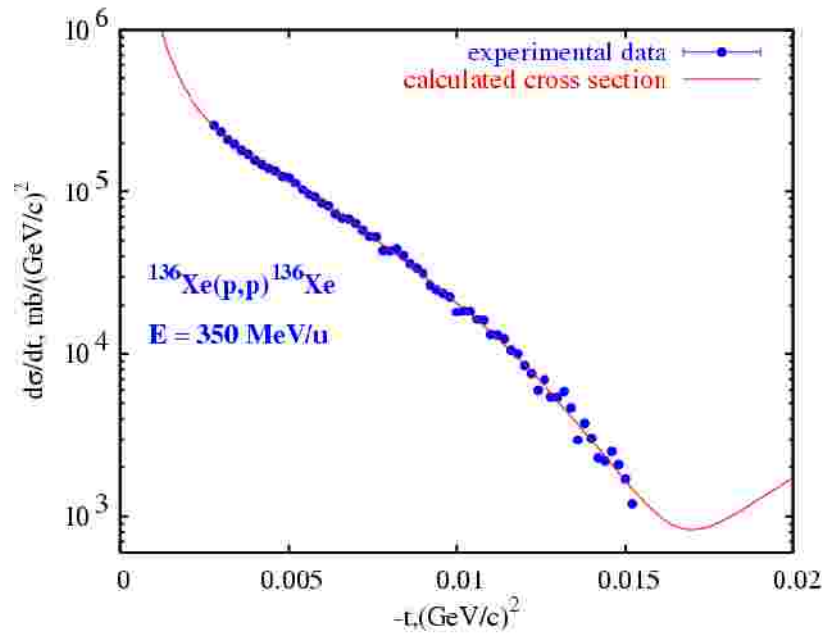
absolute luminosity measured with Si Strip Recoil Detector

deduced luminosity $\Rightarrow L = (6 \pm 2) \cdot 10^{27} \text{ cm}^{-2} \text{ sec}^{-1}$

Selected Results

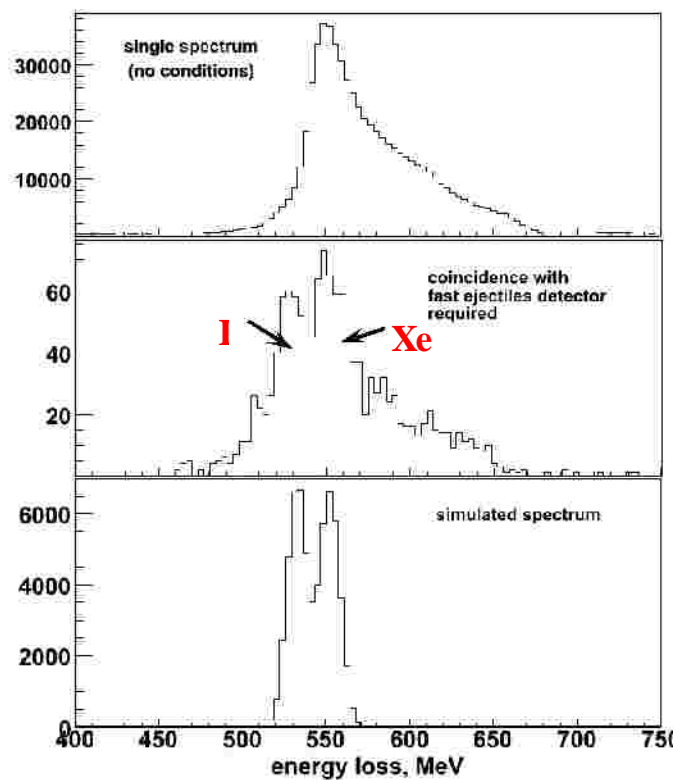
H. Moeini and S. Ilieva et al., NIM A634 (2011)77

Recoil Detector in UHV:
Differential $^{136}\text{Xe}(p,p)$ cross section



data are consistent with
nuclear matter radius: $R_m = 4.89 (10) \text{ fm}$
(expected from data on the charge radius)

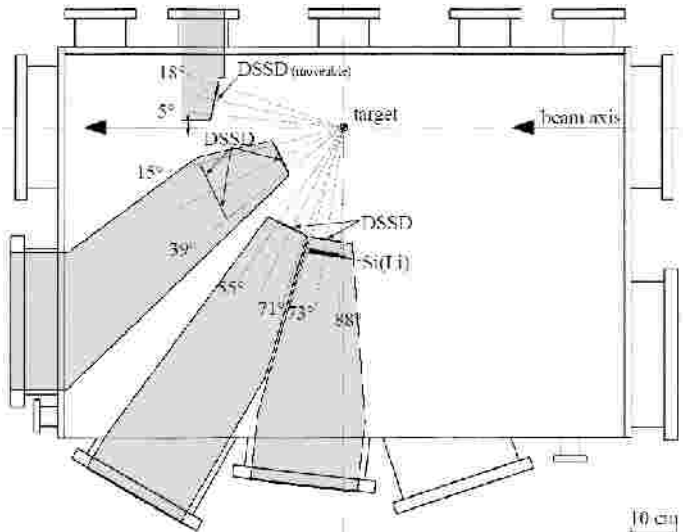
In-Ring Detectors:
Identification of reaction channels



identified reaction channels :
 $^{136}\text{Xe}(p, pn)^{135}\text{Xe}$
 $^{136}\text{Xe}(p, 2pxn)^{132,133}$

Next Step: Accepted Proposal for Feasibility Studies and First Experiments with RIB's at the ESR

(p,p), (a,a`), ($^3\text{He},\text{t}$) reactions
with ^{58}Ni and ^{56}Ni beams



reactions with ^{58}Ni :

proof of principles and feasibility studies:

- | background conditions in the environment of an internal target
- | low energy threshold
- | pulse shape analysis
- | target extension and density
- | performance of in-ring detection system

reactions with ^{56}Ni :

^{56}Ni : doubly magic, important for nucl. astrophysics:

- | (p,p) reactions: nuclear matter distr.
- | (a,a`) reactions: giant resonances ISGMR, IVGDR, parameters of the EOS
- | ($^3\text{He},\text{t}$) reactions: Gamow-Teller matrix elements, important for astrophys.

after ESR upgrade:

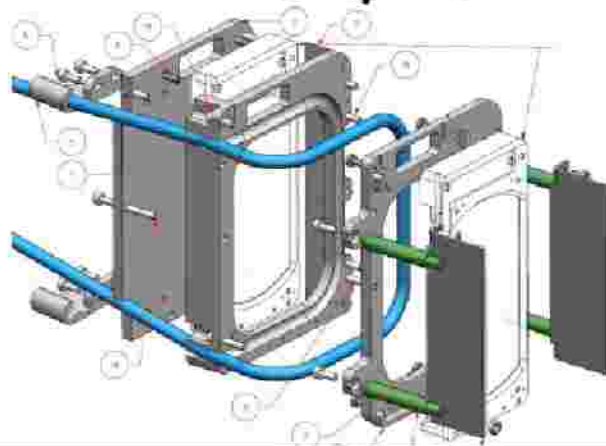
steps further away from stability

New Detector Chamber at the ESR

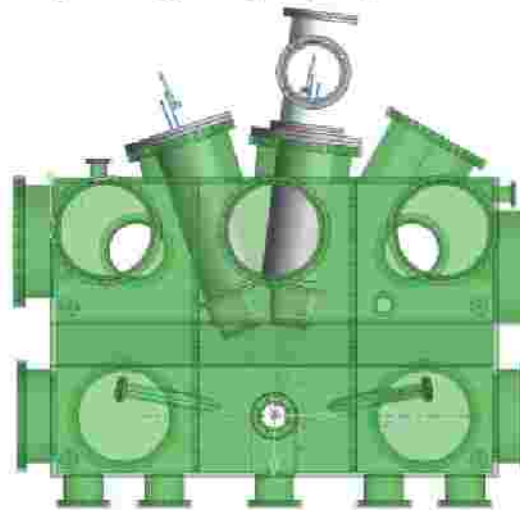
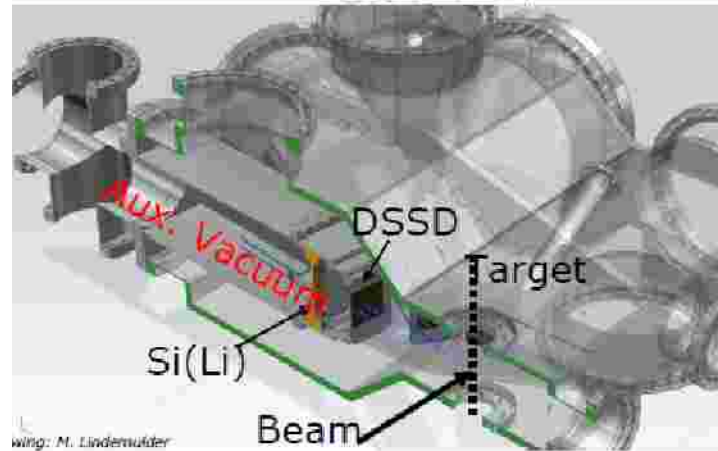


UHV capable Recoil Detectors

Assembly of the EXL's ESR Chamber

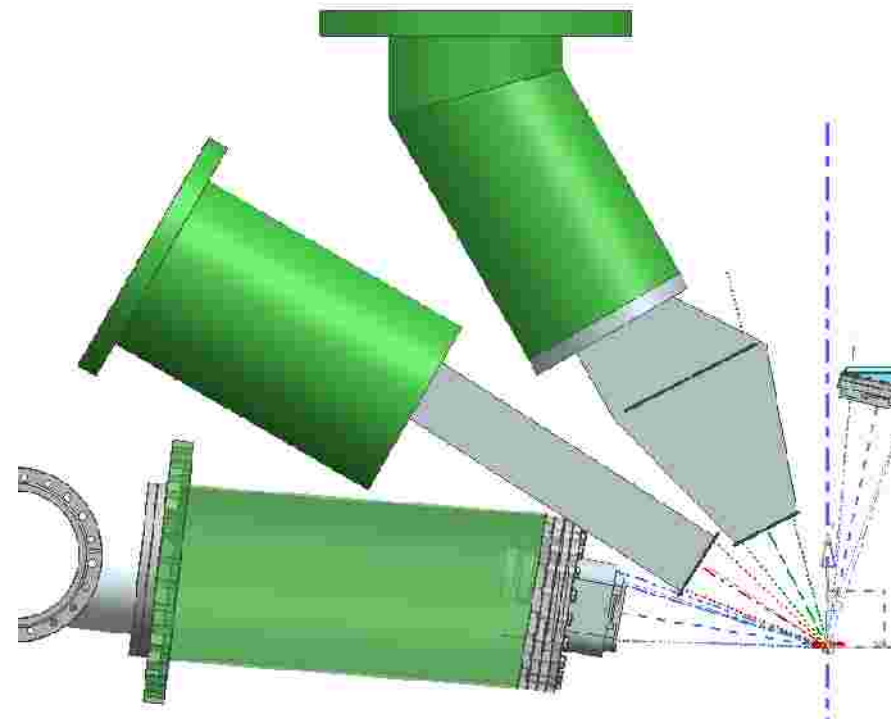
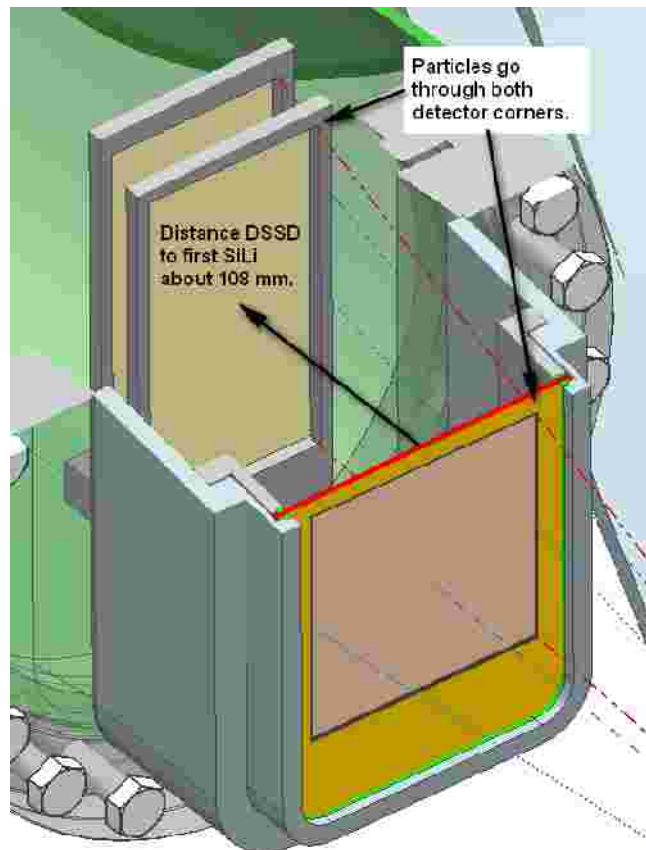


- Thermal tests using the real pocket
 - SiLi cooling vs. pocket baking
- Assembly of a vacuum system
 - Backup system required
- ASIC development + cabling
 - Interconnecting DSSDs with ASIC
 - Proper signal propagation



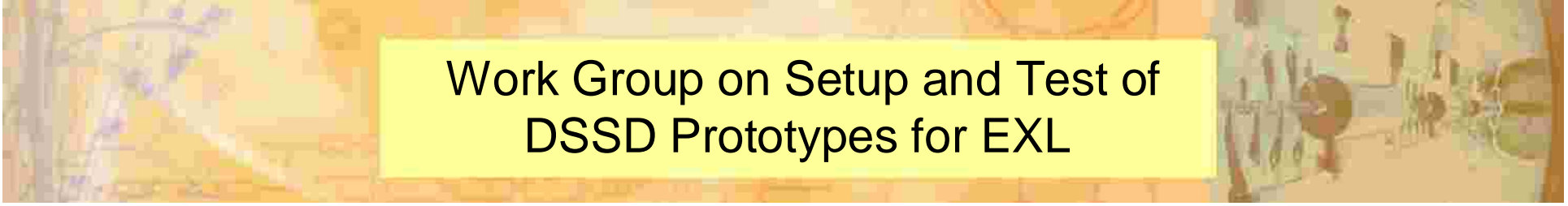
Design Study for First ESR Experiments

M. Lindemulder, KVI



Top view

DSSD – SiLi – SiLi telescope



Work Group on Setup and Test of DSSD Prototypes for EXL

R. Borger¹, T. Davinson², P. Egelhof³, V. Eremin⁴, S. Ilieva³
N. Kalantar¹, Y. Ke³, H. Kollmus³, T. Kröll⁵, X. C. Le³,
M. Lindemulder¹, M. Mutterer³, C. Rigollet¹, M. von Schmid⁵, B.
Streicher^{1,3} P. Woods²

1 KVI Groningen

2 Univ. Edinburgh

3 GSI Darmstadt

4 PTI St. Petersburg

5 TU Darmstadt

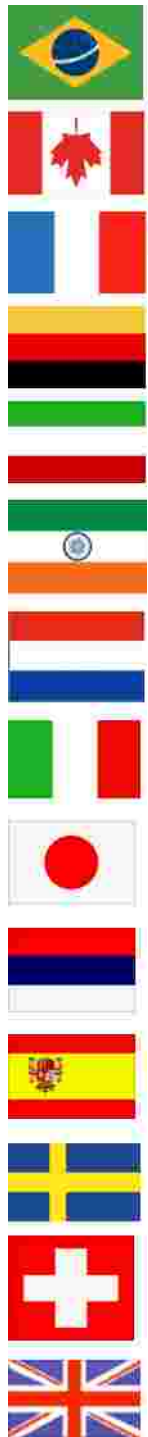


Feasibility Demonstration at the Present ESR Facility

F. Aksouh, K. Beckert, P. Beller, K. Boretzky, A. Chatillon,
A. Corsi, P. Egelhof, H. Emling, G. Ickert, S. Ilieva, J. Jourdan,
N. Kalantar, O. Kiselyov, C. Kozhuharov, T. Le Bleis, X.C. Le,
Y. Litvinov, K. Mahata, J. P. Meier, H. Moeini, F. Nolden,
S. Pascalis, U. Popp, D. Rohe, H. Simon, M. Steck, T. Stöhlker,
H. Weick, D. Werthmüller, A. Zalite
and the EXL-collaboration

Gesellschaft für Schwerionenforschung, Darmstadt, Germany
Universität Basel, Basel, Switzerland

Johannes Gutenberg Universität Mainz, Mainz, Germany
KVI, University of Groningen, Groningen, The Netherlands
University of Liverpool, Liverpool, United Kingdom



Univ. São Paulo

TRIUMF Vancouver

IPN Orsay, CEA Saclay

GSI Darmstadt, TU Darmstadt, Univ. Frankfurt, FZ Jülich, Univ. Mainz, Univ. Munich

INR Debrecen

SINP Kolkata

KVI Groningen

INFN/Univ. Milano

Univ. Osaka

JINR Dubna, Univ. St Petersburg, Moscow

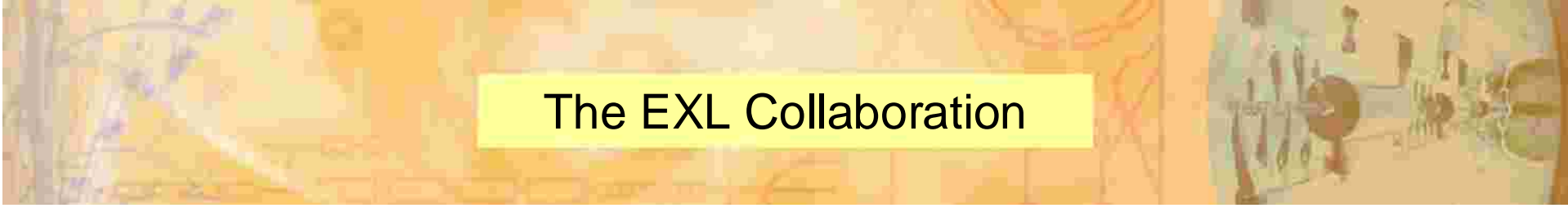
CSIC Madrid, Univ. Madrid

Univ. Lund, Mid Sweden Univ., TSL Uppsala

Univ. Basel

Univ. Birmingham, CLRC Daresbury, Univ. Surrey, Univ. York, Univ. Liverpool





The EXL Collaboration

Basel, Switzerland, Universität Basel - K. Hencken, B. Krusche, T. Rauscher, F. Thielemann
Birmingham, United Kingdom, University of Birmingham - M. Freer
Daresbury, United Kingdom, CLRC Daresbury Laboratory - P. Coleman-Smith, I. Lazarus, R. Lemmon, S. Letts, V. Pucknell
Darmstadt, Germany, Gesellschaft für Schwerionenforschung - T. Aumann, F. Becker, K. Beckert, K. Boretzky, A. Dolinski, P. Egelhof, H. Emeling, H. Feldmeier, B. Franczak, H. Geissel, J. Gerl, S. Ilieva, C. Kozhuharov, Y. Litvinov, T. Neff, F. Nolden, C. Peschke, U. Popp, H. Reich-Sprenger, H. Simon, M. Steck, T. Stöhlker, K. Sümmerer, S. Typel, H. Weick, M. Winkler
Darmstadt, Germany, Technische Universität Darmstadt - G. Schriener
Debrecen, Hungary, Institute of Nuclear Research (ATOMKI) - A. Algora, M. Csátlos, Z. Gáski, J. Gulyás, M. Hunyadi, A. Krasznahorkay
Dubna, Russia, Joint Institute of Nuclear Research - A.G. Artukh, A. Fomichev, M. Golovkov, S.A. Klygin, G. A. Kononenko, S. Krupko, A. Rodin, Yu.M. Sereda, S. Sidorchuk, E. A. Shevchik, Yu.G. Teterov, A.N. Vorontsov
Frankfurt, Germany, Universität Frankfurt - R. Dörner, R. Grisenti, J. Stroth
Gatchina, Russia, St. Petersburg Nuclear Physics Institute and St. Petersburg State University - V. Ivanov, A. Khanzadeev, E. Rostchin, O. Tarasenkova, Y. Zalite
Göteborg, Sweden, Chalmers Institute - B. Jonson, T. Nilsson, G. Nyman
Groningen, KVI The Netherlands - M. N. Harakeh, N. Kalantar-Nayestanaki, H. Moeini, C. Rigollet, H. Wörtche
Guildford, United Kingdom, University of Surrey - J. Al-Khalili, W. Catford, R. Johnson, P. Stevenson, I. Thompson
Jülich, Germany, Institut für Kernphysik, Forschungszentrum Jülich - D. Grzonka, T. Krings, D. Protic, F. Rathmann
Kolkata, India, Saha Institute of Nuclear Physics - S. Bhattacharya, U. Datta Pramanik
Liverpool, United Kingdom, University of Liverpool - M. Chartier, J. Cresswell, B. Fernandez Dominguez, J. Thornhill
Lund, Sweden, Lund University - V. Avdeichikov, L. Carlén, P. Gobulev, B. Jakobsson
Madrid, Spain, CSIC, Instituto de Estructura de la Materia - E. Garrido, O. Moreno, P. Sarriuguren, J. R. Vignote, C. Martínez-Pérez, R. Alvarez Rodriguez, C. Fernandez Ramirez
Madrid, Spain, Universidad Complutense - L. Fraile Prieto, J. López Herraiz, E. Moya de Guerra, J. Udias-Moinelo
Mainz, Germany, Johannes Gutenberg Universität - O. Kiselev, J.V. Kratz
Milan, Italy, Università da Milano and INFN - A. Bracco, P.F. Bortignon, G. Colò, A. Zalite
Moscow, Russia, Russian Research Centre, Kurchatov Institute - L. Chulkov
Mumbai, India, Bhabha Atomic Research Center - S. Kailas, A. Shrivastava
Munich, Germany, Technische Universität München - M. Böhmer, T. Faestermann, R. Gernhäuser, P. Kienle, R. Krücken, L. Maier, K. Suzuki
Orsay, France, Institut de Physique Nucléaire - D. Beaumel, Y. Blumenfeld, E. Khan, J. Peyre, J. Pouthas, J.A. Scarpaci, F. Skaza, T. Zerguerras
Osaka, Japan, Osaka University - Y. Fujita
São Paulo, Brasil, Universidade de São Paulo - A. Lépine-Szily
St. Petersburg, Russia, V. G. Khlopin Radium Institute - Y. Murin
St. Petersburg, Russia, Ioffe Physico-Technical Institute (PTI) - V. Eremin, Y. Tuboltcev, E. Verbitskaya
Sundsvall, Sweden, Mid Sweden University - G. Thungström
Tehran, Iran, University of Tehran - M. Mahjour-Shafiei
Uppsala, Sweden, The Svedberg Laboratory - C. Ekström, L. Westerberg
Vancouver, Canada, TRIUMF - R. Kanungo



V. Conclusions

- | The Future Facility NUSTAR@FAIR will allow to reach unexplored regions in the chart of nuclei, where new and exciting phenomena are expected.
- | The EXL setup is designed as universal detection system providing high resolution and large solid angle coverage for measurements at low momentum transfer.
- | The use of stored cooled radioactive beams within the EXL project will have considerable advantage over external target experiments in many cases.
- | The realization of the UHV compatible Si ball is most challenging.
- | The status of R&D and Feasibility Studies is very prom
⇒ the major technical problems are solved.
- | EXL will allow to use a world wide unique experimental technique.
- | A number of important physics questions can be only addressed by EXL.



R&D on Internal Target for EXL

new target option: cryogenic droplet targets

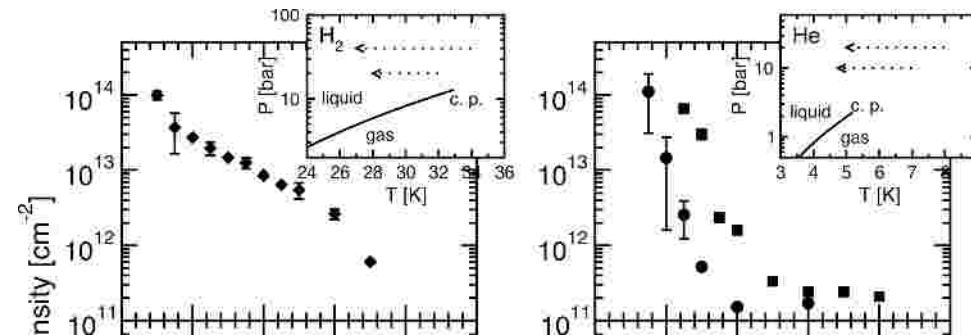
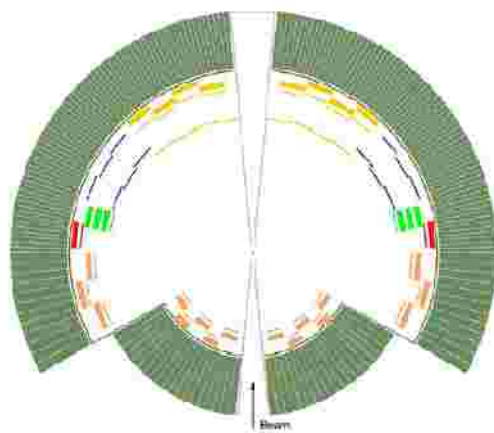
(R.Grisenti et al., Frankfurt)

as compared to conventional gas-jet target: ($d = 10^{14} \text{ cm}^{-2}$, $s = 5 \text{ mm}$):
⇒ potentially higher density and smaller target extension

first successfull tests at the ESR performed

⇒ results are promising $d = 10^{14} \text{ cm}^{-2}$ reached for H and He!
but dramatic pressure increase under ion bombardment

⇒ target extension: $s \sim 7 \text{ mm}$, expected for NESR: $s \sim 1 \text{ mm}$

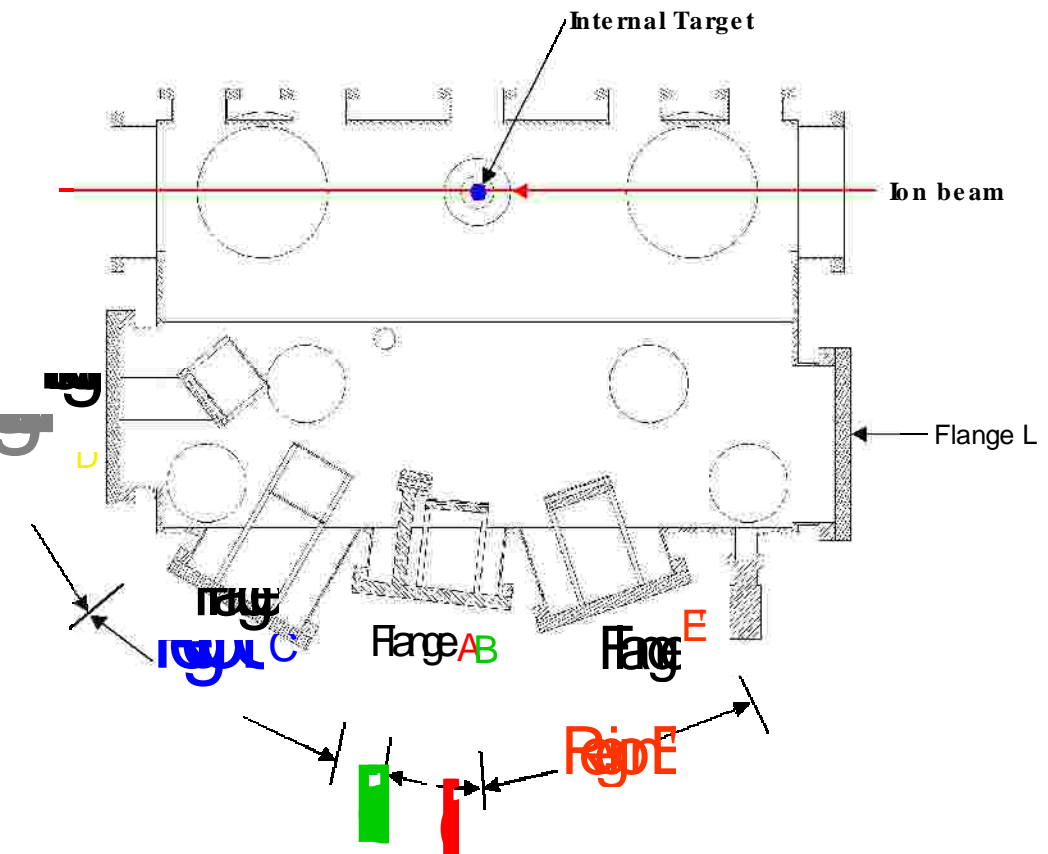


The New Recoil Detector Chamber at the ESR

Region	$\theta_{\text{Lab}}^{*})$	θ Flange axis	Covered θ range	Flange size in mm
A	90° – 80°	83°	95° - 73°	Ø250
B	80° – 75°	83°	95° - 73°	Ø250
C	75° – 45°	60°	71° - 52°	Ø 250
D	45° – 10°	0°	28° - 18°	200x250
E'	120° – 91°	109°	98° - 118°	Ø250
L		180°	136,5° – 43,5° **)	200x250

*) according to the angular regions A – E' defined in the Technical Proposal

Interaction Chamber Part (IC)



Detector Chamber Part (DC)

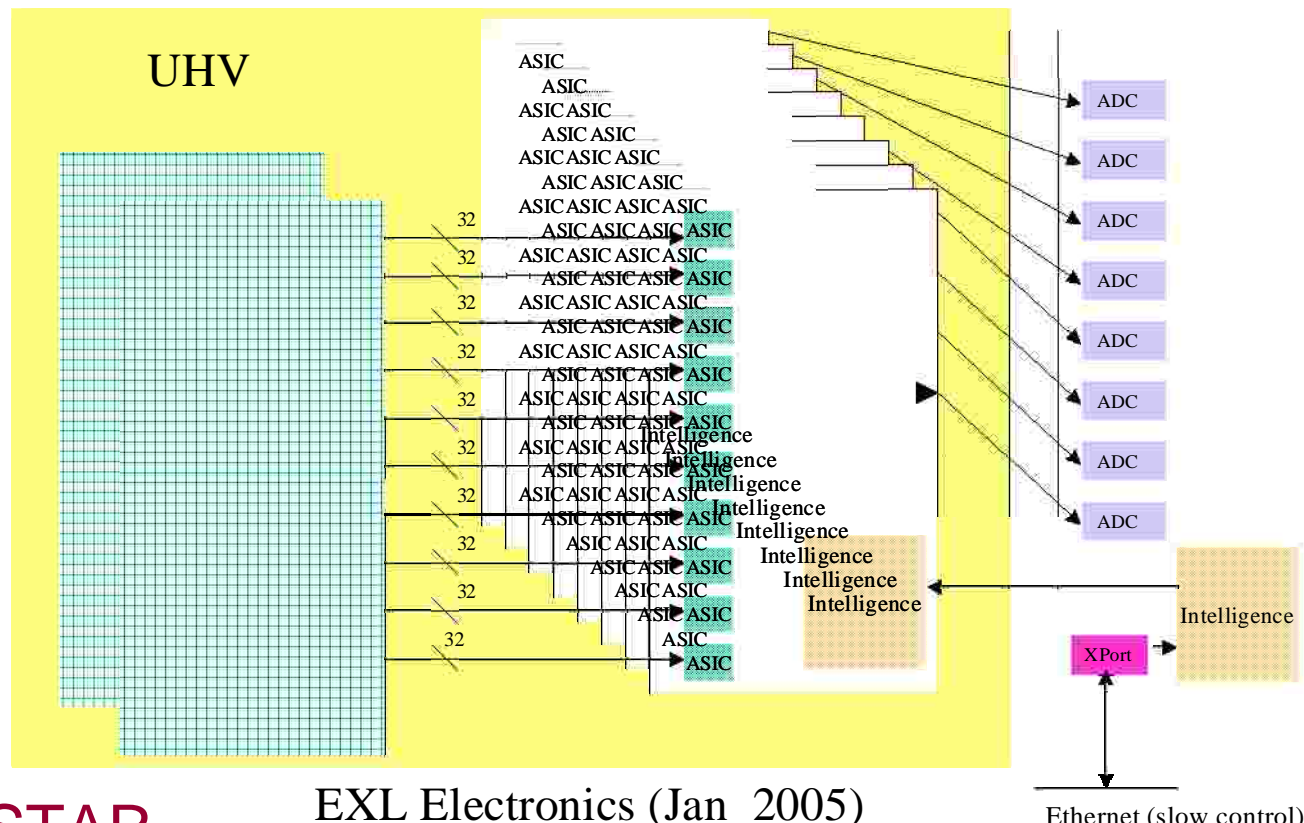
EXL Electronics

Detectors-
560000 channels
DSSD and SiLi

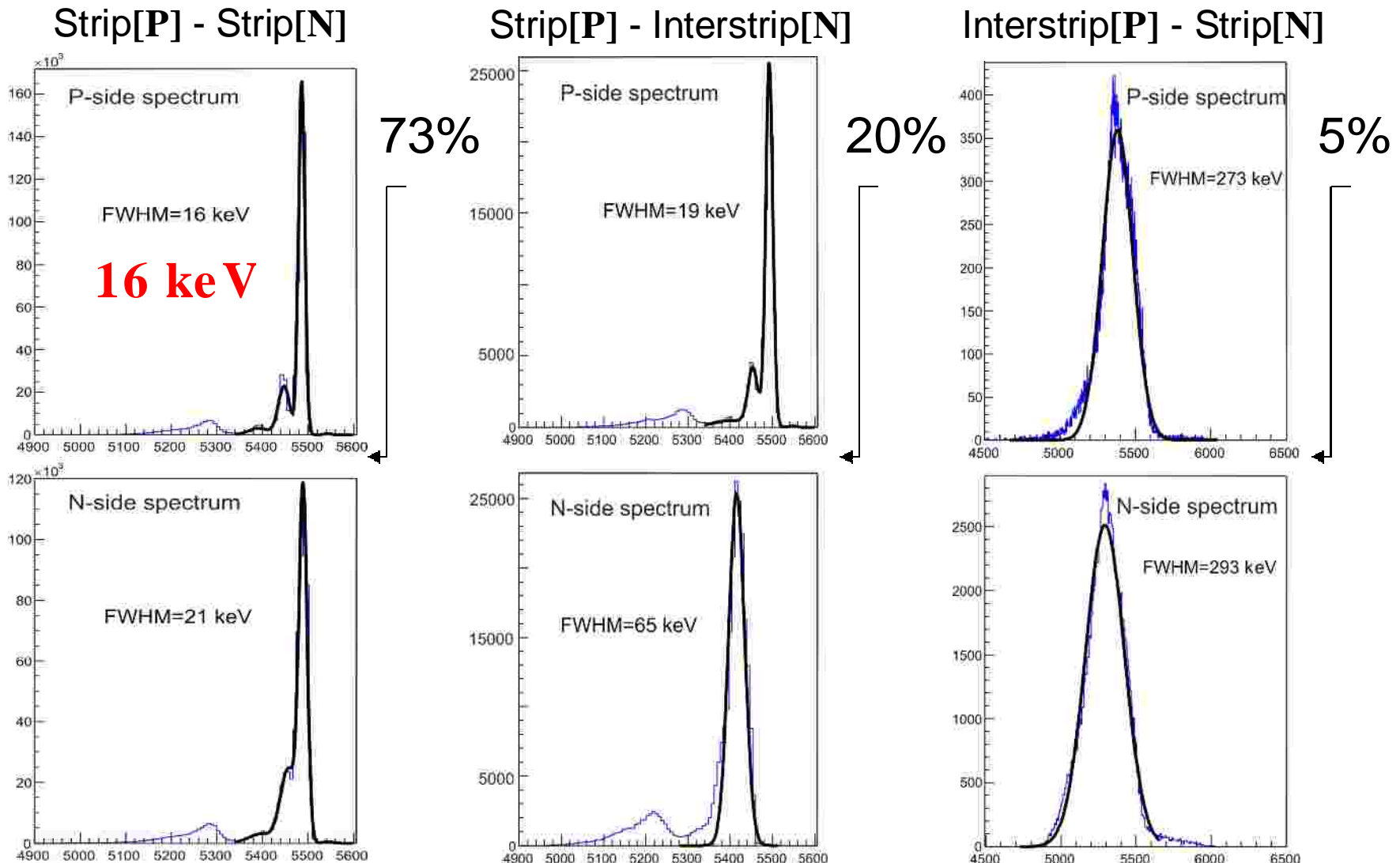
ASIC cards- approx
17500 ASICs on 1750 cards
(32 channels/ASIC)

ADC cards- 1750
ADCs on 219 cards
(320 channels/ADC)

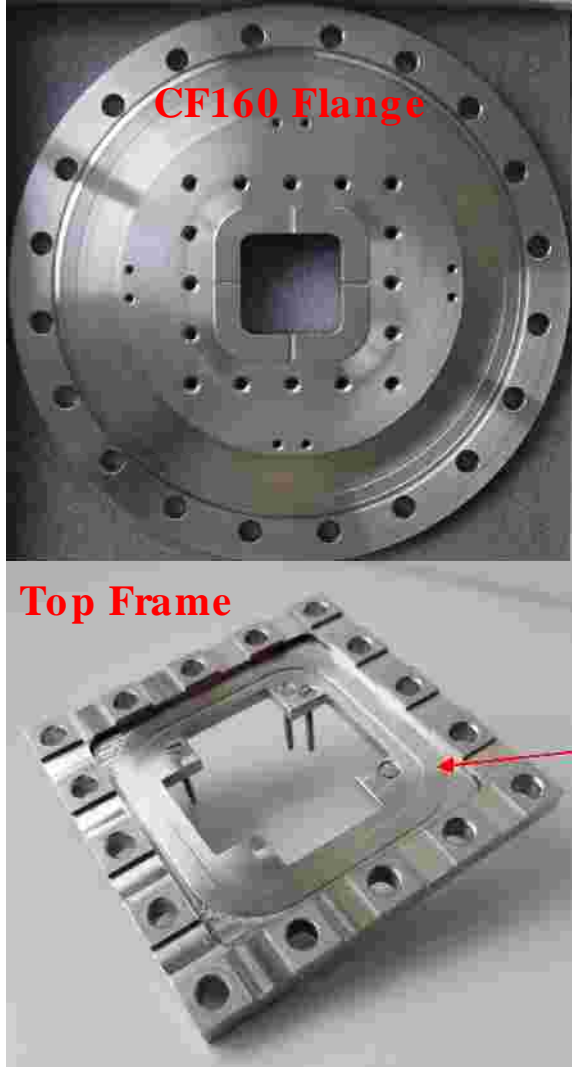
- Large number of channels
 - Large dynamic range, low threshold
 - UHV – Low power dissipation, baking
 - Space constraints



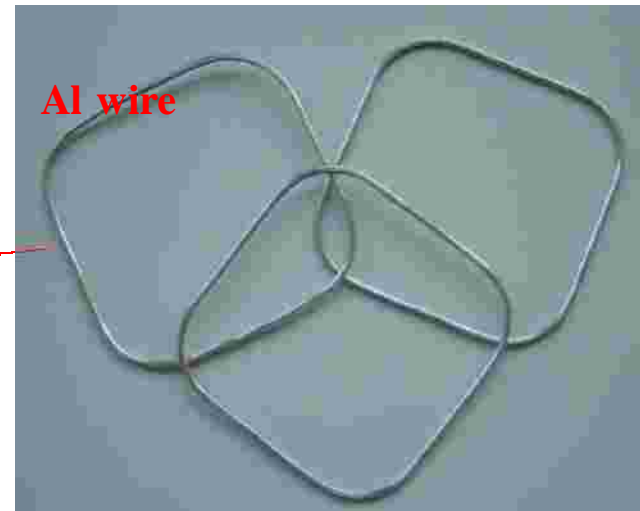
Correlation Analysis Results

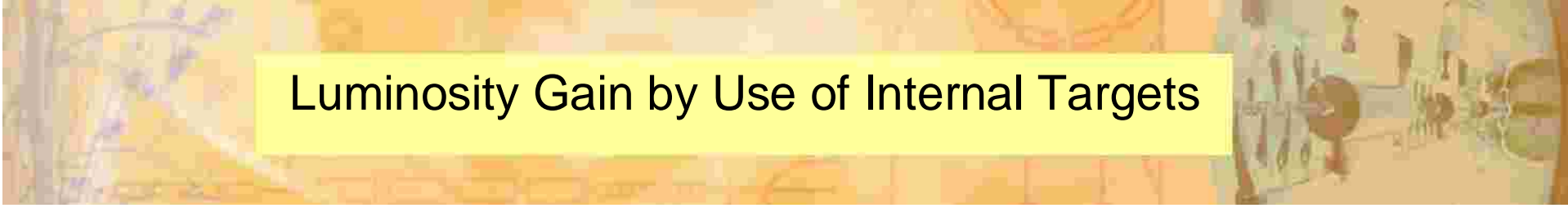


Mechanical Construction



- Base frame machined from CF160 flange
- Top frame from stainless steel has groove that presses on PCB and mounts for connectors
- Aluminium wires as a vacuum seal, used on both sides of the AlN PCB





Luminosity Gain by Use of Internal Targets

$$R(\text{int}) = I_0 \times s(\text{nuclear reactions}) / s(\text{atomic charge exchange})$$

$$R(\text{ext}) = I_0 \times s(\text{nuclear reactions}) \times N(\text{target})$$

$$\Rightarrow R(\text{int}) / R(\text{ext}) = 1 / (s(\text{atomic charge exchange}) \times N(\text{target}))$$

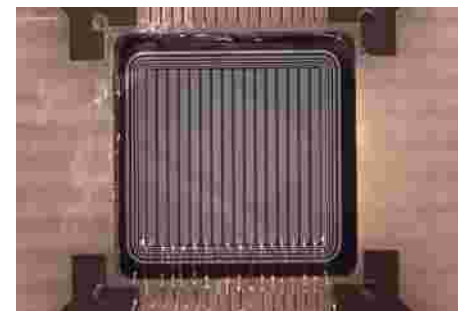
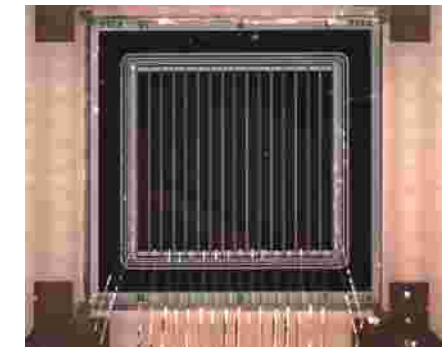
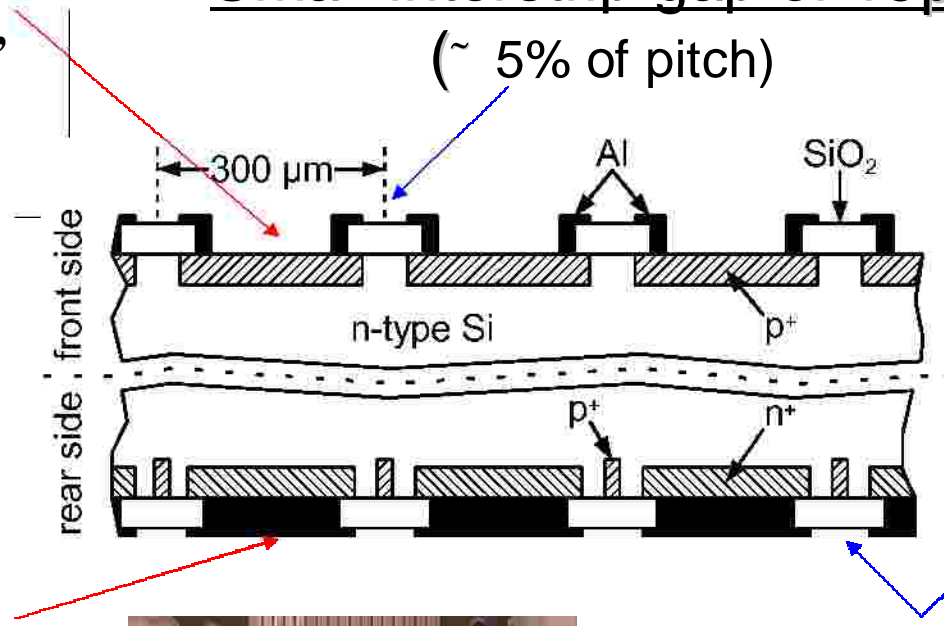
Basic DSSD Structure (16 x 16 strips, 300 μ m pitch)

P-side strips
partly metallized,
„Thin window
design“

P-side - N-side

N-side strips
metallized

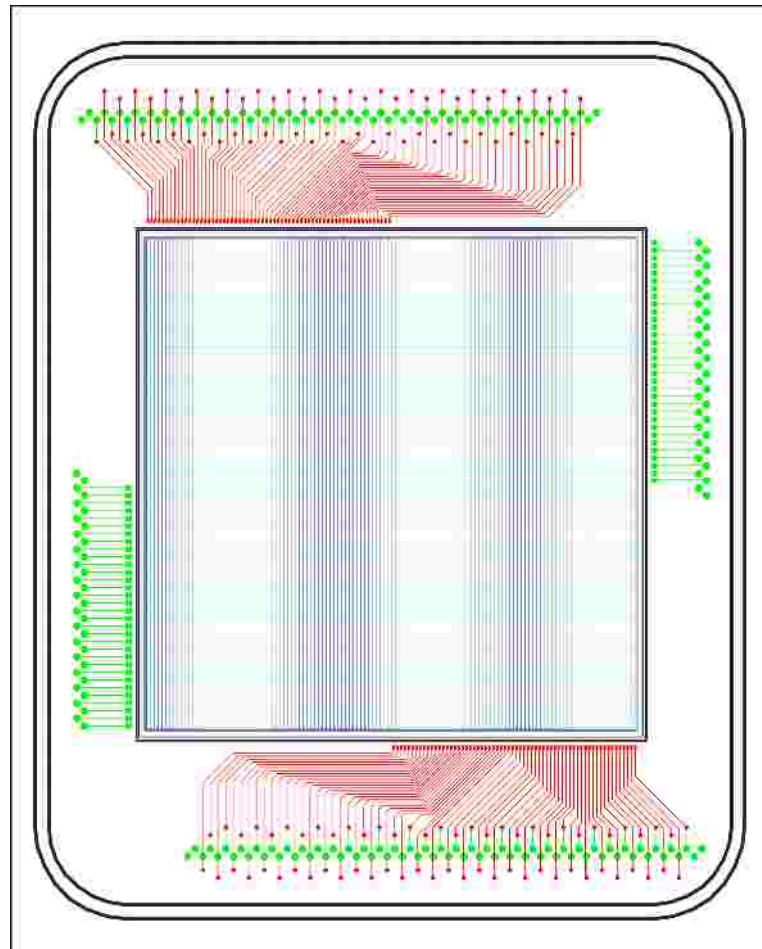
Small interstrip gap of 15 μ
(~ 5% of pitch)



Interstrip gap:
65 μ (by p+ imp.)
(~ 22 % of pitch)

Also valid for 64x64
and 64x16 DSSDs

PCB Design for 65 x 65 mm² DSSD`s

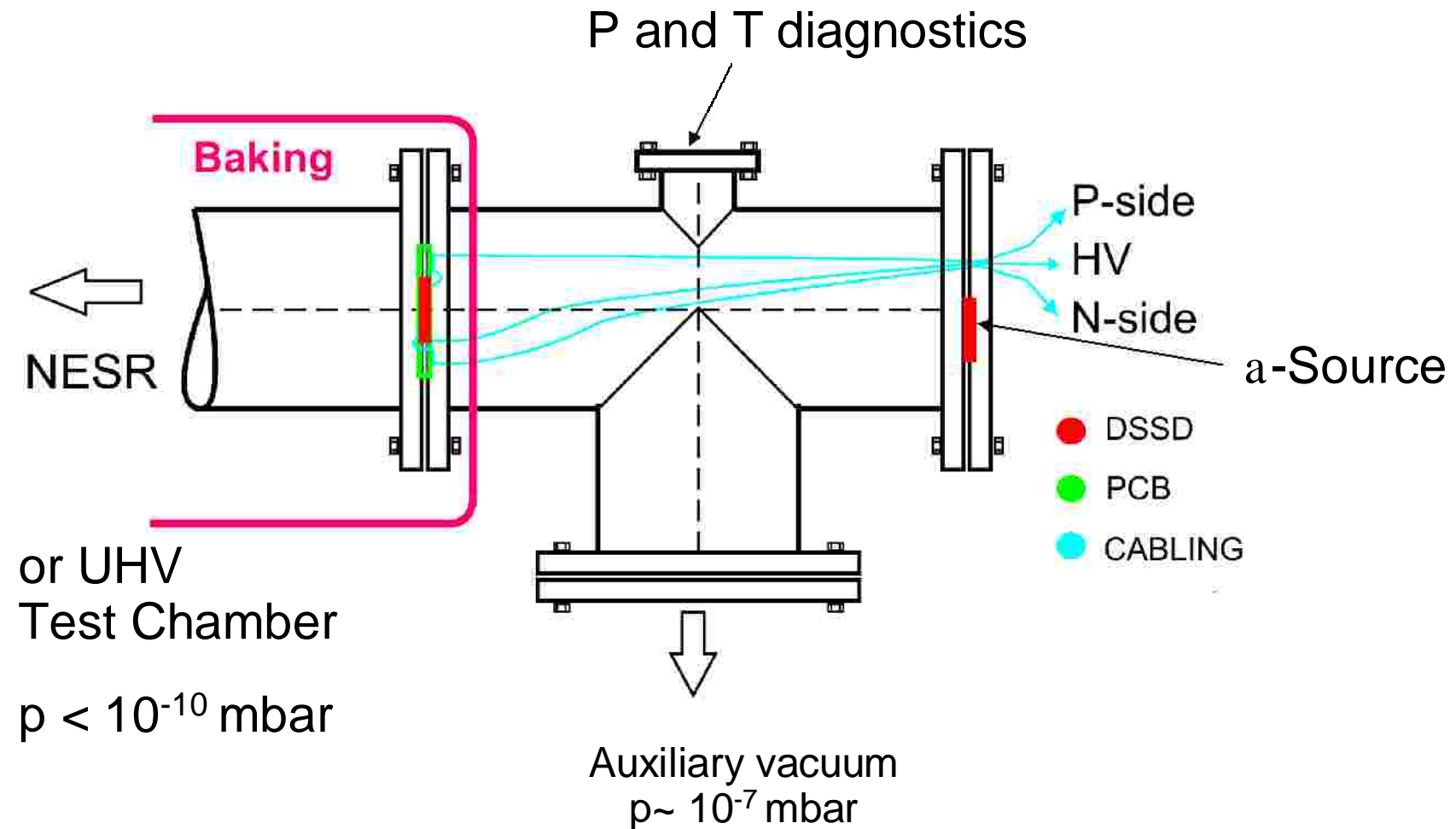


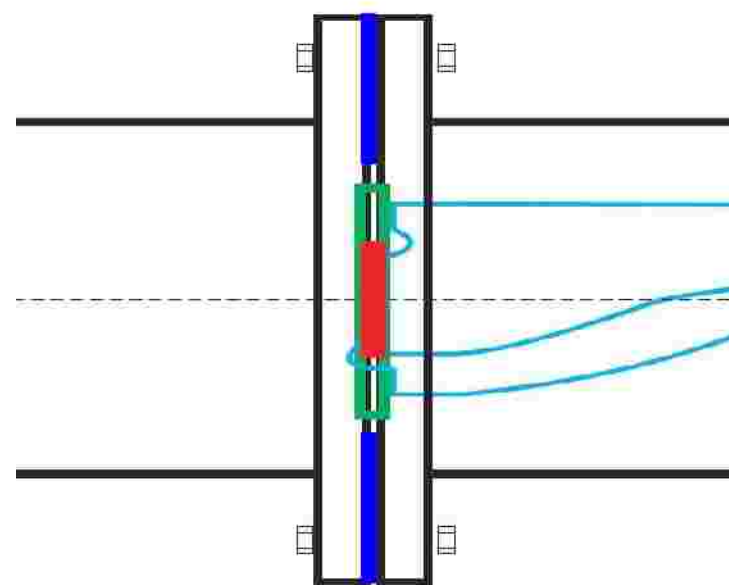
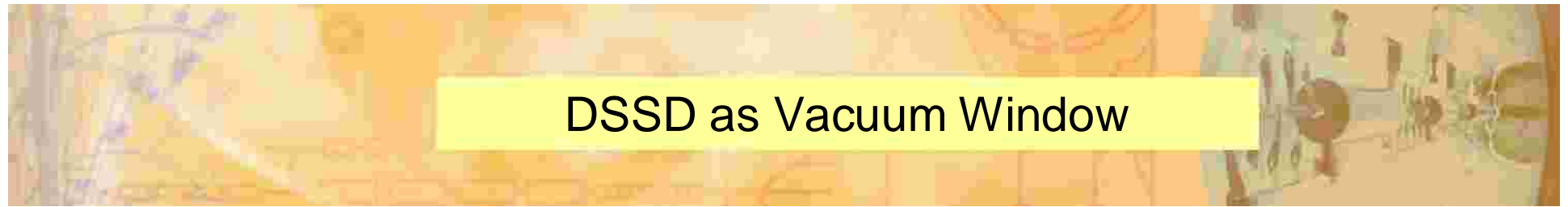
- P-side: 128 strips
- N-side: 64 strips

AlN PCB lapped and polished:
Roughness < 0.5 µm
Parallelity < 50 µm

Production: 2010

LUST
HYBRID-TECHNIK



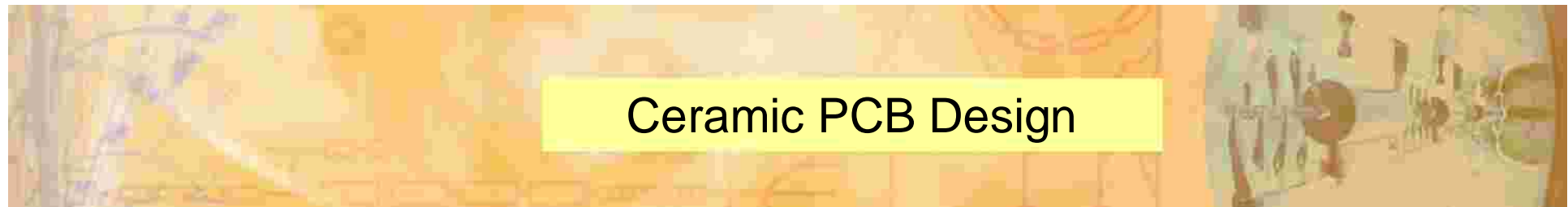


- ? DSSD
- ? ceramic PCB
- ? copper gasket

DSSD: 64 x 64 strips,
21 x 21 mm², 300µm



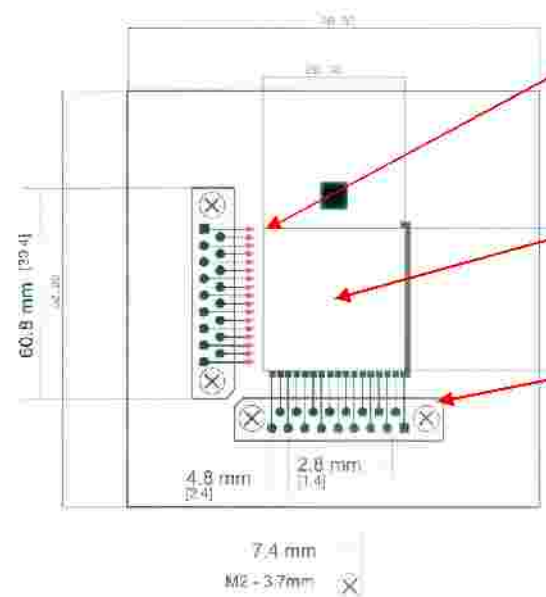
mounted on ceramic PCB,
with low-outgassing epoxy.



Ceramic PCB Design

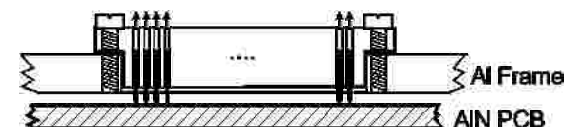
p-side in UHV,
n-side in aux.vacuum

Plate-through
contacts

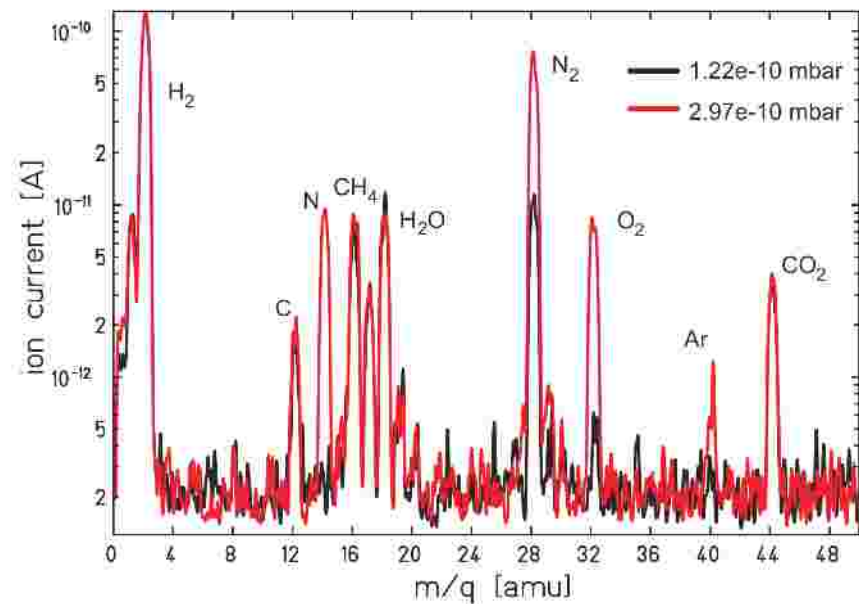
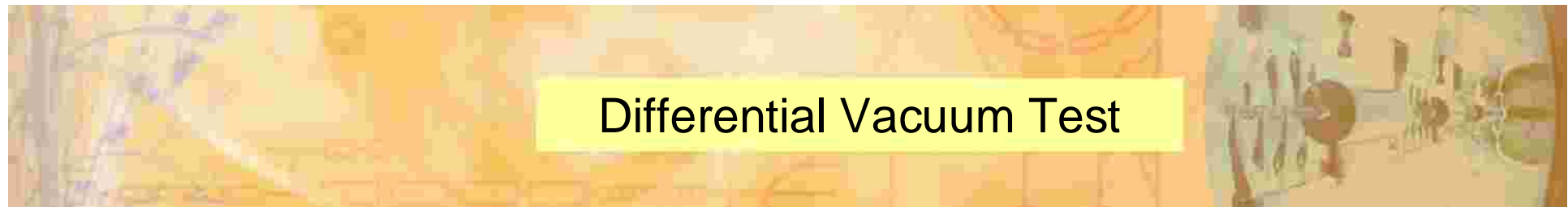


DSSD: 64 x 64 strips, 21 x
21 mm², 300µm

Spring-pin connector

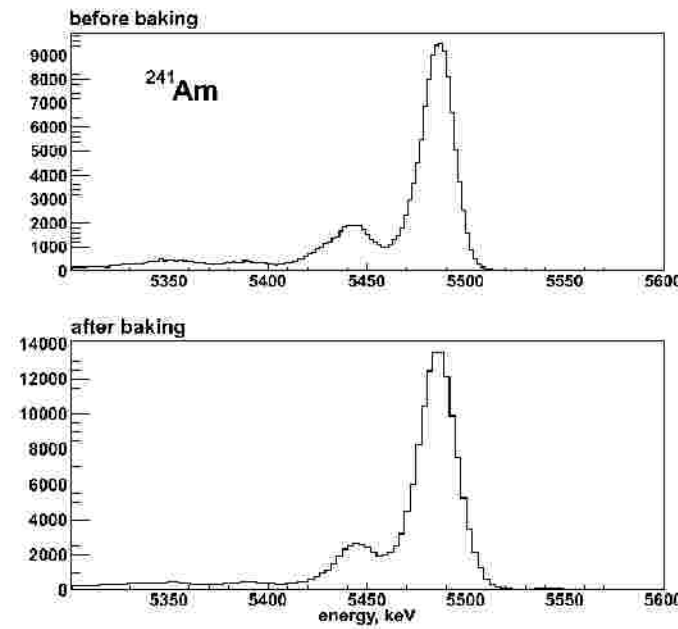


All components bakeable to 200 °C



Rest-gas analysis favourable

**DSSD as UHV – HV
vacuum barrier
works fine**



Spectral response
unchanged after three
baking cycles (to 220°)